NASA CONTRACTOR REPORT

NASA CR-2187

DESIGN OF A BLEED SYSTEM FOR A MACH 3.5 INLET

by J. Syberg and T. E. Hickcox

Prepared by
THE BOEING COMPANY
Seattle, Wash. 98124
for Ames Research Center

NATIONAL AERONAUTICS AND SPACE ADMINISTRATION • WASHINGTON, D. C. • JANUARY 1973

1. Report No.	2. Government Accession No.	3. Recipient's Catalog No.
NASA CR 2187		

4. Title and Subtitle	5. Report Date
DESIGN OF A BLEED SYSTEM FOR A MACH 3.5 INLET	January 1973
	6. Performing Organization Code

7. Author(s)	8. Performing Organization Report No.
J. Syberg and T. E. Hickcox	D6-60168
	10. Work Unit No.

9. Performing Organization Name and Address	11. Contract or Grant No.
The Boeing Company P.O. Box 3707 Seattle, Washington 98124	NAS 2-6643
	13. Type of Report and Period Covered
12. Sponsoring Agency Name and Address	Contractor Report
National Aeronautics and Space Administration Washington, D.C., 20546	14. Sponsoring Agency Code

15. Supplementary Notes

16. Abstract

An analytical bleed system design procedure is applied to a Mach 3.5, axisymmetric, translating centerbody inlet. The design features a traveling centerbody bleed system with a ducting arrangement separating low-, medium-, and high-pressure bleed. Three forward plenums and nine throat plenums are installed on the centerbody to meet the bleed requirements in the started Mach range between 1.6 and 3.5. The cowl contains four stationary plenums, three for forward and one for throat bleed. To achieve maximum bleed plenum pressure and thereby minimize bleed drag all bleed holes are inclined 20° to the surface except in the cowl throat region. Here the requirement of high stability margin with minimum total pressure recovery penalty resulted in 90° bleed holes. The bleed hole diameter varies from bleed plenum to bleed plenum to achieve the most efficient boundary layer control, while the bleed exits are sized to operate at the highest possible plenum pressure without unchoking the bleed holes. Bleed flow rates, bleed plenum pressures, and boundary layer development along the cowl and centerbody are predicted over the entire started Mach range.

17. Key Words (Suggested by Author(s))		18. Distribution Statement
Inlets	Bleed holes	UNCLASSIFIED-UNLIMITED
Boundary layer	Analytic design procedure	
Bleed systems		
Supersonic		
Axisymmetric		

19. Security Classif. (of this report)	20. Security Classif. (of this page)	21. No. of Pages	22. Price*
Unclassified	Unclassified	88	$3.00

* For sale by the National Technical Information Service, Springfield, Virginia 22151

DESIGN OF A BLEED SYSTEM

FOR A MACH 3.5 INLET

By J. Syberg and T. E. Hickcox
The Boeing Company

SUMMARY

A bleed system has been designed for a Mach 3.5 inlet using analytical procedures which promise to save many wind tunnel testing hours. The design is based on a model size compatible with the existing NASA Ames 1/3-scale inlet model and on freestream conditions corresponding to those in the NASA Ames 8- by 7-ft supersonic wind tunnel.

This report first describes the analytical procedures and tools used in the bleed system design. The operating characteristics of the inlet are then presented in the form of surface pressures and boundary layer development without boundary layer control. The proposed bleed systems for centerbody and cowl are then described, along with the design considerations for Mach 3.5 and off-design conditions. Next, the boundary layer growth is predicted throughout the started Mach number range with the bleed system operating. Finally, possible problem areas are identified and the overall system is evaluated.

Application of the analytical design procedure indicated the need for a bleed system with unusual and complex features that would be unlikely to evolve from normal wind tunnel development testing. The centerbody has a "traveling" bleed system with a ducting arrangement separating low-, medium-, and high-pressure bleed regions. Three forward bleed plenums and nine throat plenums are included, with the novel feature that one forward plenum is located among the throat plenums to provide sufficient forward bleed at off-design Mach numbers. The cowl contains four stationary plenums, three for forward bleed and one for throat bleed. The exit areas for the various bleed plenums are sized to operate at the highest possible plenum pressures without unchoking the bleed holes. All centerbody bleed holes and the forward cowl bleed holes are inclined 20° to the surface, primarily to achieve maximum bleed plenum pressure and thereby minimize bleed drag. The cowl throat bleed holes are normal to the surface to maximize the normal shock stability margin. The bleed hole diameter varies from bleed plenum to bleed plenum to achieve the most efficient boundary layer control.

With the proposed system the bleed flow rate is 13.3% of the lip flow (0.133 W_L) at Mach 3.5, with 0.089 W_L forward bleed and 0.044 W_L throat bleed. Analysis indicates that this amount of forward bleed is near the minimum bleed rate required to achieve attached flow in the supersonic diffuser and provide a full boundary layer velocity profile in the throat ahead of the normal shock. Isentropic compressions and oblique shock wave reflections at off-design Mach numbers are in general well controlled. Boundary layer separation at oblique shock reflections is predicted at some off-design Mach numbers, but rapid reattachment is expected in all of these cases due to favorable downstream pressure gradients coupled with high bleed rates near these critical regions.

INTRODUCTION

The development of bleed systems for boundary layer control in supersonic inlets has in the past depended mainly on extensive wind tunnel tests. The tests were complex, time consuming, and did not always allow optimization of the system. An analytical procedure (ref. 1) has now been developed for the design of bleed systems based on theoretical analysis and extensive experimental data. Using the procedure allows analytic definition of a bleed system, which may then be optimized in the wind tunnel with less testing.

The present work applies this procedure to the design of a bleed system for a Mach 3.5 inlet with the objective of providing satisfactory operation across a wide range of "started" Mach numbers with adequate tolerance to transient disturbances in upstream Mach number and angle of incidence, and downstream corrected weight flow. The work included the design of internal cowl and centerbody contours, design of the bleed pattern, bleed hole geometry, bleed plenum arrangement, bleed flow ducting and exits, and the prediction of bleed system performance. The inlet and bleed system geometry is sized for an existing 1/3-scale supersonic inlet model (ref. 2) operating within the flow conditions available in the NASA Ames 8- by 7-ft supersonic wind tunnel. The present work was carried out under contract NAS 2-6643 (ref. 1).

Portions of the procedure and technology have been applied before (refs. 2 and 3), but never as an entire package. The present application of the procedure is the first time a completely analytical design of the bleed system has been done prior to model testing. As such, a thorough validation of the procedure is needed from wind tunnel tests of the 1/3-scale inlet.

SYMBOLS

A	area
A_H	bleed hole area
A_L	cowl lip projected area
A/A*	sonic area ratio
D	bleed hole diameter
gw	wall temperature recovery–wall temperature/freestream total temperature
H	boundary layer shape factor–δ^*/θ
L/D	aspect ratio of bleed hole–length/diameter
M	Mach number
M_L	local Mach number
N	boundary layer power law velocity profile exponent
P	pressure
Q	bleed hole mass flow coefficient–actual flow/ideal choked flow at same conditions
R	inlet radius
R_L	cowl lip radius
S	circumferential bleed hole spacing, Y/D
T	temperature
u	axial velocity component
W_L	theoretical freestream airflow through an area equal to the cowl lip area
W/W_L	nondimensionalized bleed flow rate
X/R_L	nondimensionalized axial coordinate
$\Delta X/R_L$	nondimensional forward translation of centerbody from Mach 3.5 position

Y	half of the circumferential center-to-center spacing between holes in one row of bleed holes
y	boundary layer coordinate normal to wall
α	bleed hole angle relative to surface
δ	boundary layer thickness
δ^*	boundary layer displacement thickness
ρ	density
θ	boundary layer momentum thickness

Subscripts

i	incompressible
PL	plenum
R	property derived from analysis of Reyhner
S	static
s,c	property derived from analysis of Sasman and Cresci
th	throat
TO, T_∞	freestream total
W	wall
∞	freestream
1	upstream side of oblique shock reflection or normal shock
2	downstream side of normal shock
3	downstream side of oblique shock reflection

APPROACH

Procedure

The first step in the bleed system design procedure for a new inlet contour is to determine a centerbody translation schedule versus freestream Mach number that will provide efficient internal compression as well as adequate tolerance against transient changes in Mach number and angle of incidence. These conflicting requirements can be met by maintaining the throat Mach number near 1.25 in the mixed-compression operating range.

Once the translation schedule has been established, the inviscid flowfield solutions are computed to determine the inlet operation for that schedule. These solutions are computed with a method of characteristics program at small Mach number increments (say, $\Delta M_\infty = 0.1$) over the started Mach number range. The surface static pressure distributions are plotted along with the characteristic network and shock pattern. A map of surface static pressure versus centerbody translation, or freestream Mach number, is made to facilitate selection of bleed bands in regions of high static pressure. (High surface static pressures allow high bleed plenum pressures and therefore low bleed drag.) The surface Mach number distributions from the inviscid flow solutions are used as input for the boundary layer calculations.

The boundary layer development along both the cowl and centerbody is then computed using a boundary layer computer program (ref. 4). The first solutions are computed without bleed at each Mach number for which an inviscid solution has been calculated. The program calculates boundary layer profile distortion parameters along the surfaces, which are mapped versus centerbody translation and freestream Mach number for both the centerbody and cowl. These maps are then used to identify regions of high profile distortion (i.e., regions where boundary layer separation is likely) and thus to determine bleed locations for optimum boundary layer control.

An additional consideration when locating bleed regions is that, due to the finite cowl lip bluntness and displacement effects of the boundary layer, shock reflections and pressure gradients move forward in the actual inlet as compared to the inviscid solution. Thus, if the boundary layer analysis indicates that bleed is required in a given pressure gradient or just ahead of a shock the bleed is moved slightly forward of the location that would be selected without considering these real flowfield effects.

Next, several alternate bleed configurations are studied at the design Mach number. For each of these configurations the boundary layer solutions are obtained with bleed included. Throat bleed is not included, since for the critical normal shock position essentially all boundary layer control upstream of the normal shock must come from forward bleed. On the basis of results obtained from these solutions, the design Mach number bleed system is modified to produce the lowest throat boundary layer distortion and displacement thickness at the lowest possible bleed rates subject to the aforementioned constraints on bleed location. Knowing the bleed locations and flow rates, the bleed areas can be calculated for the selected hole angles.

Throat bleed rates are selected on the basis of past experience. Basically, the throat bleed rate required for normal shock/boundary layer interaction control and good subsonic diffuser performance has been found to be a function of throat blockage. Thus, the throat bleed rate is chosen on the basis of throat blockage with the selected forward bleed.

Based on off-design requirements, an overall bleed system compatible with the design Mach number system selected above is planned. Using the surface pressure and boundary layer distortion maps, probable off-design problem areas are determined. Selected off-design cases are then run with various bleed configurations to cover the suspected problem areas. Results from these runs are used to modify and improve the system for off-design operation, with possible modifications to the design Mach number bleed system.

This last step completes the definition of the entire bleed system. At this point, on the basis of previously determined bleed geometry and local Mach number, the bleed rates and maximum plenum pressures are determined for any remaining range of operation. The boundary layer characteristics are then computed with these bleed rates at small Mach number increments. If these solutions identify any new problem areas not anticipated in the previously computed cases, modification of the bleed system is undertaken.

The viscous flow analysis does not account for bleed within a shock interaction. For this reason, numerical problems may be encountered when bleed occurs in or just ahead of a shock reflection. Since problems may result, and since it is known that cumulative viscous effects tend to move the shock forward in the real flowfield, if a shock reflection falls within a bleed region in an off-design case that region is generally moved downstream of the reflection for the analysis. If the bleed band is fairly wide it is split into two parts—one ahead of the shock and one aft.

As a check on the validity of the final bleed system design, the Combined Flowfield Analysis (ref. 5), an inviscid-viscous flowfield solution, is used to evaluate the viscous and bleed effects on the flowfield, in particular whether the bleed is properly positioned to control the pressure gradients and shock reflections. For this bleed system two checkout cases were run, the design Mach number case and a selected off-design case.

As a check on possible inlet restart problems, several inviscid restart cases are run to determine the flowfield with large centerbody extensions. These cases are examined to determine whether boundary layer separation problems exist which could cause the started inlet to unstart as the centerbody is retracted to design position.

Design Tools

As discussed above, the analytical procedure uses several design tools. These include two computer programs to calculate inviscid and viscous inlet flowfields.

The inviscid flow solutions are calculated using Boeing program TEM 137, the MOCHA (Method Of CHAracteristics) program, which will compute two-dimensional or axisymmetric, internal or external, rotational flowfields with multiple shocks. The complete solution of

intersection of like and opposite family shocks is included, as well as shock reflections; shocks or expansions from boundary corners; pressure boundaries with separation, reattachment, and intersections with shocks; the coalescence of Mach lines to form an embedded shock; and the capability to remove mass flow at a scoop.

The boundary layer (viscous) solutions are calculated using Boeing computer program TEM 139 (ref. 4). This program provides a finite-difference solution of the boundary layer equations. It computes laminar and turbulent boundary layer development on two-dimensional or axisymmetric surfaces with or without heat transfer. It will also compute regions of bleed or blowing. Oblique shock/boundary layer interactions are computed using a control volume analysis. Boundary layer transition may be specified as occurring at a given location or given momentum thickness Reynolds number.

The inviscid and viscous programs have been combined in a procedure called the Combined Flowfield Analysis to provide a prediction of the flowfield with viscous effects. This procedure accounts for cowl bluntness, boundary layer displacement thickness effects on the inviscid core flow, shock interactions, and bleed effects. As described in reference 5, this analysis provides a much improved prediction of the real flowfield as compared to a strictly inviscid solution.

An additional consideration, discussed in reference 5, is the fact that real bleed holes are less efficient at improving the boundary layer than theoretical ideal bleed. That is, bleed holes have some roughness which tends to counteract the effect of mass removal. To correct for this effect in the analysis a bleed efficiency, η, is assigned such that for the analysis of TEM 139 the bleed removed is the actual bleed multiplied by the efficiency.

An important requirement for the design of an effective and efficient bleed system is accurate data for the flow coefficients of bleed holes. A combination of Boeing and NACA data has been used to define these flow characteristics, as shown in figure 1. The data available are valid for limited ranges of bleed hole size, spacing, and length. In addition, the characteristics were obtained with a full boundary layer velocity profile upstream of the bleed holes. These limitations may result in inaccuracies in the bleed system design. To minimize the inaccuracies, the geometric variables will be chosen as close as possible to the available data.

Boundary Layer Distortion Parameters

The bleed system design procedure is based on maintaining limits on the boundary layer profile distortion in the supersonic diffuser to prevent large separations and to provide sufficient upstream control to keep the throat boundary layer profile close to a full profile. The parameters used to evaluate boundary layer distortion are discussed below.

In previous applications of the bleed system design procedure, a different boundary layer analysis was used. The program used, TEM 123, employed the method of Sasman and Cresci, which is an integral solution. The compressible flow problem is transformed to the incompressible plane where the integral solution is computed, then retransformed to the compressible plane. The integral solution in the incompressible plane uses a power law velocity profile,

and thus the incompressible power law exponent, N_i, (called $N_{i\text{-}s,c}$ here) was used as a measure of profile distortion. Since the present application of the design procedure uses a more accurate finite-difference compressible flow solution, TEM 139, the parameter $N_{i\text{-}s,c}$ is not readily available. Instead, a velocity distortion parameter based on the actual velocity profile as computed in TEM 139 is used. The following are standard definitions:

Displacement Thickness

$$\delta^* = \int_o^\delta \left(1-\frac{\rho u}{\rho_e u_e}\right) dy$$

$$\delta_i^* = \int_o^\delta \left(1-\frac{u}{u_e}\right) dy \qquad \text{(incompressible)}$$

Momentum Thickness

$$\theta = \int_o^\delta \frac{\rho u}{\rho_e u_e}\left(1-\frac{u}{u_e}\right) dy$$

$$\theta_i = \int_o^\delta \frac{u}{u_e}\left(1-\frac{u}{u_e}\right) dy \qquad \text{(incompressible)}$$

Shape Factor

$$H = \delta^*/\theta$$

$$H_i = \delta_i^*/\theta_i \qquad \text{(incompressible)}$$

The parameter H_i is defined simply by using the existing velocity profile and neglecting the density variation that is normally included in the shape factor. This parameter is then not a function of edge Mach number or wall temperature recovery, as is $N_{i\text{-}s,c}$, which may vary for a fixed velocity profile. Because H_i is based solely on the shape of the actual velocity profile and is independent of local Mach number and wall temperature recovery, it is felt that it is a better representation of actual boundary layer distortion than the previously used $N_{i\text{-}s,c}$. The shape factor H_i is therefore used as the primary distortion parameter in the bleed system design.

The computer program TEM 139 is a finite-difference method which requires no assumption as to the shape of the velocity profile. If, however, it is assumed that the velocity profiles computed with the finite-difference procedure can be well represented by a power law relationship

$$u/u_e = (y/\delta)^{1/N_{i\text{-}R}}$$

then the shape factor H_i can be used to define a boundary layer velocity profile exponent, $N_{i\text{-}R}$.

$$H_i = \frac{\int_0^{\delta} [1 - (u/u_e)]\, dy}{\int_0^{\delta} (u/u_e)\,[1 - (u/u_e)]\, dy}$$

$$= \frac{\int_0^{1} [1 - (y/\delta)^{1/N_{i\text{-}R}}]\, d(y/\delta)}{\int_0^{1} (y/\delta)^{1/N_{i\text{-}R}}\,[1 - (y/\delta)^{1/N_{i\text{-}R}}]\, d(y/\delta)}$$

$$= \frac{1/(1 + N_{i\text{-}R})}{N_{i\text{-}R}/[(1 + N_{i\text{-}R})(2 + N_{i\text{-}R})]}$$

or

$$N_{i\text{-}R} = 2/(H_i - 1)$$

This parameter is called N_i in this report and is used as the contract-specified boundary layer distortion parameter. The relationship between the three parameters, $N_{i\text{-}s,c}$, N_i, and H_i, is shown in figure 2. An H_i value above 1.8 corresponds to a highly distorted velocity profile, and the boundary layer program will usually indicate separation if H_i exceeds a value of about 2.0. A "full" profile, normally defined as $N_i = 7$, corresponds to $H_i = 1.28$.

As previously mentioned, the design procedure is based on maintaining limits on the distortion parameter in the supersonic diffuser and keeping the throat boundary layer profile close to a full profile. An upper limit of about 1.7 is used for H_i in the supersonic diffuser, except in the regions just downstream of oblique shock reflections. Higher H_i values can be tolerated in these regions because the profile deterioration from the shock pressure rise is usually followed by a rapid natural redevelopment to lower H_i values. The upstream boundary layer control is adjusted to also provide a reasonably full profile in the throat region. Experience has shown that this ensures a controllable normal shock/boundary layer interaction when the normal shock is within the operating range of the design point. The throat bleed is therefore only used for normal shock/boundary layer control and not for profile improvement upstream of the shock.

RESULTS

Inlet Description and Operating Characteristics Without Bleed

The Mach 3.5 inlet contours, for which a bleed system has been designed, are described in reference 6. The inlet has a 10° straight cone centerbody with a 1° positive cowl lip angle. The inlet contours and area progression with centerbody translation are shown in figure 3. The point-by-point contour definition and curve-fit type are provided in table 1.

Table 1.—Inlet Contour Definition

X/R_L	R/R_L	dR/dX	Curve fit type
		Centerbody	
0.0	0.0	0.17633	
			Straight line
4.0	0.70532	0.17633	
4.1	0.7228		Smoothed cubic spline
4.2	0.7387	0.144	
4.3	0.7512		Smoothed cubic spline
4.4	0.759	0.052	
4.5	0.7625		Smoothed cubic spline
4.55	0.763	0.0	
4.6	0.7625		Smoothed cubic spline
4.65	0.7611		
4.7	0.7585	-0.0646	
4.8	0.7504		Smoothed cubic spline
4.9	0.7391	-0.1295	
5.1	0.7120		Smoothed cubic spline
5.3	0.6829		
5.5	0.6525	-0.153	
5.6	0.6362		
5.7	0.618		
5.8	0.5973		Smoothed cubic spline
5.9	0.5744		
6.0	0.5467		
6.1	0.5093		
6.2	0.4564		
6.28	0.4	-0.794	
		Cowl	
2.86	1.0	0.01745	
			Straight line
3.1	1.004188	0.01745	
3.2	1.0054		Smoothed cubic spline
3.4	1.0051	-0.011	
3.6	0.99996		Smoothed cubic spline
3.8	0.9882		
4.0	0.9681	-0.124	
4.1	0.954		Smoothed cubic spline
4.2	0.9364	-0.1942	
4.25	0.9261		Smoothed cubic spline
4.3	0.9154	-0.213	
4.4	0.8949		Smoothed cubic spline
4.5	0.8768	-0.163	
4.55	0.8695		Smoothed cubic spline
4.6	0.864	-0.093	
4.65	0.86		Smoothed cubic spline
4.7	0.8572	-0.0485	
4.8	0.8533		Smoothed cubic spline
4.9	0.8511		
5.0	0.8502		
5.1	0.85	0.0	
			Straight line
5.6	0.85	0.0	
5.8	0.8574		
5.9	0.8646		Smoothed cubic spline
6.0	0.8735		
6.1	0.8839	0.107	
6.2	0.8946		Smoothed cubic spline
6.3	0.9050		
6.4	0.9145		
6.5	0.9227	0.0729	
6.6	0.9299		Smoothed cubic spline
6.7	0.9368		
6.8	0.9435		
6.9	0.95	0.065	

The translation schedule for the inlet was developed along with the contour, and is given in reference 6. Using this schedule, the MOCHA inviscid computer program was run for each $\Delta M_\infty = 0.1$ between Mach 3.5 and Mach 1.6. The results, in the form of surface static pressures, characteristic networks, and shock patterns, are presented in the appendix. It was found that there were two portions of the Mach number range in which a relatively strong oblique shock system produced subsonic flow (locally) ahead of the throat. These are between Mach 2.8-3.3 and Mach 1.7-2.0. A map of static pressure along the surface as a function of centerbody translation, or Mach number, is shown for the centerbody and cowl, respectively, in figures 4 and 5.

For each $\Delta M_\infty = 0.1$ between Mach 3.5 and Mach 1.6 the boundary layer was calculated without bleed using TEM 139. These predictions were made for the system sized for the 1/3-scale model ($R_L = 9.788$ in.) for testing in the NASA Ames 8- by 7-ft supersonic wind tunnel. Resulting maps of H_i and N_i along the centerbody and cowl surfaces are presented in figures 6 through 9. These indicate that, without bleed, separation occurs on the centerbody in the adverse pressure gradient between the first and second shock reflection between Mach 3.5 and Mach 3.2. Between Mach 3.2 and Mach 2.5, separation occurs at the second centerbody shock reflection. Between Mach 2.5 and Mach 2.2, separation occurs between the second and third centerbody shock reflections. Between Mach 2.2 and Mach 1.7, separation occurs at the third centerbody shock reflection, and at Mach 1.6 separation is predicted at the first centerbody shock reflection.

On the cowl, without bleed, separation is indicated at the first cowl shock reflection between Mach 3.5 and Mach 2.9. Between Mach 2.9 and Mach 2.7, separation occurs at the second cowl shock reflection. Between Mach 2.7 and Mach 1.7, the solution does not separate upstream of the throat. At Mach 1.6 separation is predicted at the first cowl shock reflection.

Six summary maps of surface properties are, at this point, available for use in design of the bleed system. Figures 4 and 5 provide surface static pressure on centerbody and cowl respectively, while figures 6, 7, 8, and 9 provide boundary layer H_i along centerbody and cowl, and boundary layer N_i along centerbody and cowl, respectively. The static pressure maps are used primarily to position bleed bands, taking advantage of the highest possible surface pressure in a given region where bleed is required. The maps are also used in the initial planning of the overall system as they define regions of strong adverse pressure gradient and high-pressure-ratio shock reflections. The boundary layer distortion maps, primarily the H_i maps, are used to determine bleed location. Bleed must obviously be placed ahead of all separations to provide profile improvement. In regions of adverse boundary layer development leading to separation, bleed must be placed ahead of any steep rise in H_i and must be used to produce levels of H_i acceptably below separation in the regions of adverse development behind the bleed. For cases of separation at shock reflections, bleed must be provided upstream of the shock reflection and must be distributed to provide an improved profile going into the interaction.

Those separations that occur at a shock reflection may be caused by either a distorted boundary layer profile (high H_i) or high shock strength, or a combination of these. Bleed is used to control the boundary layer profile distortion, while shock strength can only be controlled by inlet contour modifications.

When separation is predicted at a shock reflection, no prediction is made as to the size of that separation. The separation could be a small one completely contained within the shock interaction, or it could be a massive separation. Therefore, shocks that are strong enough to always produce a separation within the interaction regardless of upstream boundary layer shape stop computation by TEM 139.

A shock may be strong enough to always produce some separation, even with a full boundary layer profile upstream. A criterion for defining the shock strength which produces separation with a full upstream profile has been developed in reference 7. Roughly, this criterion is that when the numerical value of shock reflection static pressure ratio becomes larger than the numerical value of the upstream Mach number, separation is likely. Figures 10 and 11 present the upstream Mach number and static pressure ratio versus freestream Mach number on the centerbody and cowl, respectively, for the shock reflections at which separation occurs at some Mach numbers. From this plot and the reference 7 separation criterion, it becomes obvious why some of the separations for the no-bleed cases occur. The shock reflections are so strong at some Mach numbers that the boundary layer will separate with a full upstream profile. Consequently, there may be regions in which it is not possible to get an attached solution at a shock reflection, even with the addition of upstream bleed. At Mach 1.6 both the cowl and centerbody show separation at the first shock reflection. Since these separations are so far forward and occur at this low Mach number where "started" operation may not be required, the design of the bleed system will not account for them.

The relatively strong shocks encountered are a result of the inlet contours. They are caused when one of the cowl shock reflections passes near the maximum second derivative of the contour on the cowl. Figure 12 shows the cowl shock positions with the maximum second derivative location. The rises in pressure in figures 10 and 11 may be seen to be centered about the Mach number at which one of the shocks crosses the point of maximum second derivative. This region of maximum rate of change of surface slope on the cowl is the region of maximum rate of compression of the cowl, and thus the origin of a strong compression. When a cowl shock reflection occurs near this region, the cowl compression coalesces with and strengthens the shock system, providing the high strength shock reflections noted.

Bleed Hole Geometry Requirements

The inlet operating characteristics without bleed define some requirements important in selection of bleed hole geometry. Of particular interest are the problems encountered on the centerbody at off-design conditions. These problems would seem to indicate that the forward bleed on the centerbody must remain high across the off-design range to control the high-pressure-ratio shock interactions that occur. Furthermore, it seems obvious that, to achieve adequate boundary layer control with reasonably low bleed rates throughout the operating range, great care must be taken to select a bleed hole geometry that will under all conditions be efficient at improving the boundary layer profile. The selection of bleed hole geometries meeting these requirements is discussed below.

Selection of bleed holes involved the choice of hole angle relative to the surface (α in fig. 1), hole size, and hole spacing—both circumferential and axial. To avoid problems of

recirculations within bleed plenums, and to minimize bleed area, and therefore surface roughness, it was decided to use choked bleed holes for all cases. A summary of bleed hole characteristics from figure 1 for choked bleed holes is presented in figure 13. These curves were determined as the "knee" of the bleed hole mass flow characteristics from figure 1, where the holes unchoke and Q falls rapidly with increasing plenum pressure. Both choked bleed hole mass flow coefficient and maximum allowable bleed plenum pressure for choked holes are shown versus local Mach number in figure 13. This plot shows that the lowest angle holes have the highest mass flow coefficients and the highest maximum plenum pressure. Since bleed plenum pressure is highest, for a given amount of bleed removal the lowest angle hole will produce lowest bleed drag. Also, since the mass flow coefficient is highest at a given Mach number, the lowest bleed area will be required to remove a given amount of mass flow.

Figure 14 shows the effect of varying surface Mach number on 20°, 40°, and 90° holes sized to bleed 0.010 W_L at a local Mach number of 1.0, i.e., a typical throat condition. This figure shows that if these holes move into a region of high Mach number the 20° holes will remove considerably more bleed than the steeper holes. However, if the holes move into a lower Mach number region the 90° holes provide the greatest increase in bleed. These two characteristics are extremely important in selecting bleed hole angle. Since the centerbody translates forward off-design, the throat bleed holes sized for a low local Mach number region, at the design point, become forward bleed holes in a high local Mach number environment. To avoid rapid decreases in forward bleed rate, low-angle holes for throat bleed would seem to be a logical choice. However, considering the case of throat bleed holes operating with the normal shock aft, then moving forward across the holes, the 90° holes have the greatest increase in bleed rate with the accompanying decrease in Mach number. This means they produce greater normal shock stability margin than lower angle holes.

It is obviously desirable to minimize bleed drag. Furthermore, forward bleed cannot be allowed to drop drastically on the centerbody at off-design conditions. For these reasons 20° holes will be used everywhere on the centerbody and for the forward bleed regions on the cowl. The cowl throat bleed will use 90° holes to take advantage of the increase in normal shock stability, since these holes will not operate in a high Mach number region.

The bleed hole characteristics used in the design of the bleed system are valid for $\delta^*/D = 1.0$, as indicated in figure 1. Experience with previous supersonic inlets (refs. 2 and 3), has indicated that these relatively small bleed holes are very efficient, i.e., the roughness created by the holes and the removal of boundary layer flow is small. It is also known that the hole characteristics change with δ^*/D. To reduce inaccuracies in the bleed flow predictions while maintaining an efficient bleed system, the holes will be sized to give δ^*/D near 1.0 if possible.

Circumferential bleed hole spacing is defined in figure 15. This is the spacing which determines what percentage of the circumference is actually bled in a given bleed band. The philosophy used in the bleed system design is to bleed the entire circumference in each bleed band. Mixing between bled and unbled regions, with its attendant total pressure loss, will not be relied on for boundary layer profile improvement. Therefore, a spacing as close as possible to $S = 1.0$ will be used. It is felt that the use of significantly wider spacing, $S > 1.0$, and the reliance on mixing between bled and unbled regions, will produce a less efficient bleed system

than one with a fully bled circumference. To achieve the fully bled circumference the pattern used will always be a pair or pairs of rows with staggered holes, with S = 1.0.

The criteria for selecting axial spacing between rows in a bleed band are not well established. Obviously, the minimum spacing will be determined by structural considerations. If the holes are very widely separated, considerable mixing will take place between rows. Since the concept of bleed hole selection does not rely on mixing, it would seem that very large spacing is not desirable. As a result, for 20° holes a center-to-center axial spacing of three to five hole diameters will be used, and for 90° holes a center-to-center spacing of about two hole diameters will be used.

The aforementioned criteria for selecting hole angle, hole size, and hole spacing will result in selection of bleed bands that are relatively efficient in improving the boundary layer profile. Analyses of test results from previous test programs (refs. 2, 3 and 5), indicate that an efficiency, η, of 0.80 can be used as a good approximation for the boundary layer analysis in TEM 139.

A major problem encountered in the selection of bleed holes for a Mach 3.5 inlet is the high bleed rate per hole of a given diameter. Figure 15 illustrates this problem by comparing a Mach 3.5 and a Mach 2.65 inlet for identical circumferential bleed hole spacings. The Mach 3.5 inlet has considerably higher bleed for a given bleed band (same hole diameter, spacing, and local flow condition) than the Mach 2.65 inlet, due to the greater increase in mass flow per unit area from freestream to the given local condition.. The result is that conflicts in desired bleed hole size and spacing to achieve the correct bleed hole area will arise much more often in the high Mach number inlet. The minimum effect of the problem will be that fewer rows of bleed holes may be used in a given band to achieve a given bleed rate in the higher Mach number inlet. This means that for the higher Mach number inlet, less flexibility in terms of small changes in bleed flow rates is available on a model test. Therefore the analytical bleed system design must be very accurate, as model changes for "fine tuning" are limited.

Centerbody Bleed System

A traveling centerbody bleed system featuring three forward bleed plenums and nine throat plenums on the centerbody coupled with a "triple" slot arrangement on the support tube was designed after a detailed study of the bleed requirements at Mach 3.5 and selected off-design Mach numbers. A schematic of the final system is shown in figure 16, where the centerbody slider and the support tube are unfolded to show the arrangement of the windows in the slider and the three circumferentially separated support tube slots. The centerbody is shown in the Mach 3.5 position, i.e., $\Delta X/R_L = 0$. At Mach 3.5, the bleed from the first forward plenum, F1, enters the support tube through slot S1 into duct D1. This duct is separated from duct D2, which is connected to plenum F2 through slot S2. The throat bleed is likewise separated from the forward bleed in duct D3, which at Mach 3.5 is connected to plenums T1 and T2 via slot S3. As the centerbody translates forward for off-design operation the slider windows move across the respective slots on the stationary support tube thus providing a traveling bleed system. The bleed schedule for the selected centerbody bleed system is superimposed on the static pressure map and the H_1 map in figures 17 and 18, respectively. The individual bleed requirements which led to this system are discussed in detail below.

Forward bleed at Mach 3.5.—A number of centerbody bleed configurations were examined by means of the boundary layer program to define the minimum bleed requirements at Mach 3.5 for the supersonic diffuser. Figure 19 shows the variation of δ^* and H_i along the centerbody surface for three of the best bleed configurations. Without bleed the boundary layer program predicts separation at station 4.37. A small amount of bleed upstream of the point of separation keeps the boundary layer attached through the adverse pressure gradient which ends at station 4.47 (see appendix, fig. 37). However, a relatively large amount of bleed is required in the favorable pressure gradient upstream of the second shock to keep the boundary layer attached through the reflection region. With a bleed rate of 0.0050 W_L in the front bleed region, F1, a minimum of 0.0350 W_L bleed is required in the second region, F2. With 0.0100 W_L in F1, the second shock reflection can be controlled with 0.0300 W_L in F2. The second combination appears to provide better boundary layer control in the supersonic diffuser, resulting in a thinner boundary layer in the throat. The form parameter H_i remains below about 1.7 in the supersonic diffuser, except in the redevelopment regions downstream of the two oblique shock reflections, and the throat profile is nearly full ensuring a controllable normal shock/boundary layer interaction. This centerbody bleed configuration was therefore selected for Mach 3.5.

Throat bleed at Mach 3.5.—The normal shock in a mixed-compression supersonic inlet must be operated in such a way that started operation can be maintained during small downstream flow disturbances. A stability margin of 5% of the corrected engine flow is generally considered sufficient. To accommodate an increase in corrected engine flow, the normal shock will move downstream of the operating position, reducing the recovery due to the higher normal shock losses, and thereby provide the desired increase in corrected flow supply to the engine. Correspondingly, a decrease in corrected engine flow will move the shock forward toward the throat, increasing the recovery and reducing the corrected flow supply to the engine. As the normal shock moves forward, the surface pressure in the throat region increases, and as a result the bleed flow through any bleed band located in this area increases. The corrected engine flow is thus reduced partly by an increase in recovery and partly by an increase in bleed flow. To optimize the inlet performance at the operating point, and provide the required stability margin, it is desirable to design the throat bleed system such that a significant change in bleed flow rate occurs when the normal shock moves from just downstream of the critical position to the critical position, i.e., the aerodynamic throat. As demonstrated in reference 3, this change in bleed flow rate can be achieved by means of an auxiliary normal shock stability system (vortex valves) with negligible recovery penalty at the operating point. However, this system incorporates a throat slot in the cowl, which complicates the flowfield in the throat region. To give a clear picture of the effectiveness of the forward bleed system for a future wind tunnel test program, only bleed holes are recommended in the throat region.

The recommended location of the centerbody throat bleed at Mach 3.5 is indicated in figure 17. The first throat plenum, T1, is located ahead of the geometric throat; the second, T2, just downstream of the throat station. The normal shock at the operating point, i.e., the 5% stability margin point, is expected to be situated on the bleed band in T2. At critical operation the normal shock will be located in front of the geometric throat due to the removal of flow from the inlet surfaces, which tends to move the aerodynamic throat forward. It is estimated that the critical normal shock will pressurize the bleed band in T1 such that this

bleed region both controls the critical normal shock/boundary layer interaction and increases the stability margin due to the significant change in local flow condition from the operating point to the critical point.

As described under "Bleed Hole Geometry Requirements," it is advantageous to use 90° rather than slanted bleed holes in the throat region because of the larger change in flow coefficient with local Mach number. However, the Mach 3.5 throat plenums act as forward plenums at some off-design Mach numbers (see fig. 17) and therefore are also required to provide good boundary layer control in a high supersonic Mach number environment. This requirement calls for slanted bleed holes, as shown in figure 14. Consequently, a hole inclination of 20° to the surface was selected for the Mach 3.5 throat plenums.

The next step in the centerbody bleed system design was to determine the amount of throat bleed needed at Mach 3.5. The throat blockage at Mach 3.5 with the selected forward centerbody and cowl bleed configurations is about 6% of the throat area. Experimental data on two Mach 2.65 inlets (refs. 2 and 3), indicate that good normal shock/boundary layer control was obtained with a total throat bleed rate of about 0.020 W_L (cowl and centerbody). In both of these inlets the throat blockage was estimated to be about 3% of the throat area. The blockage in the Mach 3.5 inlet is approximately twice as high as in the Mach 2.65 inlets. The bleed rate required to achieve comparable normal shock/boundary layer control and subsonic diffuser performance is, therefore, probably in the order of 0.040 W_L. The centerbody throat bleed holes should thus be sized to provide approximately 0.020 W_L bleed at Mach 3.5.

Bleed at off-design Mach numbers.—An indication of the centerbody bleed requirements at off-design Mach numbers is obtained from figures 6 and 10. Without bleed the boundary layer separates in front of the throat at all Mach numbers, and control must be provided upstream of the point of separation. Oblique shocks with pressure ratios greater than the numerical values of the upstream Mach numbers occur in the Mach ranges 1.8 to 2.1 and 2.7 to 3.3, indicating the need for very effective boundary layer control at the centerbody positions corresponding to these Mach ranges.

A detailed investigation was carried out at selected off-design Mach numbers to more accurately define the bleed requirements at the worst cases for which MOCHA provided a solution past the throat. A series of bleed configurations were run in TEM 139 at Mach 2.0, 2.8, and 3.3. In all cases the oblique shock (third reflection at Mach 2.0 and 2.8, second reflection at Mach 3.3) separates the boundary layer even when very square profiles (for example $H_i = 1.2$, $N_i = 10$) have been produced just upstream of the shock reflection by means of very high bleed rates.

It is apparently not possible to maintain fully attached shock reflections throughout the Mach range, primarily because of the high-pressure-ratio shock systems occurring when the first or second cowl shock sweeps across the region of maximum increase in cowl slope at station 4.20 (see fig. 12). However, the requirement of attached shock reflections is probably too conservative in these cases, especially because the shocks always are followed by a favorable pressure gradient (see appendix, figs. 39 through 45 and 51 through 54). Reattachment will probably occur just downstream of the shock in the favorable gradient, or the separation

may even be confined to the shock/boundary layer interaction with negligible effect on the inlet performance. Existing bleed design technology does not include an analysis of boundary layer separation and reattachment. The bleed rates required in front of these shock interactions to achieve high inlet performance can presently only be estimated on the basis of experience with similar conditions in other supersonic inlets.

To reduce the possibility of off-design performance problems in this inlet, it is necessary to design the centerbody bleed system in such a way that high bleed rates are provided in front of the relatively strong shock interactions. However, this requirement must be met without compromising the bleed configuration selected for Mach 3.5. An important requirement at Mach 3.5 is to separate the two forward bleed regions, F1 and F2, so that each plenum can be operated at the highest possible plenum pressure to reduce the bleed drag. A number of plenum and support tube slot arrangements were studied, including systems similar to those designed for the two Mach 2.65 inlets described in references 2 and 3. The "triple" slot arrangement shown in figure 16 was chosen primarily because it allows full use of the large bleed area in plenum F2 for control of the second shock reflection in the Mach range of 2.7 to 3.5, as shown in figure 17. The Mach 3.5 configuration is thus compatible with the off-design bleed requirements.

The selection of the number of throat plenums and the bleed hole areas in the individual plenums are based on maintaining high throat bleed rates at off-design conditions, using the full capacity of the forward bleed system in the Mach ranges with relatively strong shock reflections, and minimizing the surface roughness from the inactive throat bleed holes at Mach 3.5. As shown in figures 16 and 17, a third forward plenum, F3, is installed between throat plenums T5 and T6 to provide additional bleed in front of the third centerbody shock in the Mach range of 1.7 to 2.1. This plenum does not communicate with the throat duct, D3, and is only active when located over support tube slot S2 (see fig. 16).

Because of the high bleed flow rate required in plenum F2 at Mach 3.5, 50% of the support tube duct area is assigned to duct D2. The other half of the support tube flow area is split evenly between the other forward bleed duct, D1, and the throat bleed duct, D3 (see fig. 16). The flow capacities of these ducts are discussed later. As the centerbody translates forward, the various throat plenums slide across the two forward bleed slots, S1 and S2. The windows in the throat plenums are arranged such that some of the plenums will bleed into duct D1 during part of the translation while other plenums communicate with duct D2 (see fig. 17). Since duct D2 has the larger flow area, more plenums can use this flow channel simultaneously without unchoking any of the bleed holes.

Bleed geometry and flow rates.—The bleed hole areas for the Mach 3.5 bleed configuration, i.e., F1, F2, T1, and T2, were defined based on the Mach 3.5 bleed requirements. To minimize potential off-design performance problems the bleed areas in plenums T3 through T9 and F3 were sized to make full use of the flow capacity of the three separate duct systems in the support tube. The recommended bleed hole configurations, including hole size, hole area, and hole spacing, are listed in table 2. A unique feature of this system is the variation in bleed hole diameter from bleed band to bleed band along the centerbody. This was done to achieve the desired bleed hole areas and maintain a hole spacing close to S = 1.0 in each bleed band. Another requirement affecting the selection of the bleed hole diameter was to keep the

Table 2.—Centerbody Bleed Holes

Bleed band station	Plenum number	Hole diameter, in.	Number of holes/row	Number of rows	Row station	Hole area, A_H/A_L	Spacing, S = Y/D
4.27-4.32	F1	0.060	388	2	4.280 4.304	0.00729	0.99
4.45-4.54	F2	0.050	481	4	4.455 4.480 4.505 4.530	0.01255	0.98
4.62-4.64	T1	0.026	900	2	4.625 4.635	0.00318	1.00
4.72-4.74	T2	0.026	900	2	4.725 4.735	0.00318	0.99
4.87-4.90	T3	0.036	624	2	4.875 4.890	0.00422	1.01
5.02-5.05	T4	0.036	624	2	5.025 5.040	0.00422	0.99
5.17-5.20	T5	0.040	530	2	5.177 5.193	0.00443	1.02
5.26-5.31	F3	0.040	530	4	5.264 5.276 5.288 5.300	0.00885	0.99
5.35-5.39	T6	0.050	406	2	5.360 5.380	0.00530	1.02
5.47-5.51	T7	0.050	406	2	5.480 5.500	0.00530	0.99
5.61-5.66	T8	0.060	308	2	5.620 5.645	0.00579	1.05
5.76-5.81	T9	0.060	308	2	5.770 5.795	0.00579	1.01

hole diameter in the same order of magnitude as the upstream boundary layer displacement thickness. A comparison of the hole sizes listed in table 2 with the displacement thickness for the selected Mach 3.5 configuration (0.010 W_L in F1, 0.030 W_L in F2) in figure 19 shows that this requirement is closely met for the two forward plenums and the throat plenums at Mach 3.5. The matching between D and δ^* at off-design conditions is discussed later.

The bleed rates through the individual plenums were calculated at each $\Delta M_\infty = 0.10$ to determine the total bleed rate and the maximum allowable plenum pressure for choked bleed holes for each of the three duct systems. The results for the two forward bleed ducts, D1 and D2, are shown in figures 20 and 21. The estimated actual bleed rates and plenum pressures are shown, together with the maximum flow capacity of the bleed duct exits in the 1/3-scale inlet model. (The total bleed exit flow capacity on this model is approximately 70% of the flow capacity in the support tube ducts). In duct D1 the exit capacity is well utilized at the low Mach numbers. Approximately 80% of the capacity appears to be required to maintain choked bleed holes at all Mach numbers. In duct D2 the choked bleed flow rate exceeds the maximum exit capacity near Mach 2.7 by a small amount. However, the increase in plenum pressure needed to allow all of the choked bleed hole flow to pass through the exit is relatively small, so that the resultant unchoking of some of the bleed holes is negligible. Note that to maintain choked bleed holes at all off-design Mach numbers the exit areas for both ducts must be set so that the Mach 3.5 plenum pressures are much lower than the maximum allowable plenum pressures. The resultant bleed drag penalty will be discussed later.

The estimated throat bleed rate versus Mach number for the design centerbody translation schedule is shown in figure 22. Again, the off-design requirements result in inefficient operation at Mach 3.5, i.e., the throat plenum pressure is lower than required for choking the holes. The calculations of the flow rates are based on a local Mach number of 1.2 at the throat bleed bands. This is believed to be a representative average local Mach number for the normal shock at the operating point. The corresponding maximum plenum pressure obtained from figure 13 is 0.30 P_{TO}. Notice on figure 1, however, that the bleed reduction is relatively small for plenum pressures up to 0.40 P_{TO}. The indicated bleed hole unchoking between Mach 2.1 and 2.8 is therefore small and the bleed rates and plenum pressures should be only slightly less than the levels shown in figure 22. The desired throat bleed rate at Mach 3.5 was found to be 0.020 W_L based on the relative throat blockage. For a bleed hole spacing of 1.0 the hole diameter providing the required hole area is 0.022 in. As shown in table 2, a hole diameter of 0.026 in. was chosen, increasing the Mach 3.5 throat bleed rate (through T1 and T2) to 0.024 W_L, so that higher bleed flow rate is available to control the high-pressure-ratio second centerbody shock reflection in the Mach range of 2.8 to 3.3 (where the Mach 3.5 throat plenums, T1 and T2, act as forward bleed plenums, see figs. 17 and 18).

The above comparisons of bleed hole flow rates and bleed system capacity for the 1/3-scale inlet model are based on zero pressure loss between bleed plenums and bleed exits. Some pressure losses will occur from the bleed plenums through the slots to the support tube, in the turning from the support tube to the support tube struts, and in the strut channels leading to the exit. The losses will reduce the bleed capacity for a given bleed plenum pressure and thus increase the Mach range in which bleed hole unchoking occurs. However, the bleed exit flow capacities on the 1/3-scale model can be increased to compensate for these losses, if required, by improved flow ducting near the bleed exits.

Cowl Bleed System

The design of the cowl bleed system is considerably different from that of the centerbody system. A "traveling" system is not necessary, as the supersonic diffuser always occupies essentially the same portion of the cowl contour.

The cowl bleed system is illustrated in figure 23. Four plenums are used, each with its own bleed plenum exit. The first three plenums provide forward bleed removal, and the fourth acts as throat bleed. The cowl bleed bands are shown superimposed on the inviscid pressure map and the no-bleed H_i map in figures 24 and 25, respectively.

Forward bleed.—Since the same forward bleed system that operates at Mach 3.5 will operate across the entire Mach number range, off-design operating conditions must be considered in the design of the system. Examination of the cowl boundary layer distortion maps without bleed, figures 7 and 9, shows that the first cowl shock reflection separates without bleed between Mach 3.5 and 2.9. Forward bleed will be required to control this interaction and provide a boundary layer prediction downstream. This bleed must be positioned to remain ahead of the first cowl shock reflection when viscous effects are included at the lowest Mach number at which separation is predicted. This consideration, together with the existing 1/3-scale model hardware, resulted in positioning the first bleed band (plenum zero) as shown in figures 23, 24, and 25. This bleed plenum is located so far forward to control the low Mach number cases that it will have limited effect for the higher Mach number conditions. The bleed flow rate was therefore selected as the minimum to provide an attached solution only at the lower end of the affected Mach range when other forward bleed would be behind the shock reflection. This gave a bleed rate of 0.003 W_L at Mach 3.5.

This plenum alone would not adequately control the first cowl shock reflection at Mach 3.5. Additional bleed is required just ahead of the first shock reflection, and ahead of the second shock reflection. Figure 26 gives the results of four bleed configurations which provide attached flow all the way to the throat at Mach 3.5. These all include forward plenum zero. The minimum bleed configuration requires a bleed rate of 0.010 W_L just ahead of the first shock (plenum one) and 0.025 W_L ahead of the second shock (plenum two). This configuration would work quite well at Mach 3.5, but would not provide control over an adequate off-design range of Mach number or angle of incidence. Analysis of off-design Mach number cases and previous experience with similar inlets at angle of incidence has shown that the first shock would move ahead of the bleed band used to control it at these off-design conditions, leading to probable separation. To maintain attached flow over an acceptably wide range of off-design Mach numbers and angles of attack, the bleed band ahead of the first shock was moved forward. The result was that for the same bleed rate in this plenum, 0.010 W_L, the boundary layer distortion behind the first shock reflection increased considerably and more bleed, 0.030 W_L, was required ahead of the second shock reflection. The bleed ahead of the first shock was then increased to 0.015 W_L at the same station. This resulted in decreased δ^* and slightly lower H_i behind the first shock. In addition, the bleed ahead of the second shock was reduced to 0.025 W_L, with the result that total forward bleed was the same. Both of these configurations had considerably higher H_i behind the first shock reflection than the first configuration.

This work then showed that moving the bleed forward to obtain a wider operating range decreased its effectiveness in improving the boundary layer at Mach 3.5. As a result, the bleed ahead of the first shock was split into two bands, both in forward plenum one. Moving a portion aft while maintaining a bleed rate of 0.015 W_L should produce more effective bleed, decreasing δ^* and H_i downstream of the first cowl shock reflection. This also allows the front band to be positioned far forward to stay ahead of the first cowl shock reflection over a wide range of Mach numbers and angles of attack, while positioning the second band closer to the shock at Mach 3.5. In addition, a bleed rate of 0.03 W_L was used in forward plenum two to improve the control of the second shock reflection. The results at Mach 3.5, shown in figure 26, show better control of the first shock reflection with decreased downstream H_i with this configuration. Better control also results at the second shock reflection, with lower downstream H_i and lower H_i at the throat. In addition the throat blockage with this system is significantly less than with the other systems evaluated, due to the thinner boundary layer displacement thickness (see fig. 26). As figure 26 shows, this system provides bleed ahead of indicated regions of separation in the off-design range, which should result in good off-design performance.

Throat bleed.—As discussed in the "Bleed Hole Geometry Requirements" section, 90° holes were chosen for the cowl throat bleed because of the advantage they offer in increased normal shock stability margin over slanted holes. As discussed in the "Centerbody Bleed System" section, the Mach 3.5 supercritical bleed rate based on the blockage should be 0.02 W_L. The cowl throat bleed band (plenum three) is positioned at the Mach 3.5 throat location opposite the centerbody throat bleed to provide normal shock/boundary layer interaction control and maximum stability margin at the design Mach number. As a result of the inlet throat moving forward as the centerbody is translated forward from the design position, this bleed band is aft of the throat for all but small translations. This may be seen in figure 25. As translation increases, the geometric throat moves into the bleed band of forward plenum two. As a result, this forward bleed band will, in conjunction with plenum three, provide throat and normal shock control at off-design conditions.

Bleed geometry.—Table 3 provides a description of bleed hole diameter, location, and spacing. Comparing the hole diameter to the displacement thickness, shown in figure 26, shows that δ^*/D remains near 1.0 at Mach 3.5 in plenums one, two, and three. Because of the very small bleed rate in plenum zero and the advantage of using choked holes to prevent any problems of recirculation, the diameter of the holes in this plenum is on the order of $D = 0.6\ \delta^*$. This is felt to be acceptable since the bleed rate is quite small. With these hole sizes the circumferential bleed hole spacing in all plenums is maintained very close to $S = 1.0$. Thus, in each plenum the entire circumference of the inlet is bled, and mixing within the boundary layer does not have to be relied on for profile improvement.

Overall Bleed System Performance

The work described in the previous sections represents the most complete design and analysis of a supersonic inlet bleed system prior to the first model test. The analysis predicts the performance of the system as well as areas where problems may be encountered. Wind tunnel testing can then be planned so that final system definition is obtained much more efficiently.

Table 3.—Cowl Bleed Holes

Bleed band station	Plenum number	Hole diameter, in.	Number of holes/row	Number of rows	Row station	Hole area, A_H/A_L	Spacing, S = Y/D
3.83-3.85	0	0.026	1165	2	3.835 3.845	0.00411	1.00
4.21-4.24	1	0.040	709	4	4.217 4.233 4.317 4.333	0.00592	1.01
4.31-4.34						0.00592	0.99
4.515-4.585	2	0.036	743	4	4.523 4.541 4.559 4.577	0.01005	1.00
4.66-4.74	3	0.030	880	6	4.665 4.670 4.695 4.700 4.725 4.730	0.01240	1.00

An illustration of the proposed bleed system bleed hole pattern is shown approximately to scale on the inlet contours in figure 27. The bleed rates predicted for this system are shown across the started operating Mach number range in figure 28. This figure illustrates that relatively high forward bleed rates are maintained at off-design conditions to control the high-pressure-ratio shock system.

The proposed bleed system as described was investigated with the boundary layer analysis throughout the started Mach number range. As discussed previously, only forward bleed has been included in the analysis. The results of the analysis, in the form of centerbody and cowl H_i and δ^* maps, are shown in figures 29 through 32. Figure 29 presents a map of boundary layer H_i on the centerbody with the proposed bleed system.

The centerbody boundary layer is predicted to separate upstream of the throat at several Mach numbers at the relatively strong second or third centerbody shock reflections. As mentioned earlier, the third shock reflection also produces subsonic flow in the reflection for Mach 2.9 and Mach 2.0 to 1.8. These separations are expected to be small, contained within the shock/boundary layer interaction, or reattaching very quickly with rapid boundary layer redevelopment, particularly since for all these cases the bleed system provides for upstream profiles which generally have low H_i, indicating a "full" profile. Additionally, the solutions are generally close to the throat before separation is encountered. Thus it is expected that these problems will result in little or no degradation of inlet performance.

Figure 29 also shows that there are no regions of excessive profile distortion, high H_i, except behind oblique shock reflections. It may be seen that rapid boundary layer redevelopment occurs in these regions, and H_i returns to acceptable levels quite rapidly.

The results for the cowl bleed system are presented in the form of an H_i map in figure 30. The solution stops with a prediction of separation at the relatively strong second cowl shock reflection between Mach 3.4 and 2.8. Since the upstream H_i is quite low over this entire range the separations are expected to be small with rapid redevelopment or be contained within the shock/boundary layer interaction. In addition, the shock reflection is close to the throat, and thus subject to throat bleed control. As a result, little or no degradation of inlet performance is expected. Over the remainder of the started Mach number range, except at Mach 1.6, the solution extends past the cowl throat. The only regions of high H_i are behind shock reflections, and these redevelop rapidly to acceptably low values. The throat profiles are quite good, with low H_i throughout this Mach number range and are probably also satisfactory between Mach 2.8 and 3.4. Near Mach 3.5 the second cowl shock reflection is just ahead of the throat, with resulting high H_i values. Figure 30 illustrates that the downstream redevelopment is rapid in this Mach number range. In the actual inlet this shock reflection will be moved forward somewhat due to cumulative viscous effects. This greater length for redevelopment will improve the throat boundary layer H_i. Additionally, cowl throat bleed will be active in this region to provide profile improvement. Because of these effects, no problems on the cowl throat are expected.

Both the centerbody and cowl show separation at the first shock reflection at Mach 1.6 as shown in figures 29 and 30. This was predicted in the boundary layer analysis without bleed, as previously discussed, but the bleed system was not altered to account for it. If it is found in testing that these separations are significant, it is recommended that the started Mach number range be selected beginning at Mach 1.7.

Maps of displacement thickness, δ^*, on the centerbody and cowl obtained with the recommended bleed system are shown in figures 31 and 32, respectively. It may be seen by comparing δ^* with the bleed hole sizes listed in tables 2 and 3 that at Mach 3.5 the design requirement of $\delta^*/D = 1.0$ is met. However, at off-design conditions the match between δ^* and hole diameter is not always as good. This is particularly true in some regions on the centerbody, and to a lesser degree on the cowl. In those ranges where the hole size is considerably smaller than the displacement thickness, the actual bleed rates are expected to be smaller than the predicted bleed rates. This trend was demonstrated in reference 3.

The bleed exit areas for the proposed bleed system are presented in table 4. These exit areas are sized on the basis of zero pressure loss from the bleed plenum to exit, and would have to be somewhat larger on a model to account for duct pressure losses. This is primarily a consideration in sizing the centerbody bleed exits. Table 4 presents two sets of exit areas, one sized strictly for the Mach 3.5 case without regard for off-design bleed requirements, the other sized to keep the bleed holes choked at all operating conditions. Note the large change in bleed exit area between these two cases. This includes shutting off plenum zero on the cowl. A significant penalty in terms of bleed drag is paid at Mach 3.5 to maintain choked bleed holes across the entire range of operation as specified in the design procedure. Since centerbody translation is a function of freestream Mach number, a system is conceivable in which the bleed exit area would vary with centerbody translation. Exit area requirements could then be matched as desired. For example, a two-position system could be built which provides sufficient exit area off-design and is closed down near the design Mach number centerbody position to minimize design point drag.

Surface	Plenum	Bleed rate, W/W_L	Exit area, A/A_L
Off-design			
Centerbody	F1 F2 T1 + T2	0.0100 0.0300 0.0244	0.0233 0.0428 0.0158
Cowl	0 1 2 3	0.0030 0.0155 0.0305 0.0200	0.0077 0.0290 0.0188 0.0191
		0.1334	0.1565
Mach 3.5			
Centerbody	F1 F2 T1 + T2	0.0100 0.0300 0.0244	0.0136 0.0234 0.0119
Cowl	0 1 2 3	0 0.0155 0.0305 0.0200	0 0.0222 0.0188 0.0191
		0.1304	0.1090

Table 4.—Mach 3.5 Bleed—Exists Adjusted for Off-Design and Mach 3.5

Alternate Bleed Hole Configurations

The purpose of the bleed system design procedure is to reduce the amount of wind tunnel testing required to develop an optimum bleed system. However, flexibility should be available for "fine tuning" the system in the wind tunnel.

Table 4 presents the proposed system with exits sized to maintain choked holes at all conditions, and with exits sized to maintain choked holes at Mach 3.5. An obvious test variation would be to test the smaller exit area configuration to determine how adverse the effects are of unchoking bleed holes off-design.

Table 5 presents an absolute minimum bleed configuration for the proposed model which maintains choked holes and paired rows of holes. This is not being recommended as a test configuration without step-by-step bleed reduction to explore the minimum possible bleed at Mach 3.5. This configuration would be achieved by closing two rows of holes in centerbody plenum F2 and closing two rows of holes in each of cowl plenums one, two, and three.

Table 5.—Mach 3.5 Bleed—Minimum Bleed Configuration

Surface	Plenum	Bleed rate, W/W_L	Exit area, A/A_L
Centerbody	F1	0.0100	0.0136
	F2	0.0150	0.0117
	T1 + T2	0.0244	0.0119
Cowl	0	0	0
	1	0.0078	0.0111
	2	0.0153	0.0094
	3	0.0133	0.0127
		0.0858	0.0704

Increased flexibility in optimizing the bleed system may be achieved by providing additional holes so that bleed bands may be relocated. Table 6 presents the bleed hole pattern recommended for a 1/3-scale model to be tested in the NASA Ames 8- by 7-ft supersonic wind tunnel. The starred rows of holes are those added to the proposed system given in tables 2 and 3. Their inclusion allows the repositioning of the bleed bands, or increasing the bleed rates in a plenum. The use of markedly higher bleed rates may be restricted by available exit area. This bleed hole pattern will allow final wind tunnel optimization of the bleed system.

Table 6.—Bleed Holes for 1/3-Scale Inlet Model

Plenum	Row number	Row station	Number of holes/row	Hole diameter, in.	Hole angle, α, deg
Centerbody					
F1	1* 2* 3 4 5* 6*	4.200 4.224 4.280 4.304 4.328 4.352	388	0.060	20
F2	7 8 9 10 11*	4.455 4.480 4.505 4.530 4.555	481	0.050	20
T1	12 13 14* 15*	4.625 4.635 4.655 4.665	900	0.026	20
T2	16 17 18* 19*	4.725 4.735 4.780 4.790	900	0.026	20
T3	20 21	4.875 4.890	624	0.036	20
T4	22 23	5.025 5.040	624	0.036	20
T5	24 25	5.177 5.193	530	0.040	20
F3	26 27 28 29	5.264 5.276 5.288 5.300	530	0.040	20
T6	30 31	5.360 5.380	406	0.050	20
T7	32 33	5.480 5.500	406	0.050	20
T8	34 35	5.620 5.645	308	0.060	20
T9	36 37	5.770 5.795	308	0.060	20

*Alternate bleed rows

Table 6.—Concluded

Plenum	Row number	Row station	Number of holes/row	Hole diameter, in.	Hole angle,α, deg
Cowl					
0	1 2	3.835 3.845	1165	0.026	20
1	3* 4* 5 6 7* 8* 9 10 11* 12*	4.167 4.183 4.217 4.233 4.267 4.283 4.317 4.333 4.349 4.365	709	0.040	20
2	13* 14 15 16 17 18*	4.505 4.523 4.541 4.559 4.577 4.595	743	0.036	20
3	19 20 21 22 23 24 25* 26*	4.665 4.670 4.695 4.700 4.725 4.730 4.755 4.760	880	0.030	90

*Alternate bleed rows

Combined Flowfield Analysis

The Combined Flowfield Analysis is a procedure for prediction of the real flowfield with viscous effects. The effects of cowl lip bluntness, boundary layer growth, bleed, and shock/boundary layer interactions are simulated. Cowl lip bluntness produces a detached lip shock that is displaced from the attached shock position and is initially stronger. Boundary layer growth has the effect of displacing the walls into the flowfield, thus generally increasing the local compression. Bleed removes mass from the stream, with an initial expansive effect as the local streamlines are turned toward the wall, followed by a compressive turning of the streamlines back parallel to the wall at the termination of the bleed region. Shock/boundary

layer interactions modify the boundary layer properties, as well as tending to move the reflected shock forward relative to an inviscid solution. These effects produce significant changes in the flowfield as compared to an inviscid solution.

This analysis is described in detail in reference 5, and is shown there to produce results that agree well with experimental data from large-scale models. Because the use of the Combined Flowfield Analysis is time consuming, it is not suited to use as a design tool in the initial steps of defining a bleed system. However, it does lend itself nicely to evaluation of that system. The use of the Combined Flowfield Analysis in the bleed system design provides a definition of the flowfield with viscous effects included. These results are used to determine whether bleed bands are correctly positioned to allow control of shock interactions and pressure gradients. Because of the complexity and time required to apply the analysis, only two cases are considered.

A Combined Flowfield Analysis has previously been applied to an inlet using the 1/3-scale model hardware. Reference 5 presents the results of the analysis for the inlet tested and described in reference 2. This work showed the cowl lip bluntness effect for the 1/3-scale model to be negligible, so this effect was not accounted for in the following analyses.

The Combined Flowfield Analysis procedure was applied to the Mach 3.5 inlet with the proposed bleed system at Mach 3.5. The results, in the form of surface pressure distributions and characteristic network and shock patterns, are presented in figure 33. The bleed regions are indicated by the shaded arrows. This figure shows that shock reflections of the primary shock system fall behind or in the aft portion of the bleed bands designed to control those reflections. This means that the bleed bands are correctly positioned, even with viscous effects included. Repositioning of bleed bands to control shock interactions will not be required. Figure 33 shows that the primary shock system is becoming continuously stronger, particularly following the first cowl shock reflection. Part of this strengthening comes from the shocks off the second and third cowl bleed bands and the second centerbody bleed band. Much of the shock strengthening comes from the distributed compression due to boundary layer growth. The primary oblique shock system is predicted to have too great a deflection angle to allow a simple reflection with supersonic flow downstream at the second cowl shock reflection. As stated in reference 5, the full significance of this is not presently understood. The deflection angle is too large, by about 1.2°, to allow supersonic flow downstream. In addition, this reflection occurs in a favorable pressure gradient. As a result, it is felt that at worst a small subsonic pocket would exist that would be rapidly accelerated to supersonic conditions. Further, the Combined Flowfield Analysis done previously in reference 5 for the 1/3-scale M = 2.65 inlet tested in reference 2 showed a similar occurrence, but reference 2 shows no problems encountered in the operation of the inlet.

An additional case at Mach 2.7, chosen to be representative of off-design conditions, was computed using the Combined Flowfield Analysis. The results are presented in figure 34. The primary shock system shock reflections are found to be well positioned relative to the bleed bands used to control them. The primary shock system deflection angle is too large to allow a simple oblique shock reflection at the third centerbody shock reflection. As in the Mach 3.5 case the turning is only slightly too great to allow supersonic flow downstream, and the shock reflection occurs in a region of favorable pressure gradient. Thus, it is felt the situation will be the same as at Mach 3.5, accelerating to supersonic conditions with no significant adverse effect.

Restart At Mach 3.5

Experience from the development of supersonic inlets has indicated that restart of translating centerbody inlets may be difficult to achieve. As the centerbody translates forward, following an inlet unstart at the design position, the throat area will increase and the capture flow will decrease due to the conical spillage. A position will be reached where the throat area is large enough to accommodate the low recovery flow downstream of the normal shock without requiring external normal shock spillage. At this point the normal shock will move downstream of the inlet throat, and the inlet will be started. It should then be possible to retract the centerbody to the design position, maintaining a started inlet. However, boundary layer separation may occur on the centerbody in the supersonic diffuser during the restart process, resulting in premature unstart as the centerbody is retracted toward the design position. This phenomenon, referred to as "semistart," is not fully understood but has been found to be affected by the strength of the first centerbody shock reflection coupled with the internal flow area variation in the inlet.

A study was undertaken to determine whether semistart is a potential problem in the present Mach 3.5 inlet. Figure 35 shows the properties of the first centerbody shock reflection as a function of centerbody position at Mach 3.5. A comparison of the location of the shock reflection with the bleed schedule from figure 17 shows that the shock is always located ahead of the bleed regions. The Mach number upstream of the shock is higher than the pressure ratio across the shock for centerbody positions inside $\Delta X/R_L = 1.3$. Using the shock separation criterion of reference 7, the boundary layer will remain attached through the shock interaction if the upstream profile is full in this range of centerbody positions. The centerbody position at which restart will occur based on inviscid calculations is shown in figure 36. At $\Delta X/R_L = 1.1$ the throat area is sufficiently large, and the normal shock will move downstream of the throat when the centerbody is extended to this position. The boundary layer development along the centerbody was therefore calculated at $\Delta X/R_L = 1.1$. The results confirmed that the boundary layer remains attached through the shock reflection. The internal flow area variation for extended centerbody positions is favorable for restart because the geometric throat moves forward to the lip. Experience with similar Mach 2.65 inlets has indicated that this type of area progression feature alleviates semistart. Consequently, no inlet starting problems are expected and the bleed system need not be modified.

CONCLUDING REMARKS

The work described here is the application of analytical procedures to the design of a bleed system for a supersonic (M = 3.5) inlet. Analysis of the proposed system indicates that adequate boundary layer control is provided over the "started" Mach number range. Several off-design conditions have been identified as possible problem areas. The possibility of boundary layer separation exists in these areas. In addition to predicting the boundary layer development with bleed, the bleed system geometry, complex ducting, and basic bleed exit areas have been described.

The present work has illustrated that several areas within the bleed system design procedure need improved analysis or further information to achieve a more complete and

accurate design. These areas and the improvements needed are identified below. While quite comprehensive analytic and isolated experimental work was used to define the bleed system, a large-scale wind tunnel test with the proposed bleed system is needed not only to validate the procedure but to provide valuable experimental data for future bleed system design.

The bleed hole data presently available are limited in terms of variation of bleed hole parameters. The bleed geometry for the proposed bleed system was chosen in part on the basis of existing experimental bleed hole data derived from isolated wind tunnel tests on flat plates with fully developed boundary layers. The bleed hole data presently used are limited in variation of hole diameter, hole length, hole spacing, and upstream boundary layer profile. A comprehensive parametric study of bleed hole performance from isolated tests would be of great value in future inlet design. With the added information the designer could perform tradeoffs not presently possible between the various parameters to arrive at a configuration, and have greater confidence in the accuracy of the design.

At several off-design conditions the possibility of boundary layer separation exists. These separations are, in each case, predicted downstream of shock reflections. The current analysis does not predict the size of separations or the flow behavior within separated regions. On the basis of prior experience with supersonic inlets it is felt that the separations, if they exist, would be small and would not significantly affect inlet performance. The development of the capability to predict interactions with local separation, and to predict flow conditions downstream if the separation does not immediately reattach, would be of great benefit because interactions of this type may be overcontrolled using current methods. The ability to predict the effect of a local separation on the inlet flowfield would be extremely valuable in determining the amount of boundary layer control required. In addition, the capability to predict the effects of bleed within a shock interaction would be of great help in determining optimum bleed location. Also, analytic understanding of normal shock/boundary layer interactions would allow predictions of throat bleed requirements without reliance on empirical data.

At several off-design Mach numbers, local subsonic flow was predicted. Since the method of characteristics is valid only for supersonic flow, the analytical procedure cannot be applied when any subsonic point is encountered. The analytical procedure would be significantly improved if an analysis were created which allowed computation through and past locally subsonic regions, allowing a more complete analytical design of the bleed system.

The present bleed system design procedure requires a considerable amount of time for data preparation. A significant decrease in the complexity and time required in the procedure could be achieved by modifying the input and output of the boundary layer and inviscid flow programs to make them more compatible. This type of improvement would also make the Combined Flowfield Analysis easier to use for bleed system evaluation. Further work of this kind, plus development of an analysis defining the structure of shock/boundary layer interactions, could allow a more automated Combined Flowfield Analysis, thus encouraging greater application in final bleed system evaluation.

The bleed system design procedure in its present form is, however, extremely valuable. Its use has allowed analytical definition of a bleed system incorporating features that are unlikely to evolve from wind tunnel testing. Furthermore, possible problem areas have been

identified before testing has been undertaken. The analytical bleed system design procedure is felt to be an important advancement in supersonic inlet design technology and promises to save many wind tunnel testing hours in the development of future supersonic inlet systems.

APPENDIX

The inlet described in reference 6 was analyzed using the inviscid flow MOCHA program. At each $\Delta M_\infty = 0.1$ along the translation schedule between Mach 3.5 and Mach 1.6 the inviscid flowfield was computed. Figures 37-56 present the results of the study in the form of plotted surface static pressures, together with the contours, characteristic network, and shock pattern for flowfield visualization.

This analysis revealed that the flowfield solution extended past the throat over most of the Mach number range. Between Mach 2.8 and 3.3 and between Mach 1.7 and 2.0 the oblique shock system becomes so strong that it produces subsonic flow ahead of the throat. This condition may be restricted to a local subsonic pocket.

REFERENCES

1. *Design of Bleed Systems for a NASA M=3.5 Inlet,* technical proposal, D6-24854, The Boeing Company, March 1971.

2. J. L. Koncsek and J. Syberg, *Transonic and Supersonic Test of a Mach 2.65 Mixed-Compression Axisymmetric Intake,* NASA CR-1977, The Boeing Company.

3. J. Syberg and J. L. Koncsek, *Transonic and Supersonic Test of the SST Prototype Air Intake,* report FAA-SS-72-50, prepared for FAA by The Boeing Company, April 1972.

4. T. A. Reyhner, *A Computer Program for Finite-Difference Calculation of Compressible Turbulent Boundary Layers,* D6-23236, The Boeing Company, June 17, 1970.

5. T. A. Reyhner and T. E. Hickcox, "A Procedure for Combined Viscous-Inviscid Analysis of Supersonic Inlet Flow Fields," AIAA paper 72-44, January 17, 1972.

6. T. E. Hickcox, *Report of Work Performed Under Contract NAS2-6643, Design of Bleed Systems for a NASA M=3.5 Inlet,* D6-40559, The Boeing Company, March 28, 1972.

7. G. C. Paynter, *Shock and Ramp Induced Incipient Separation of a Turbulent Boundary Layer,* D6-11487, The Boeing Company, November 3, 1967.

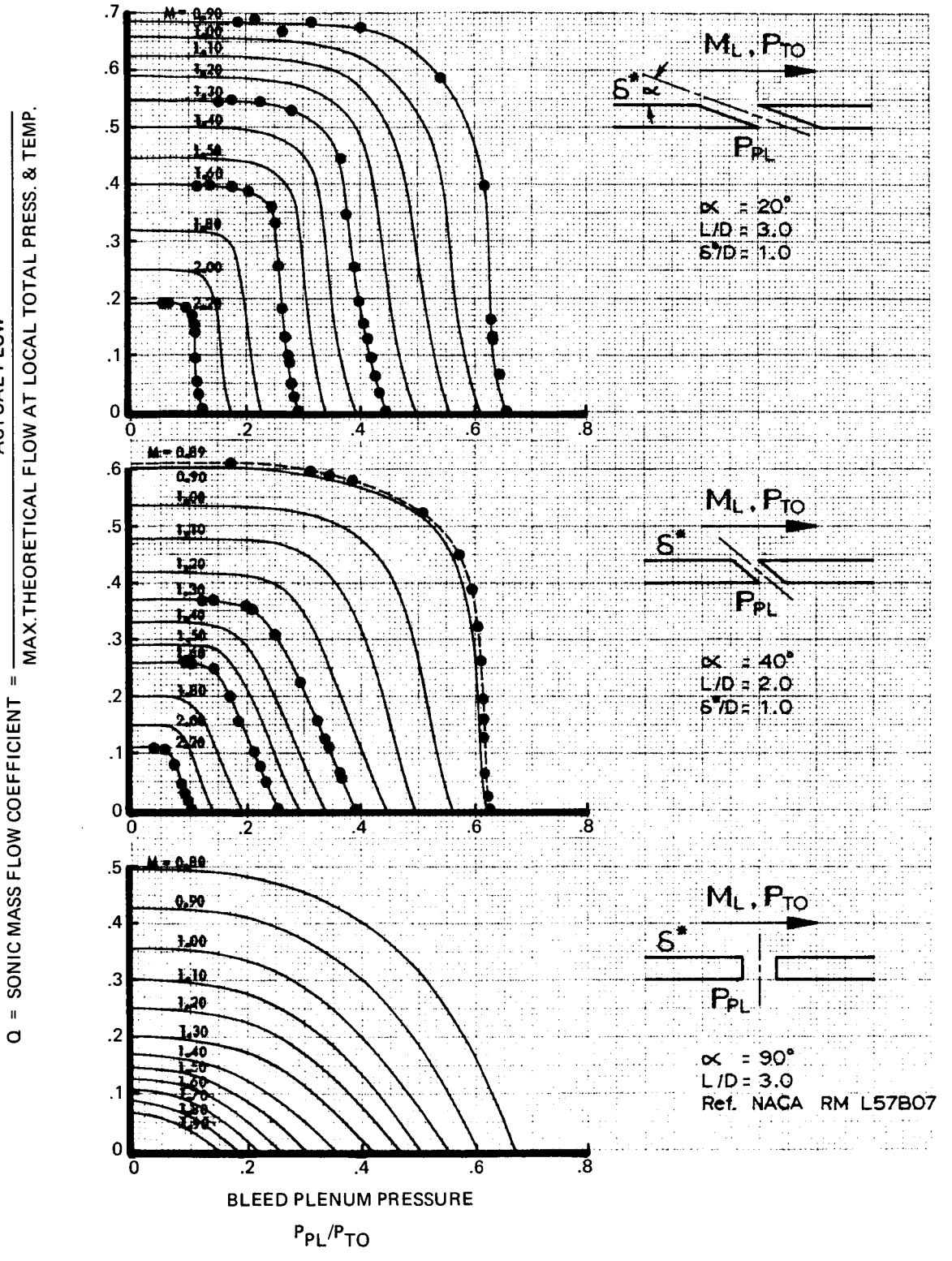

FIGURE 1.–BLEED HOLE CHARACTERISTICS

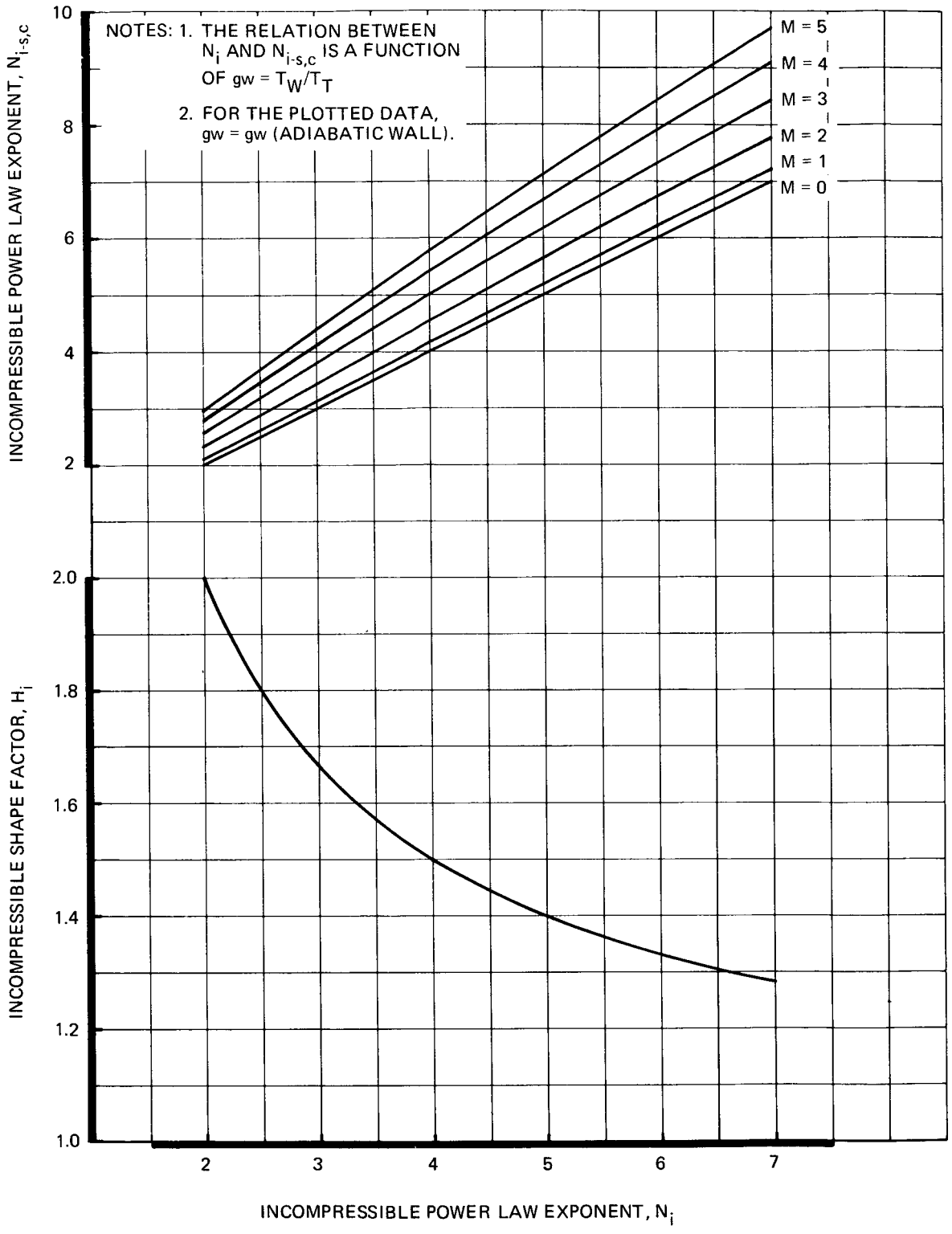

FIGURE 2.–BOUNDARY LAYER DISTORTION PARAMETERS

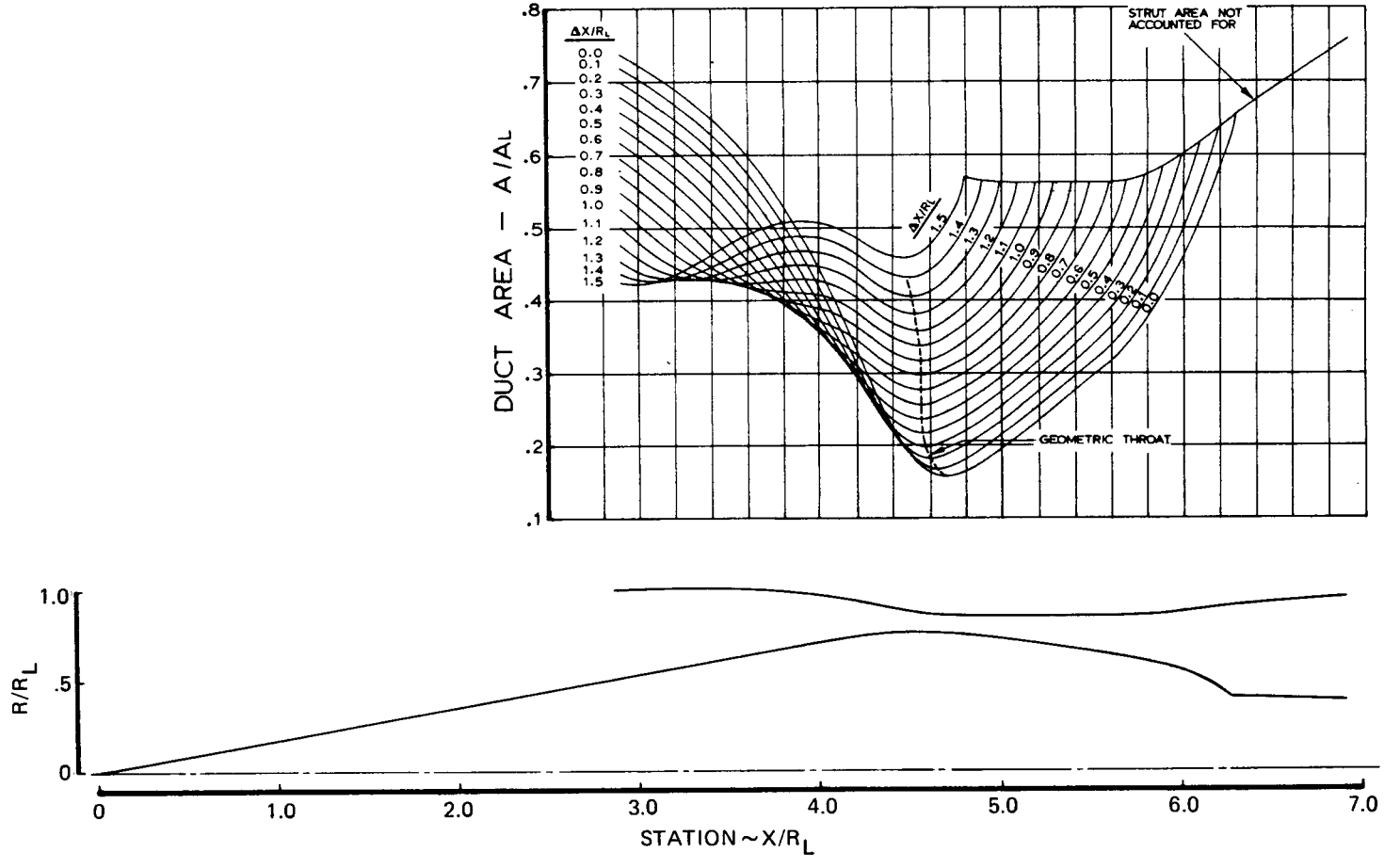

FIGURE 3.–INTERNAL AREA VARIATION WITH CENTERBODY TRANSLATION MACH 3.5 INLET

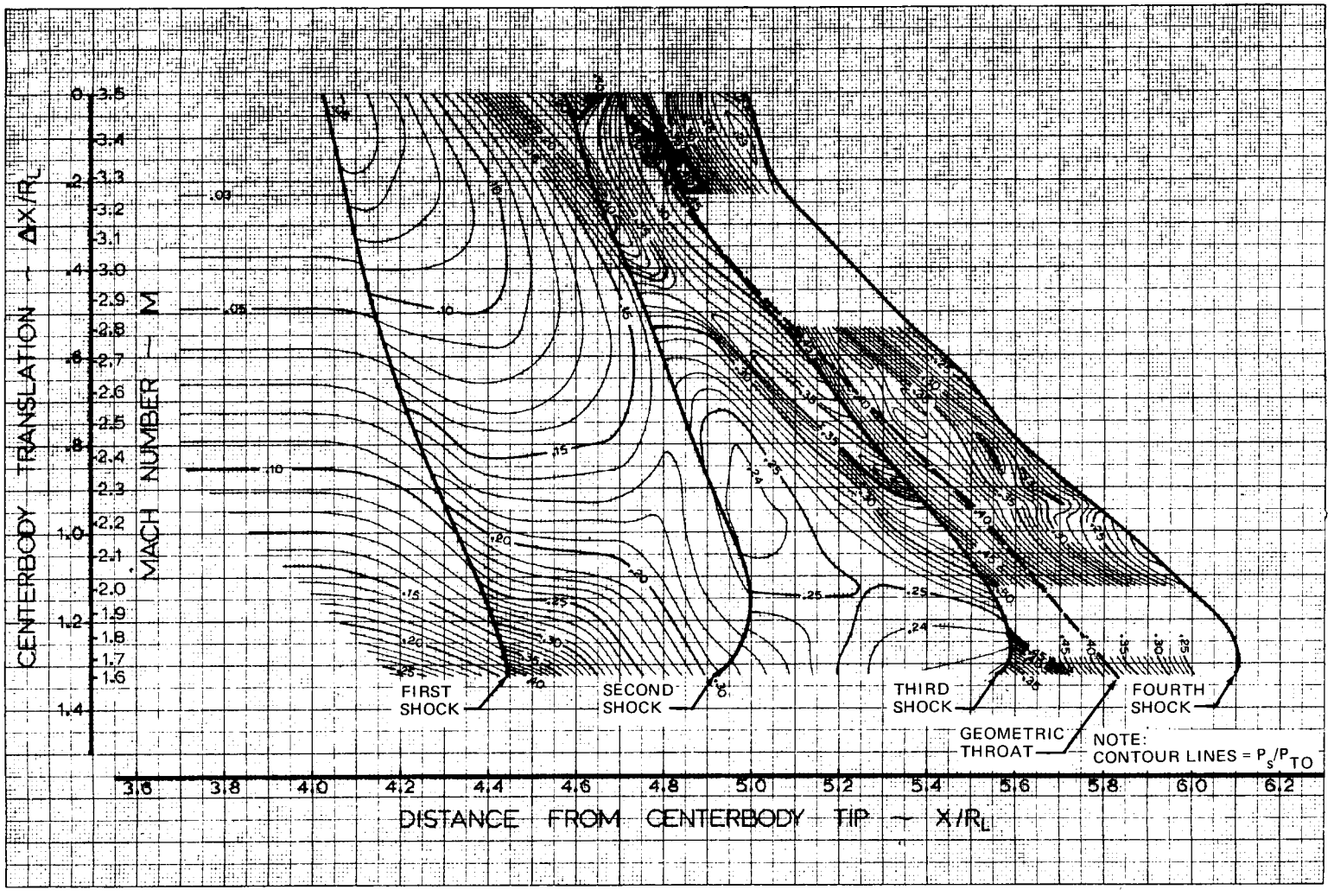

FIGURE 4.– MAP OF CENTERBODY SURFACE PRESSURE. INVISCID ANALYSIS

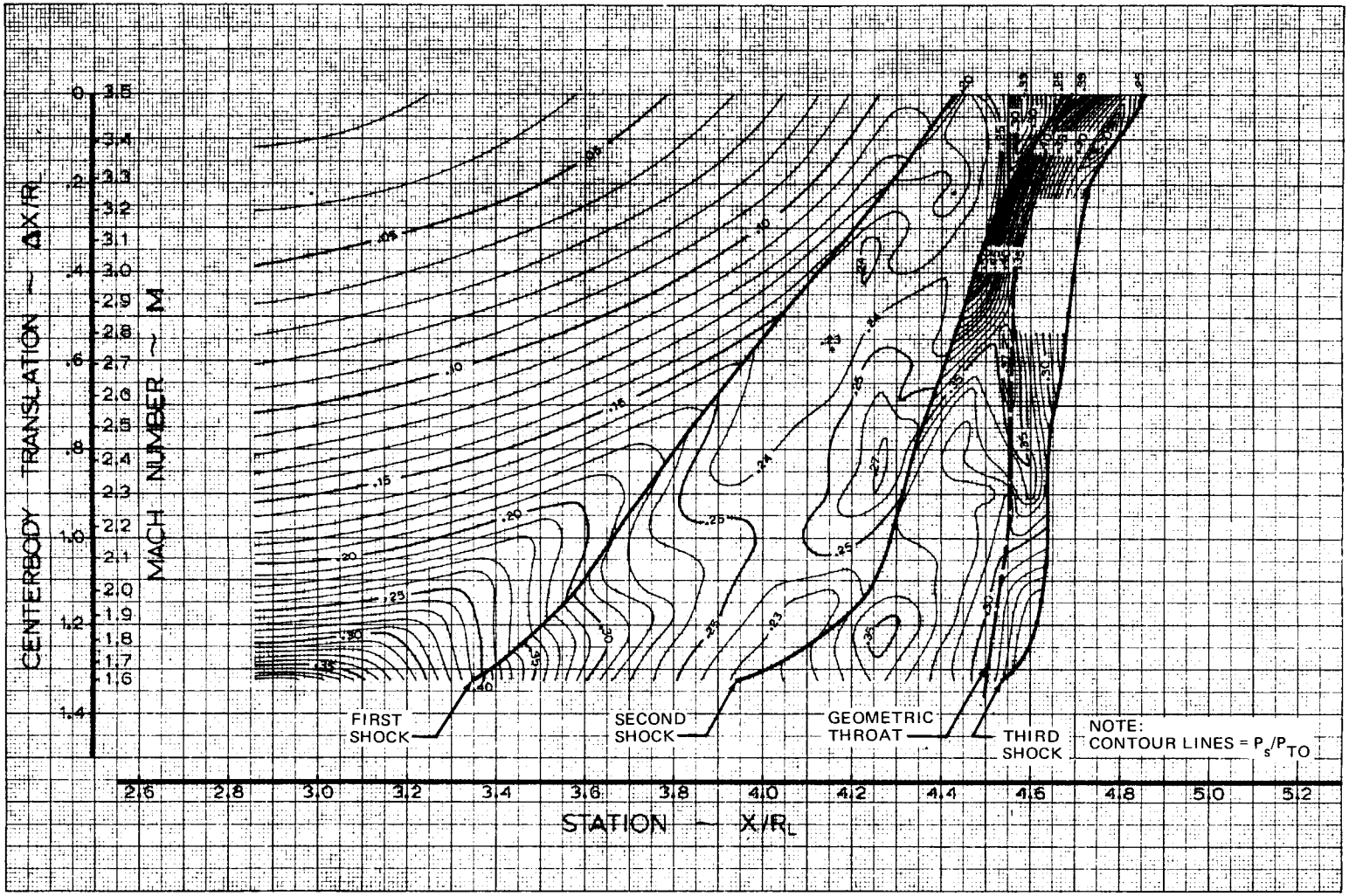

FIGURE 5.–MAP OF COWL SURFACE PRESSURE.INVISCID ANALYSIS

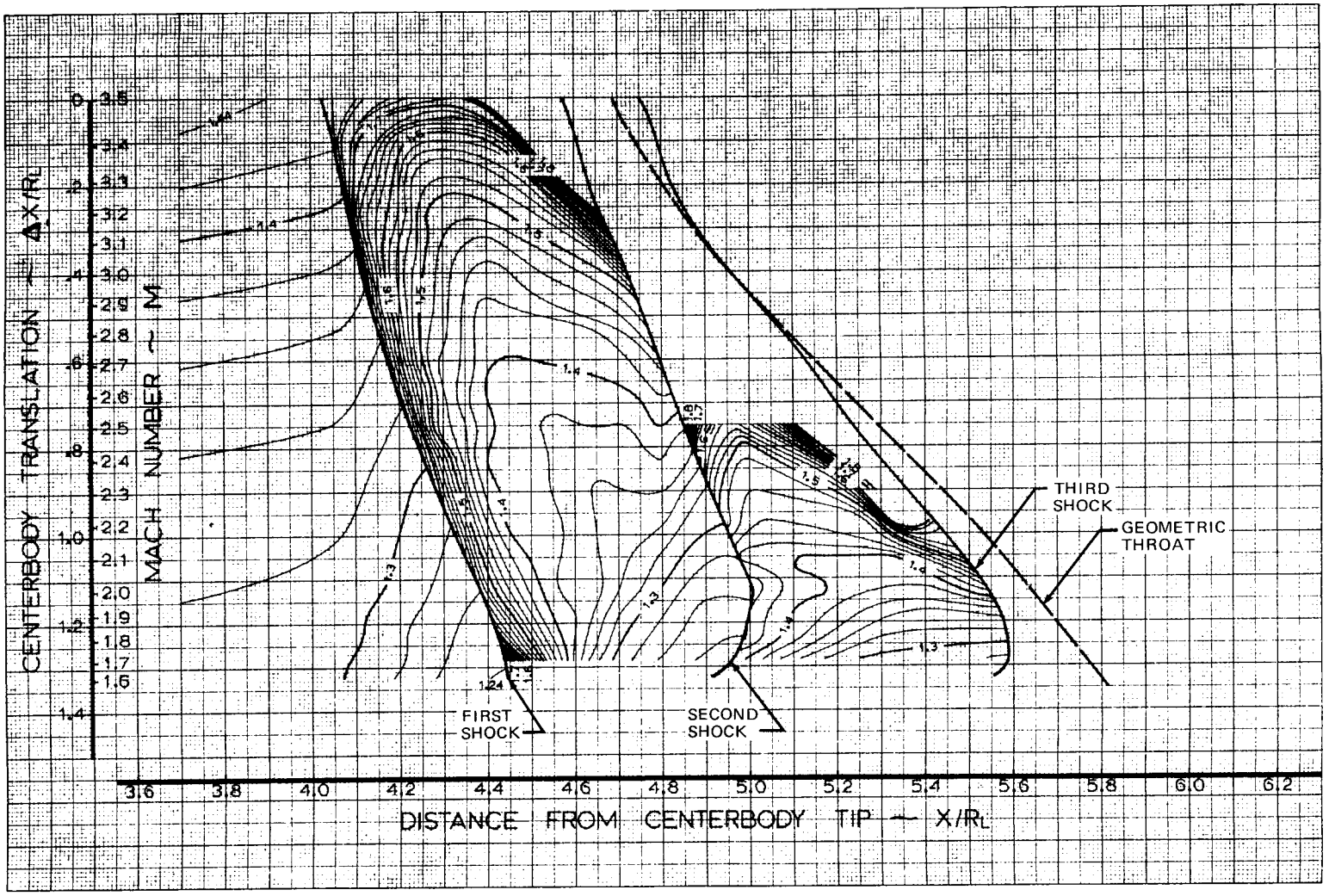

FIGURE 6.–MAP OF CENTERBODY BOUNDARY LAYER SHAPE FACTOR, H_i. NO BLEED

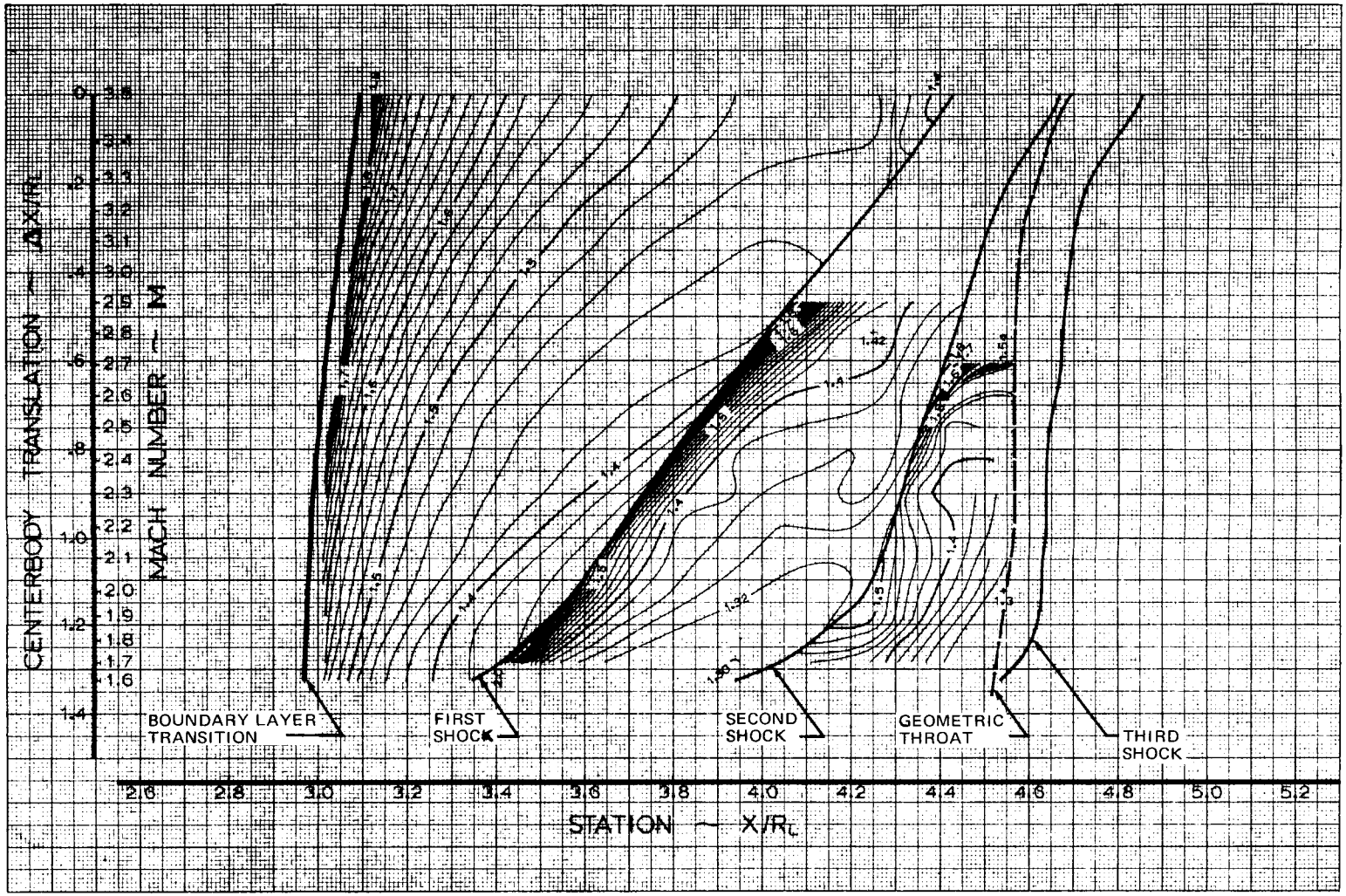

FIGURE 7.–MAP OF COWL BOUNDARY LAYER SHAPE FACTOR, H_i. NO BLEED

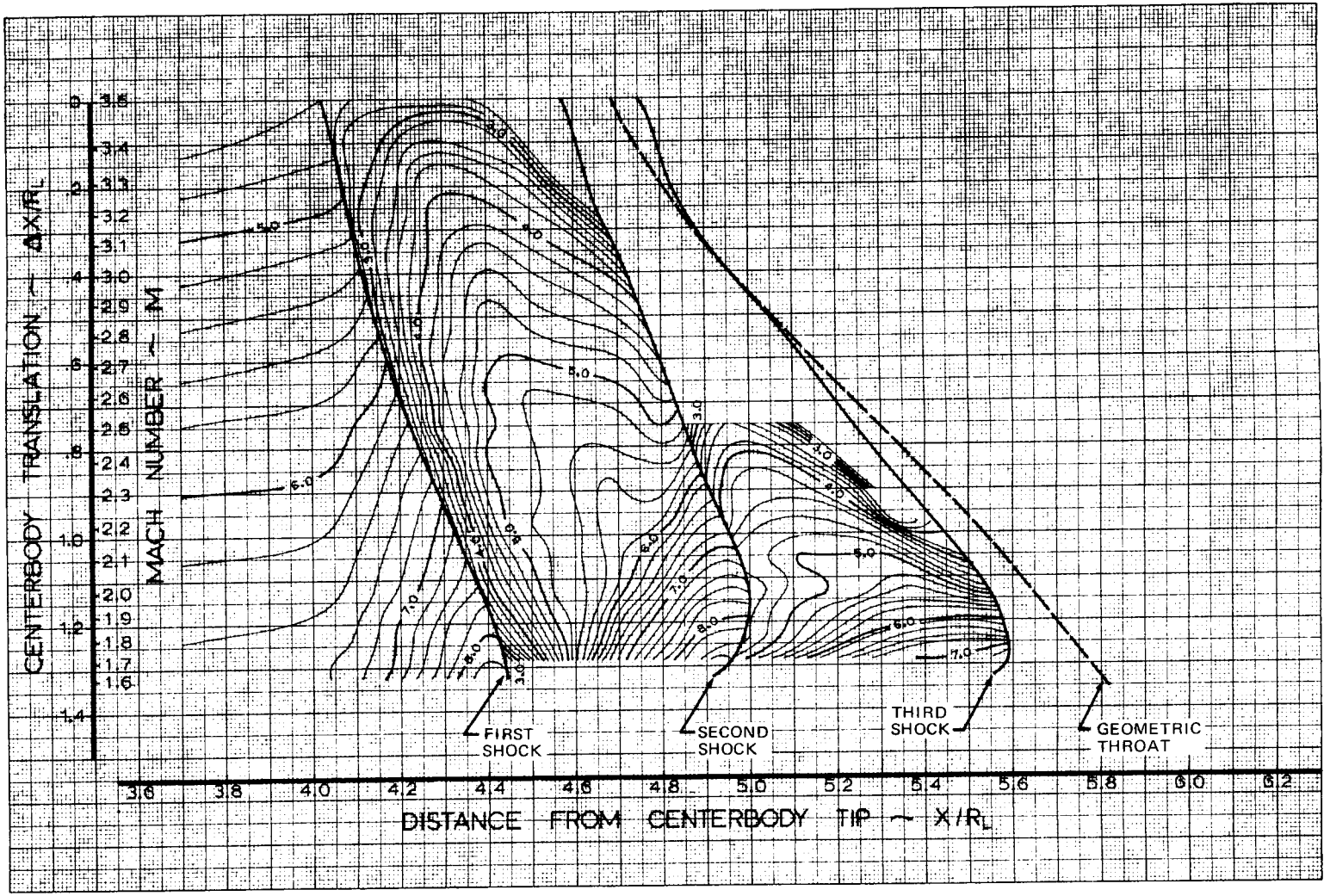

FIGURE 8.–MAP OF CENTERBODY BOUNDARY LAYER POWER LAW EXPONENT, N_i. NO BLEED

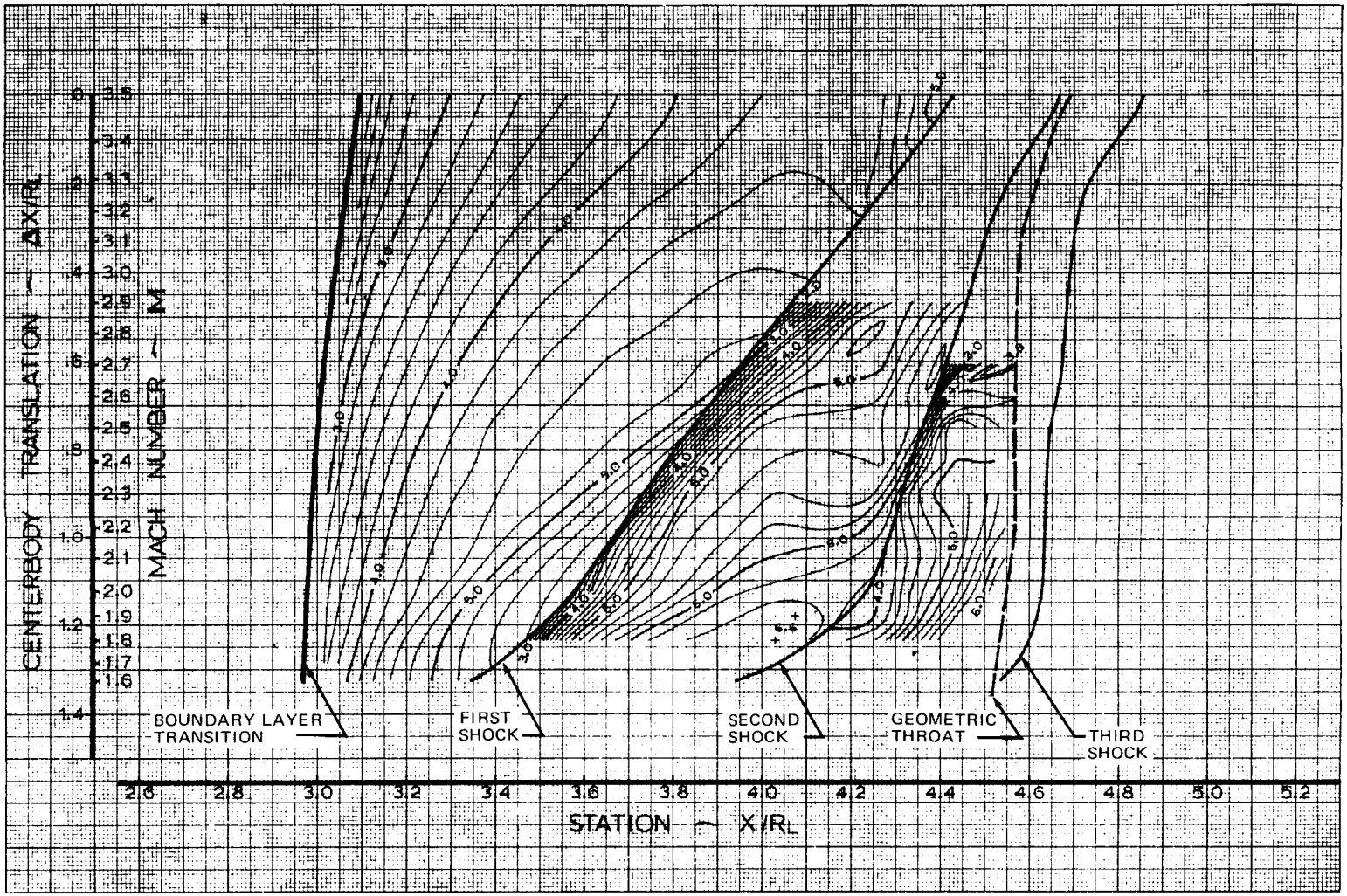

FIGURE 9.–MAP OF COWL BOUNDARY LAYER POWER LAW EXPONENT, N_i. NO BLEED

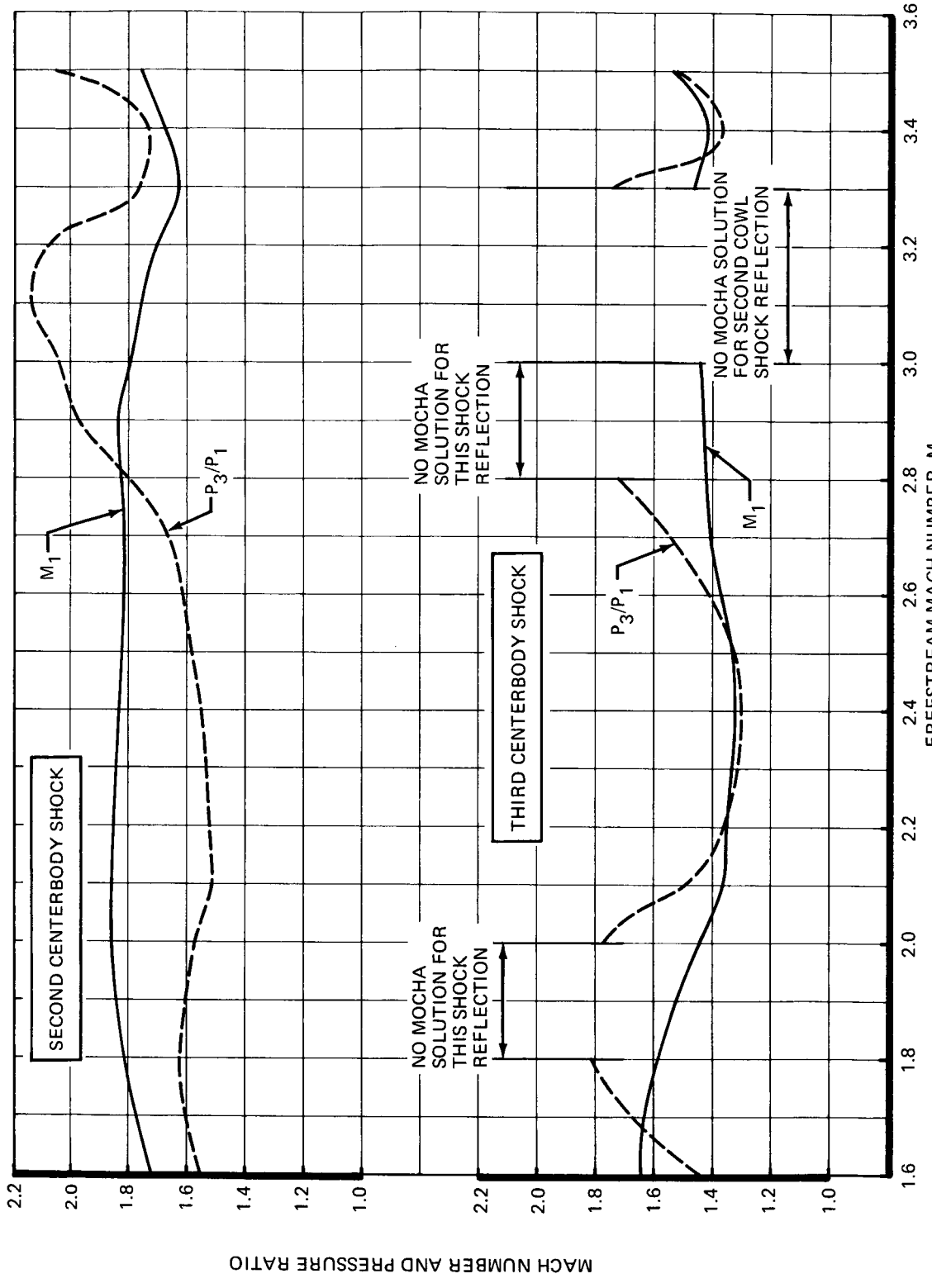

FIGURE 10.– CENTERBODY SHOCK REFLECTION PROPERTIES

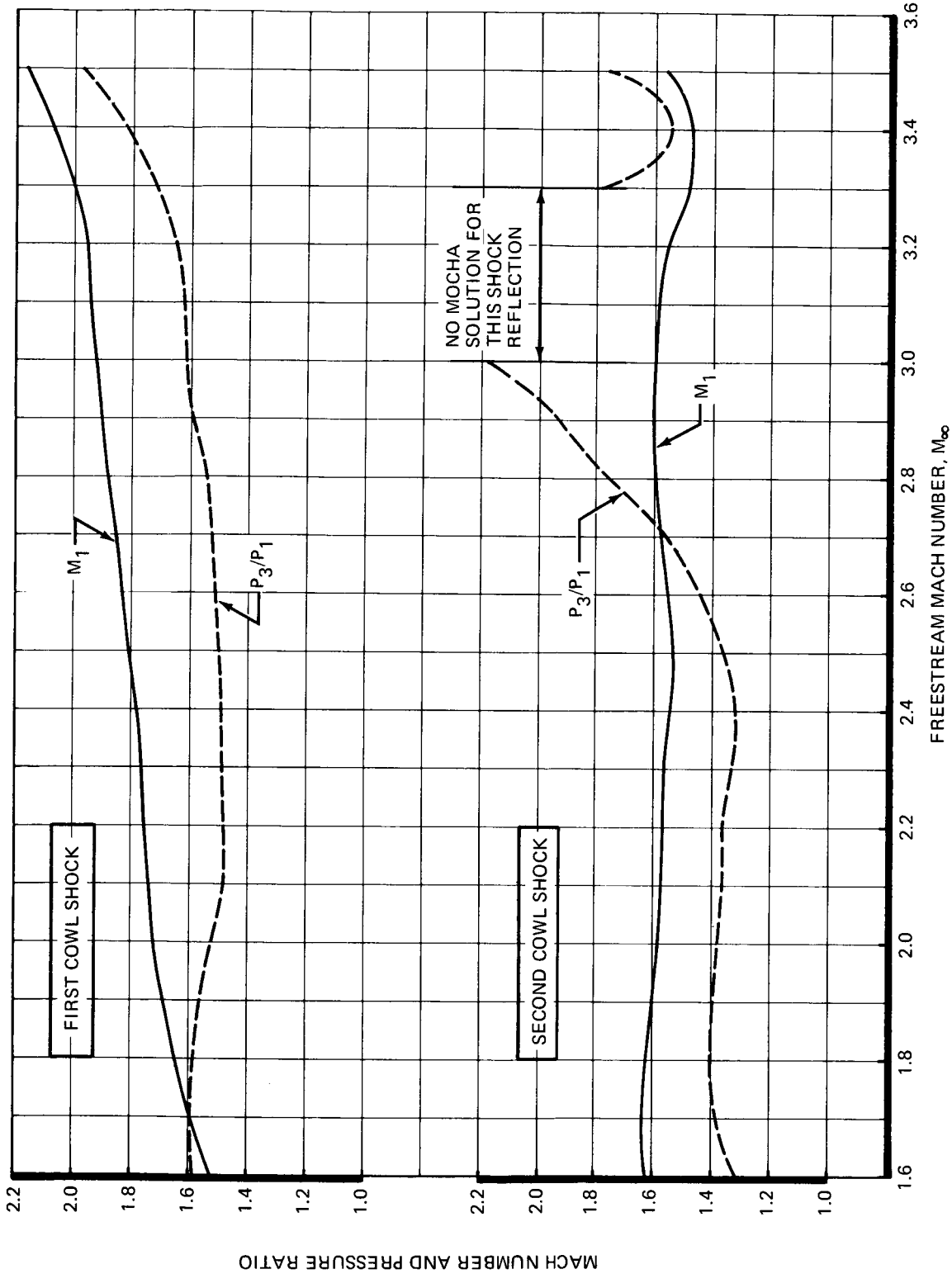

FIGURE 11.–COWL SHOCK REFLECTION PROPERTIES

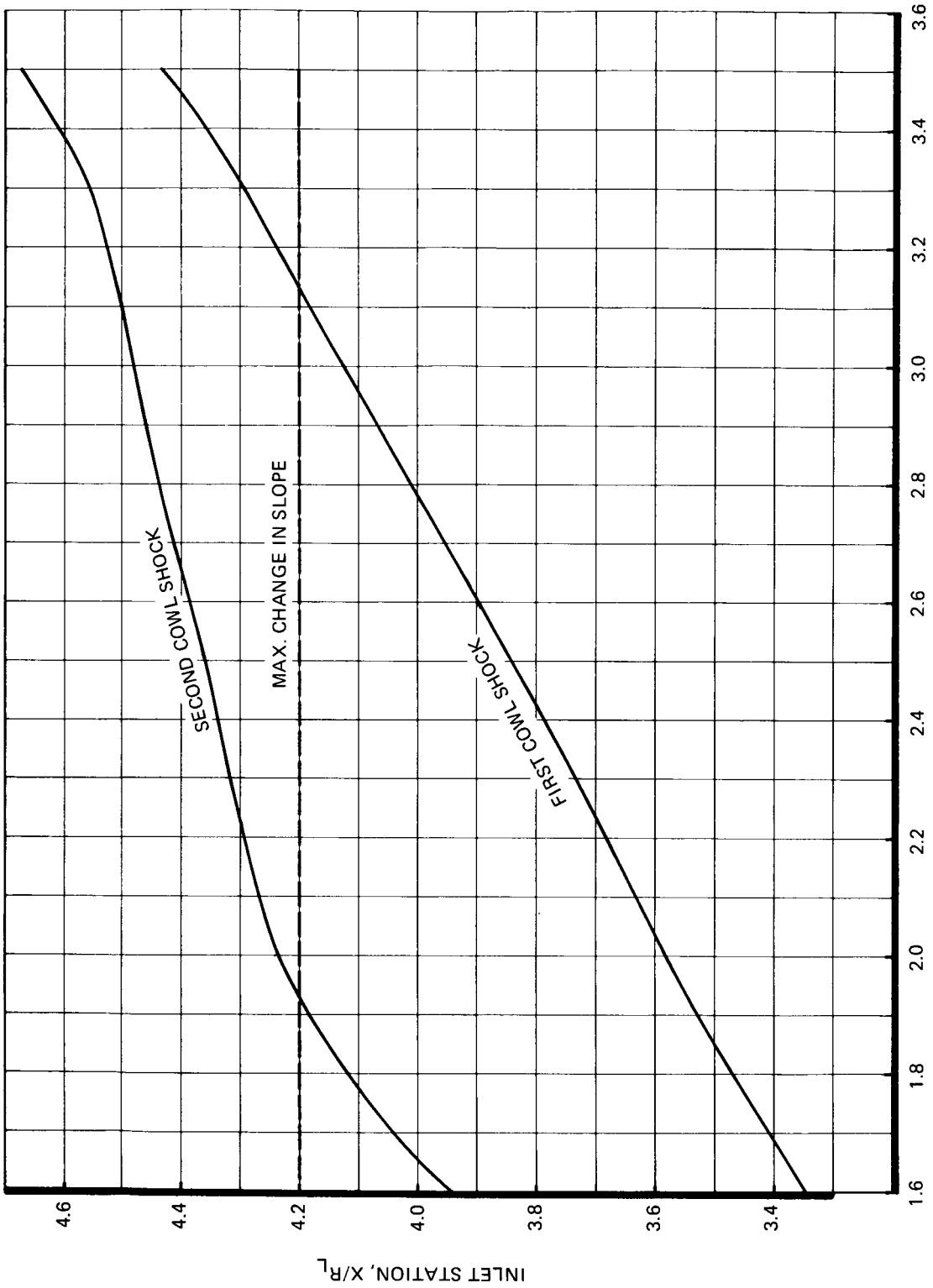

FIGURE 12.–POSITION OF COWL SHOCK REFLECTIONS

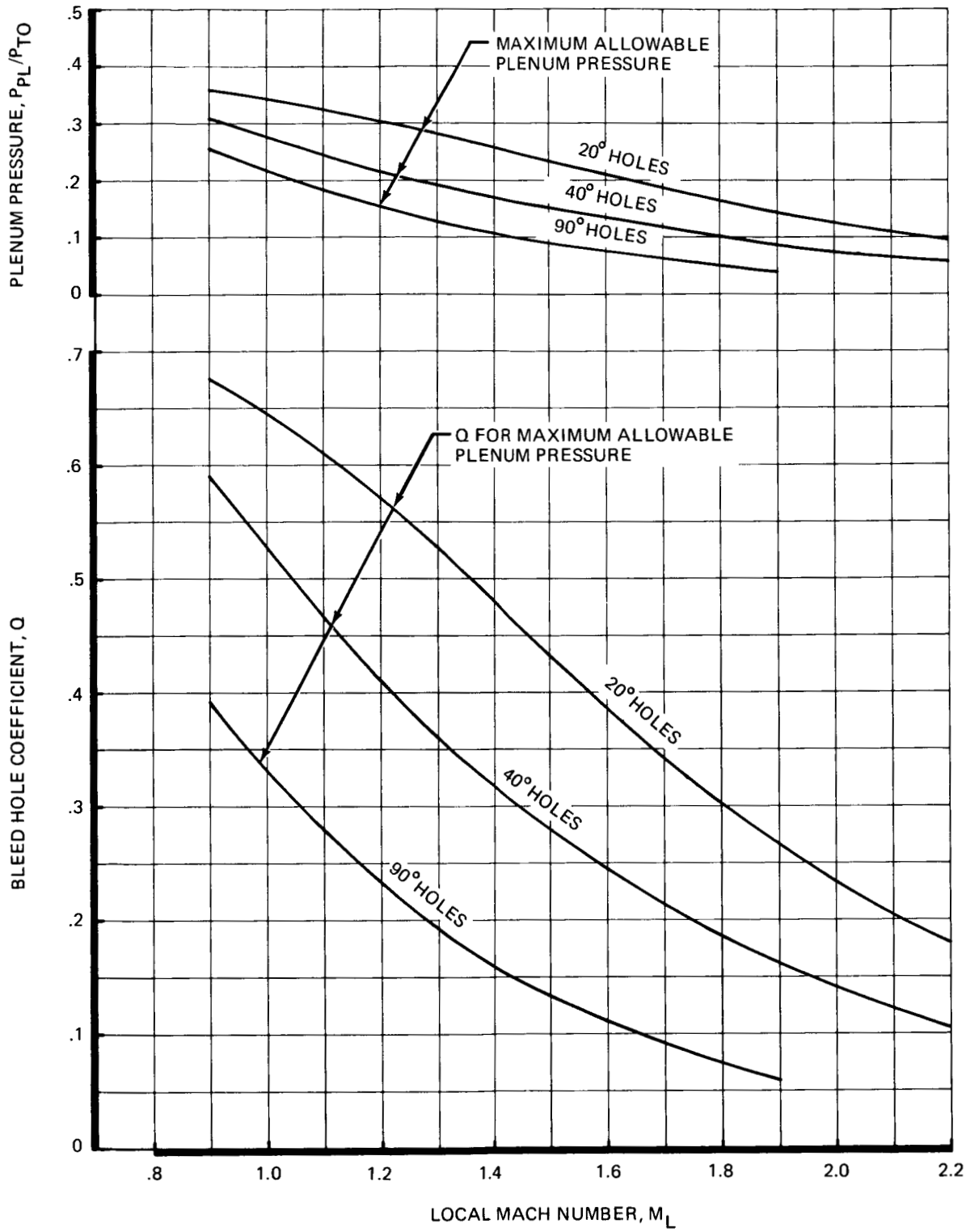

FIGURE 13.–BLEED HOLE CHARACTERISTICS FOR CHOKED HOLES

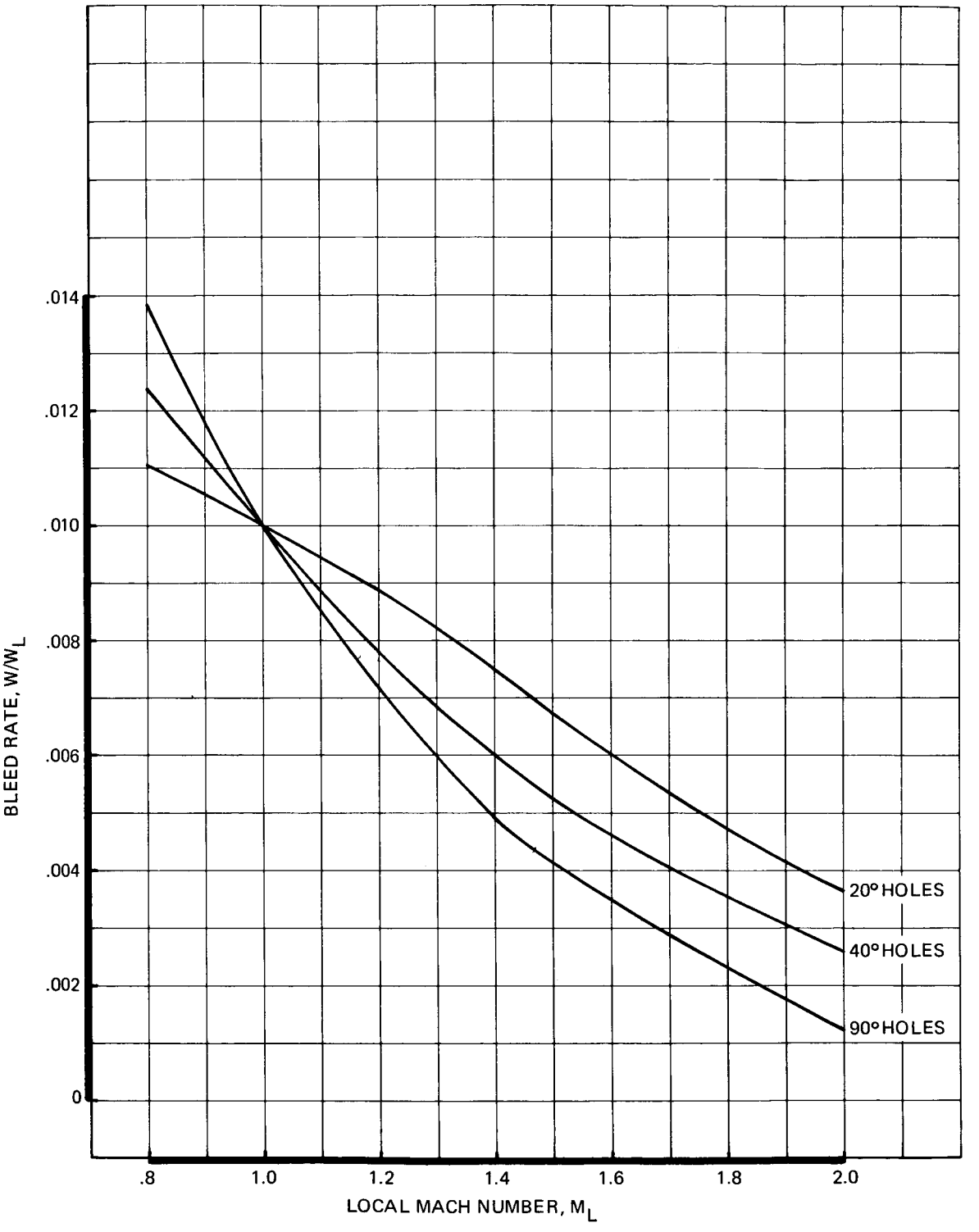

FIGURE 14.–EFFECT OF LOCAL MACH NUMBER AND BLEED HOLE ANGLE ON BLEED MASS FLOW

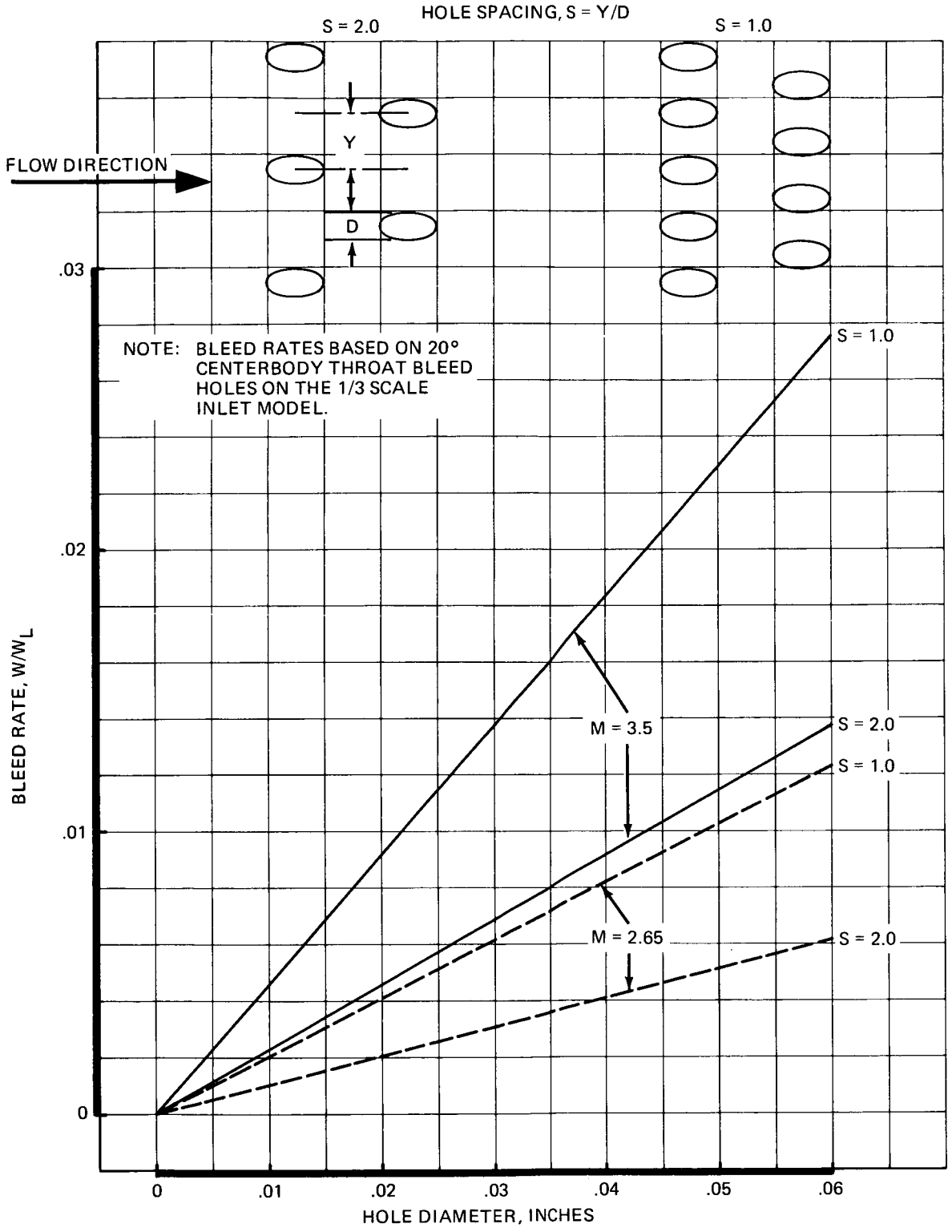

FIGURE 15.–EFFECT OF HOLE DIAMETER, HOLE SPACING, AND FREESTREAM MACH NUMBER ON BLEED MASS FLOW

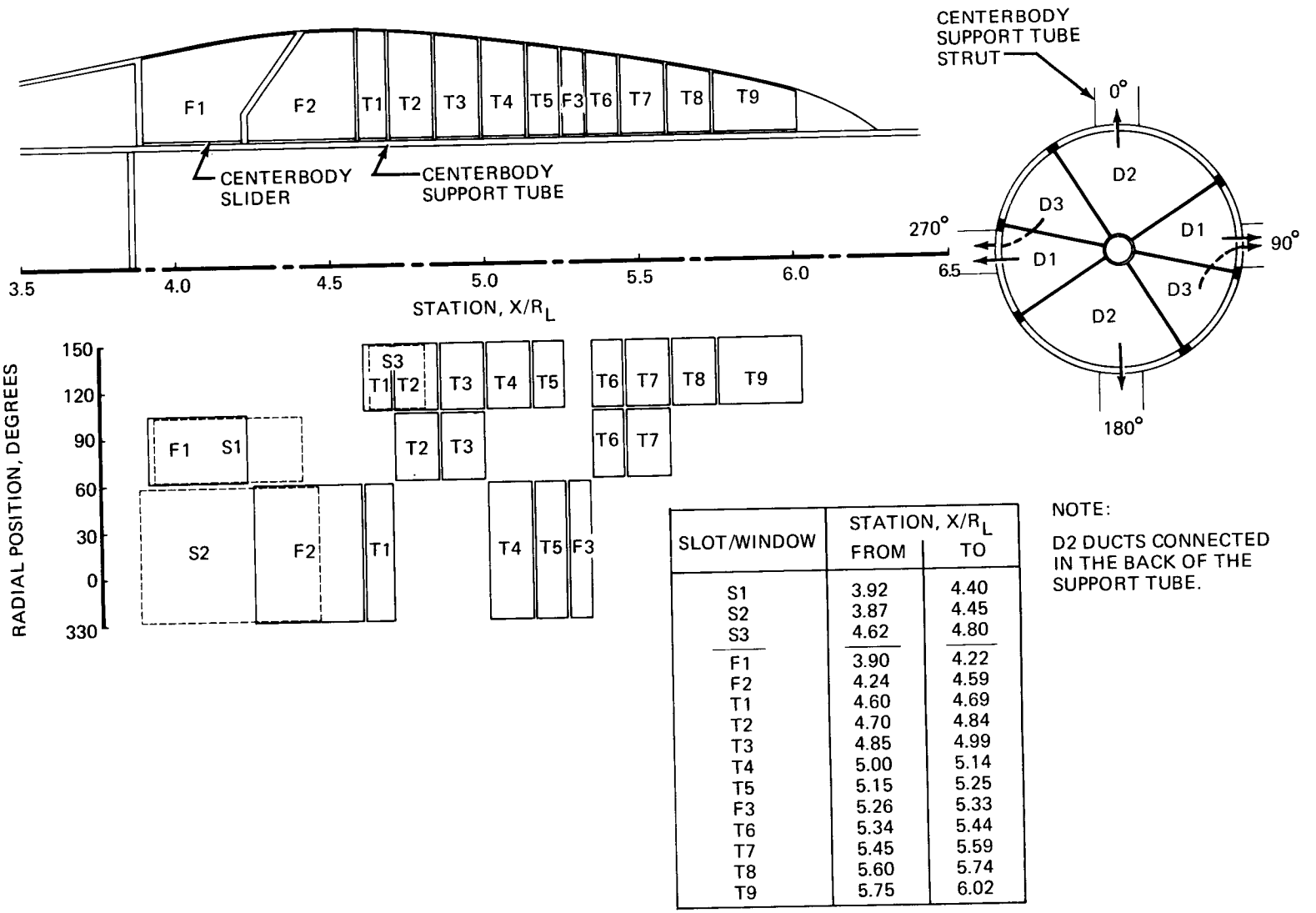

SLOT/WINDOW	STATION, X/R_L FROM	TO
S1	3.92	4.40
S2	3.87	4.45
S3	4.62	4.80
F1	3.90	4.22
F2	4.24	4.59
T1	4.60	4.69
T2	4.70	4.84
T3	4.85	4.99
T4	5.00	5.14
T5	5.15	5.25
F3	5.26	5.33
T6	5.34	5.44
T7	5.45	5.59
T8	5.60	5.74
T9	5.75	6.02

NOTE:

D2 DUCTS CONNECTED IN THE BACK OF THE SUPPORT TUBE.

FIGURE 16.–CENTERBODY BLEED SYSTEM

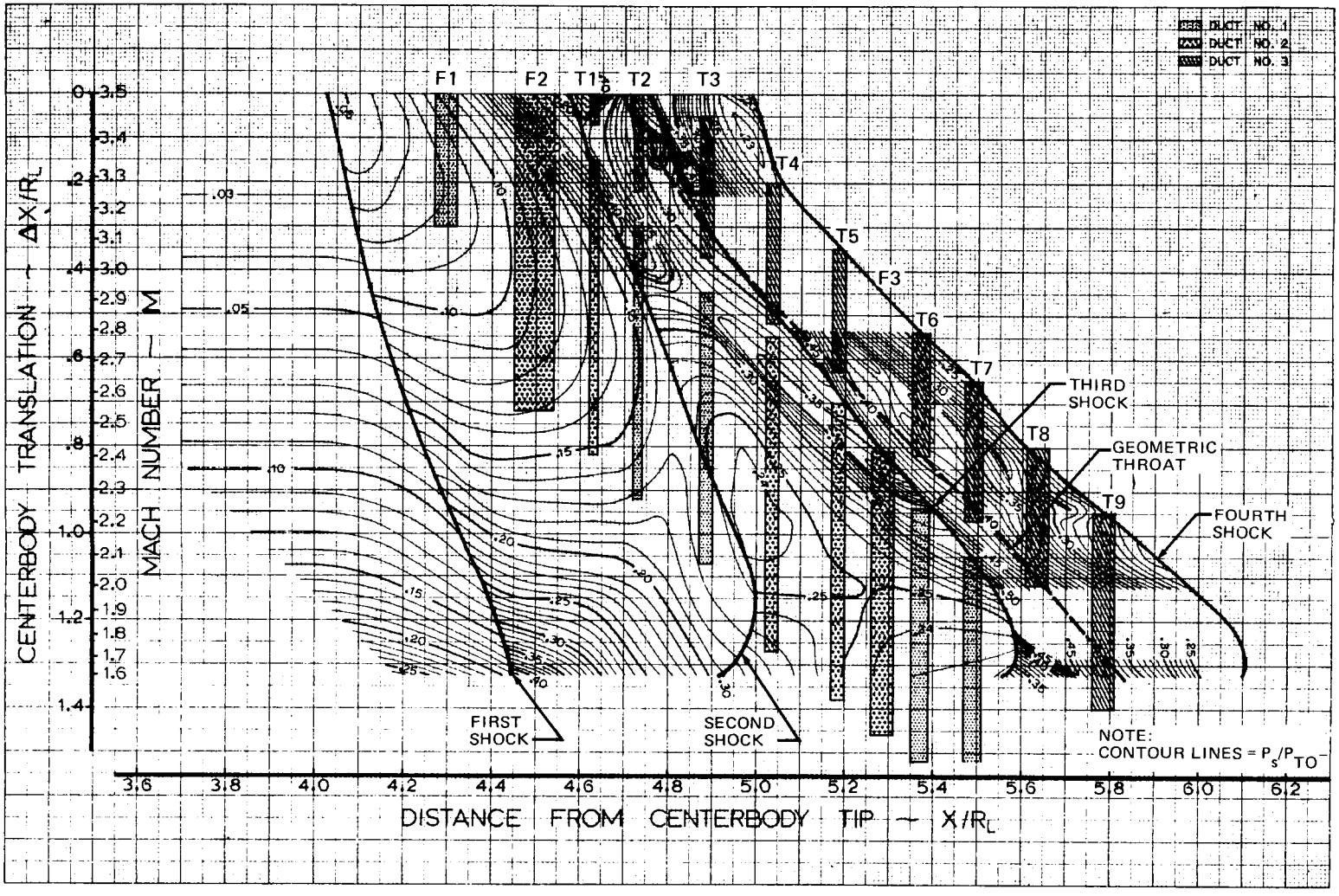

FIGURE 17.–BLEED SCHEDULE SUPERIMPOSED ON INVISCID CENTERBODY SURFACE PRESSURE MAP

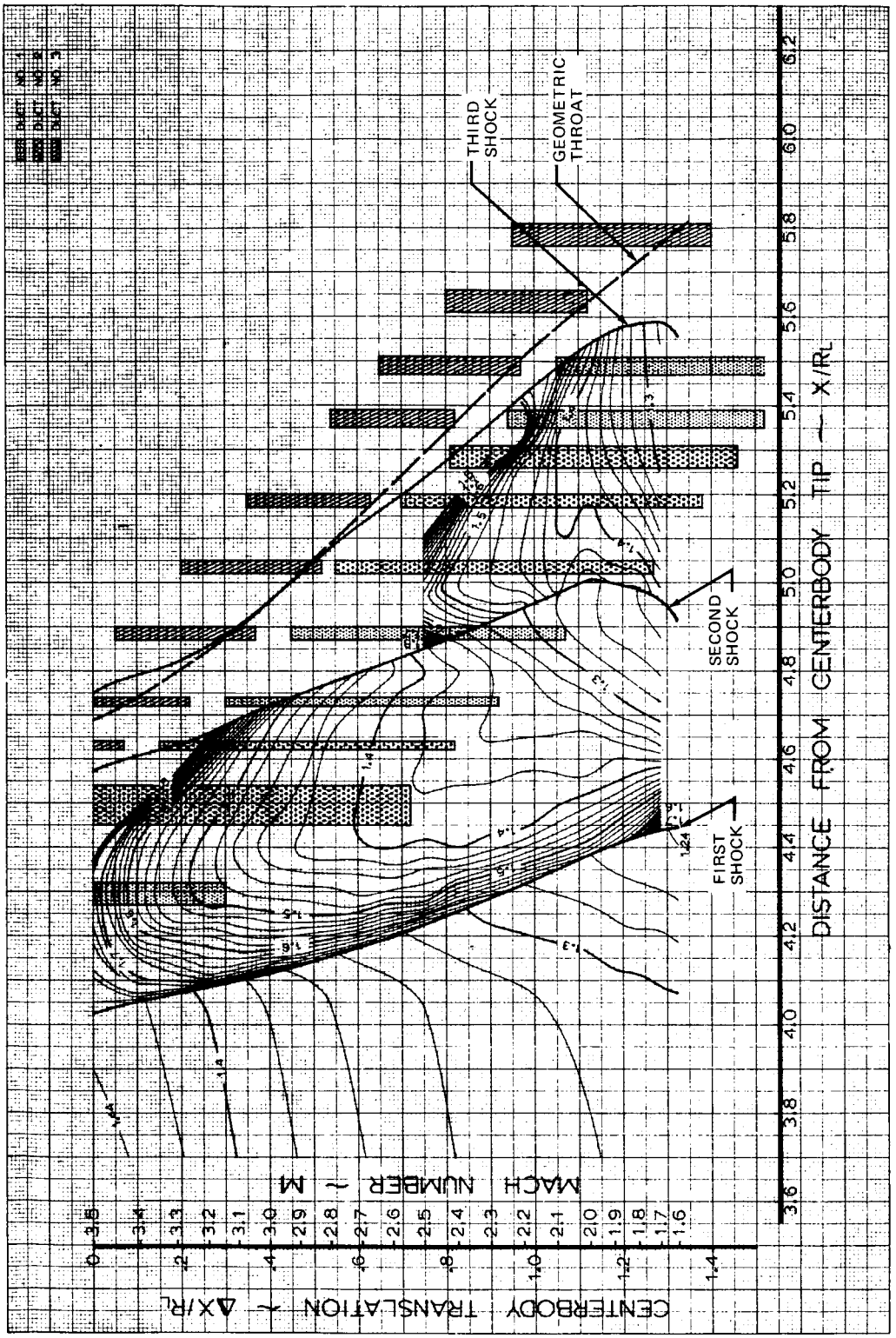

FIGURE 18.– BLEED SCHEDULE SUPERIMPOSED ON CENTERBODY H_i MAP WITHOUT BLEED

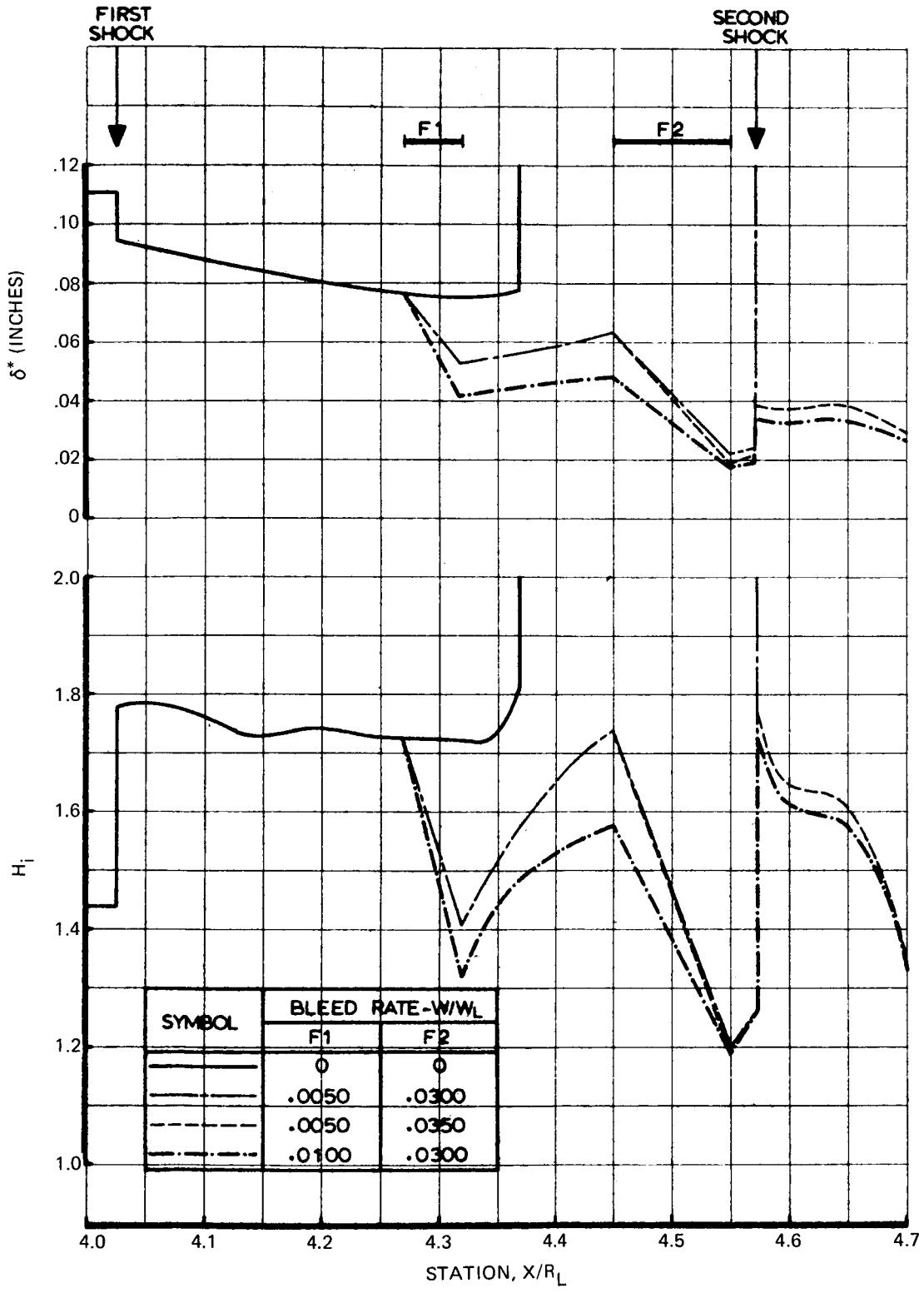

FIGURE 19.—FORWARD CENTERBODY BLEED REQUIREMENTS AT MACH 3.5

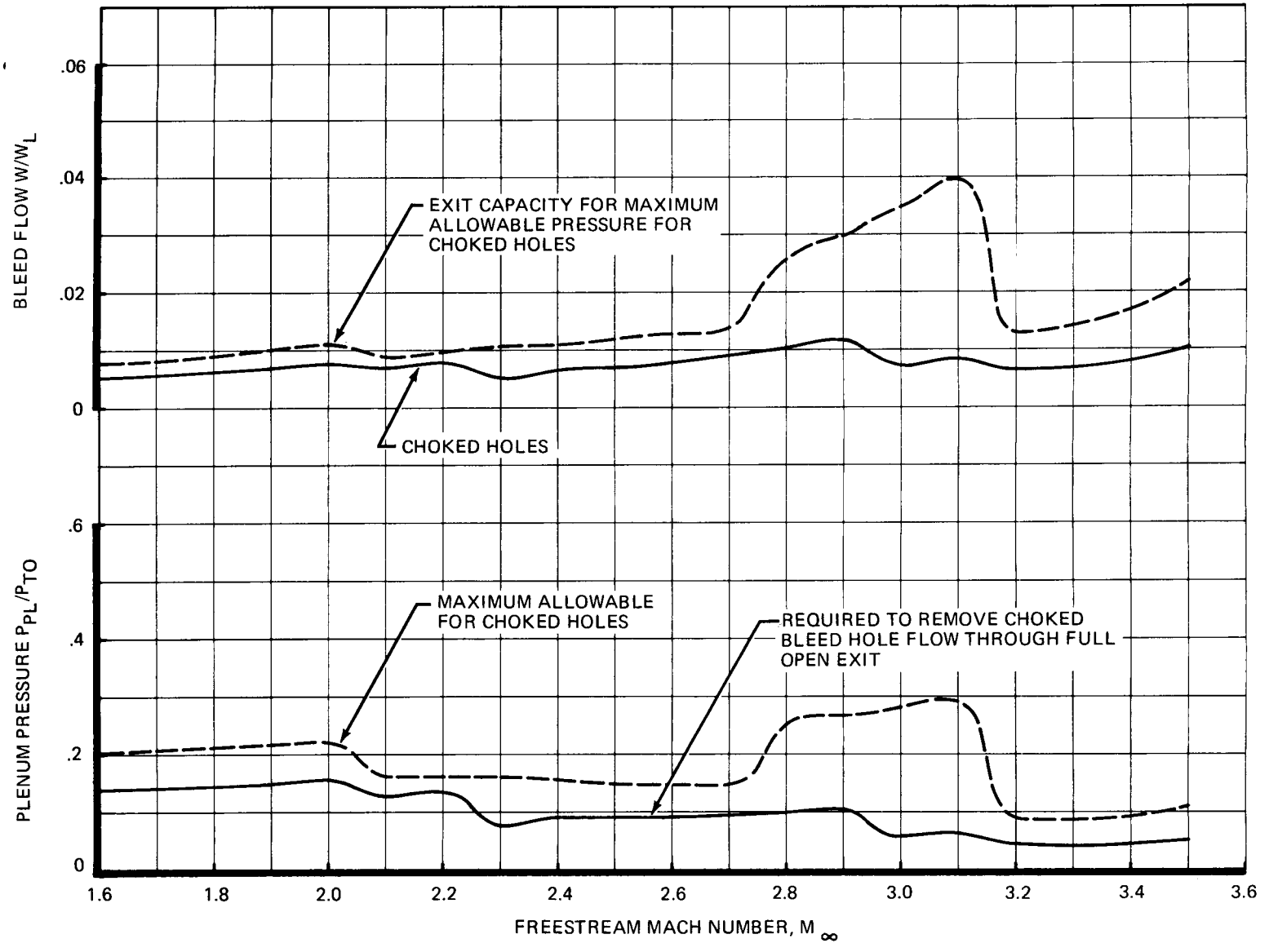

FIGURE 20.–FLOW RATES AND CAPACITY OF 25% DUCT AREA FOR FORWARD CENTERBODY BLEED

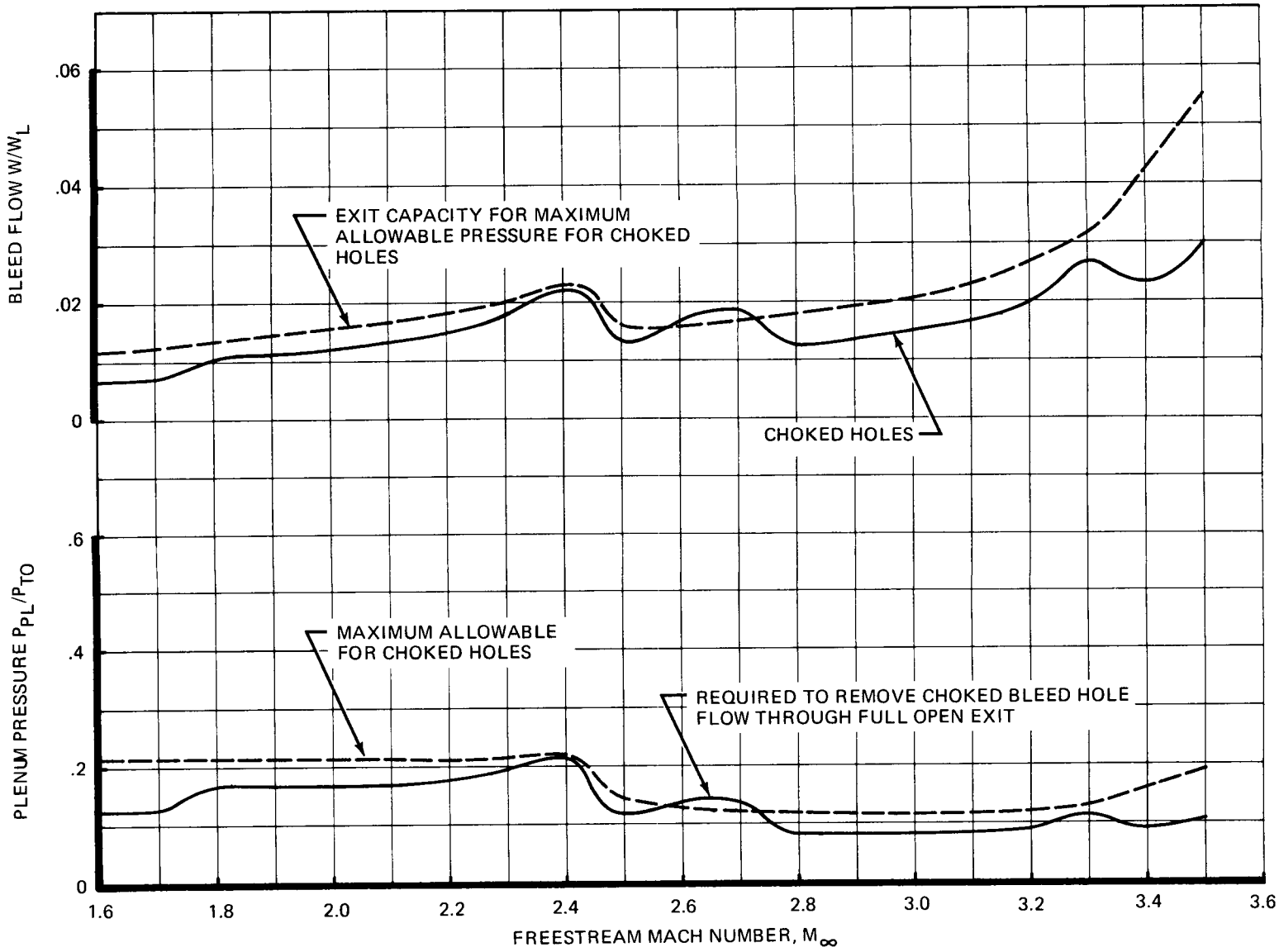

FIGURE 21.–FLOW RATES AND CAPACITY OF 50% DUCT AREA FOR FORWARD CENTERBODY BLEED

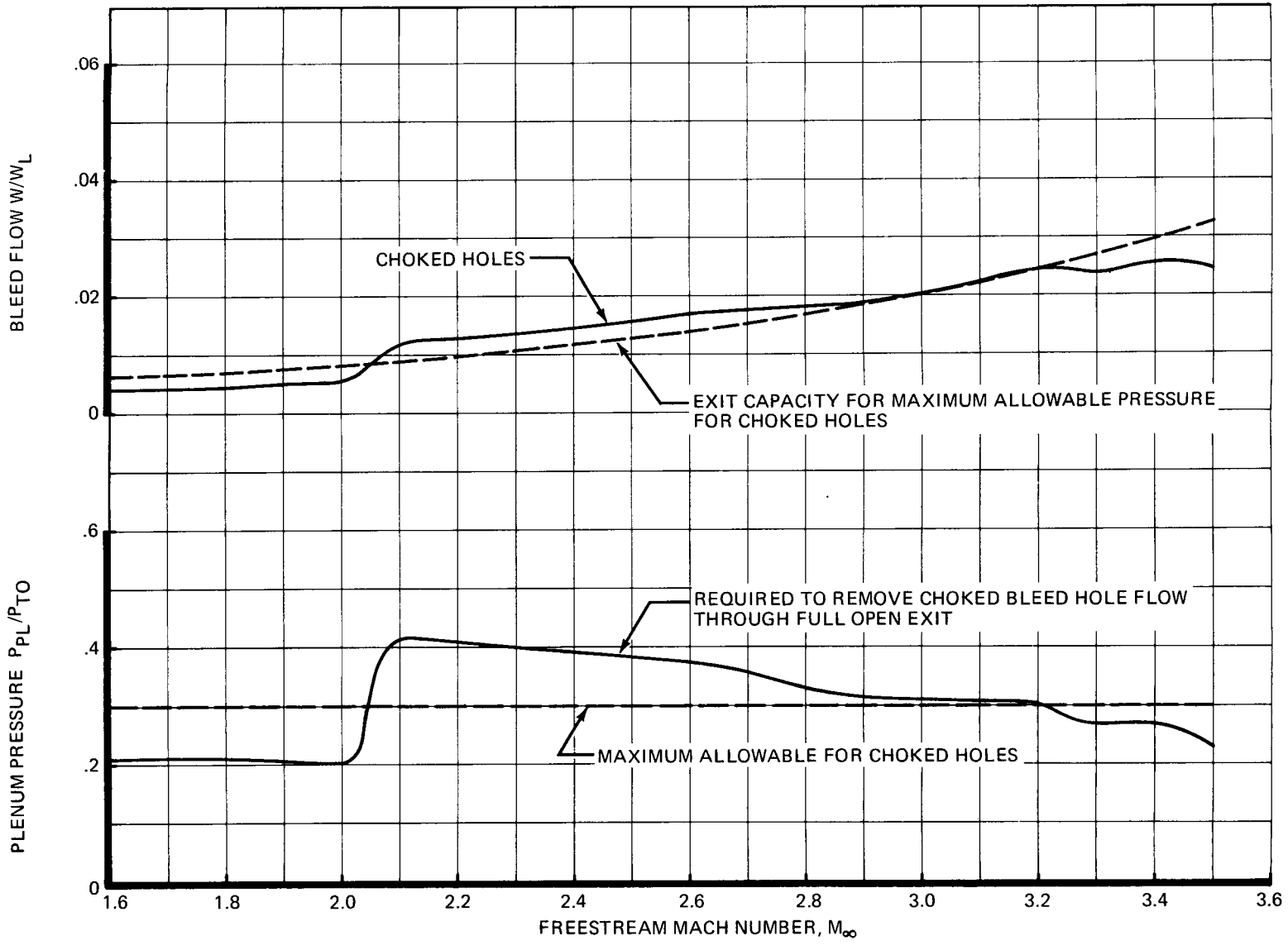

FIGURE 22.–FLOW RATES AND CAPACITY OF THROAT DUCT FOR CENTERBODY BLEED

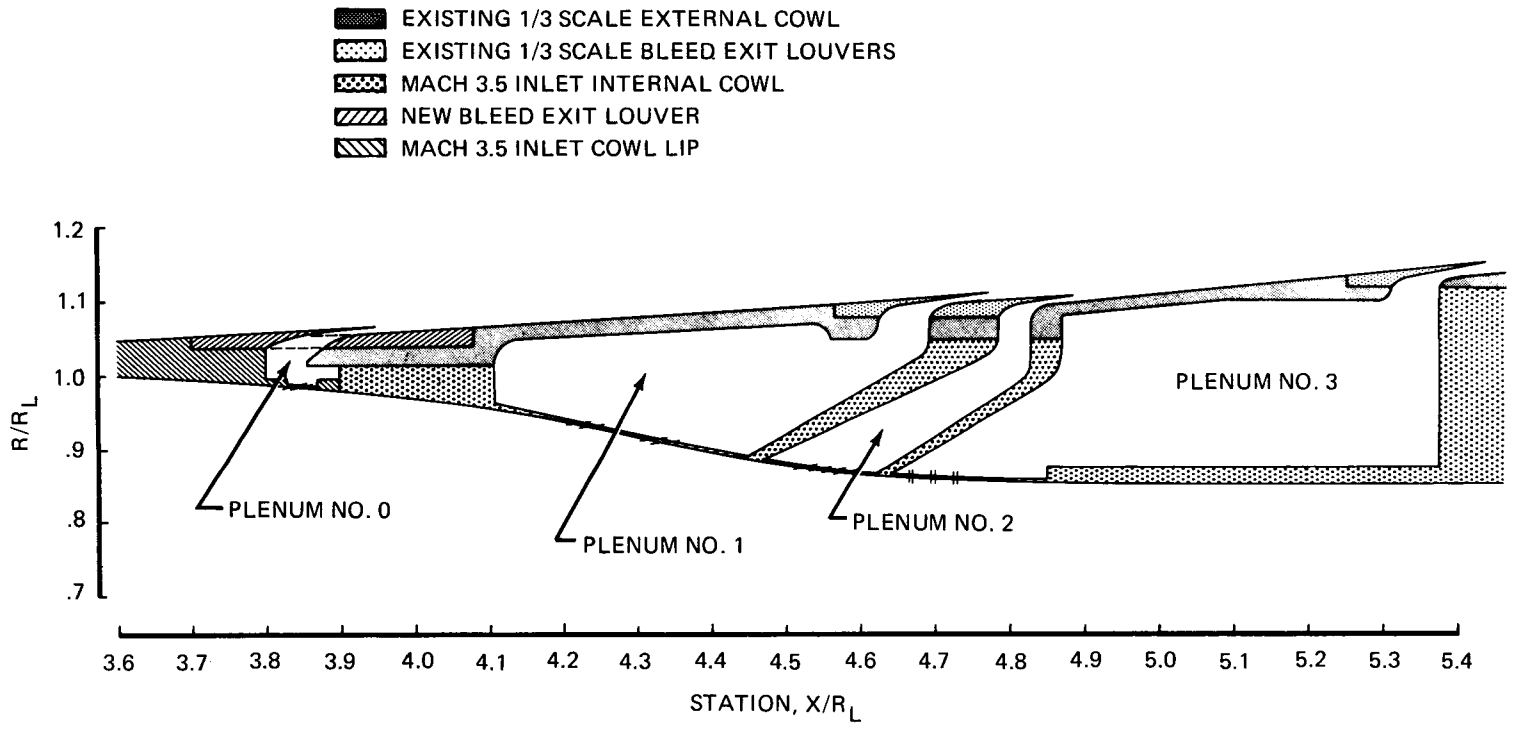

FIGURE 23.–COWL BLEED SYSTEM

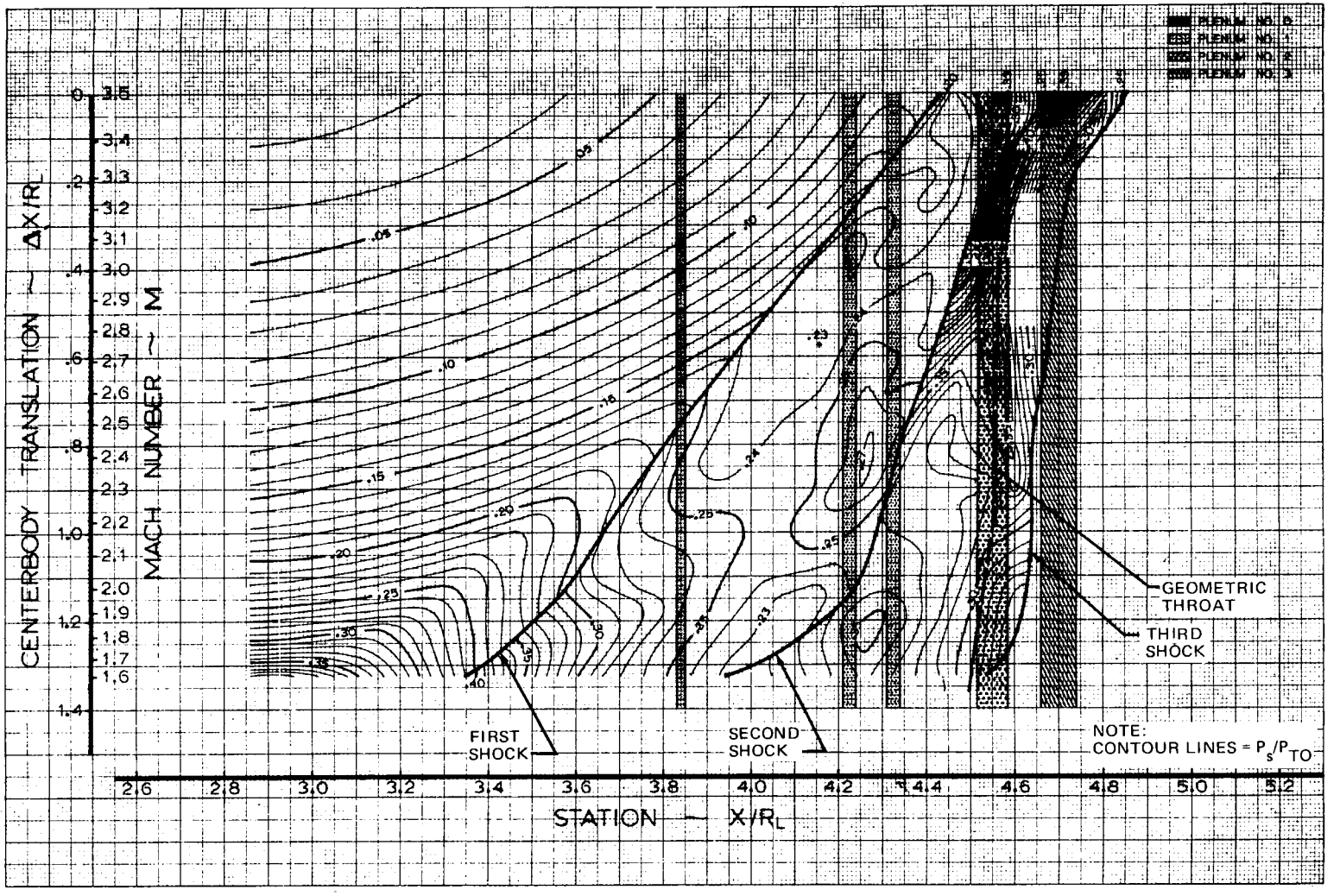

FIGURE 24.—BLEED BANDS SUPERIMPOSED ON INVISCID COWL SURFACE PRESSURE MAP

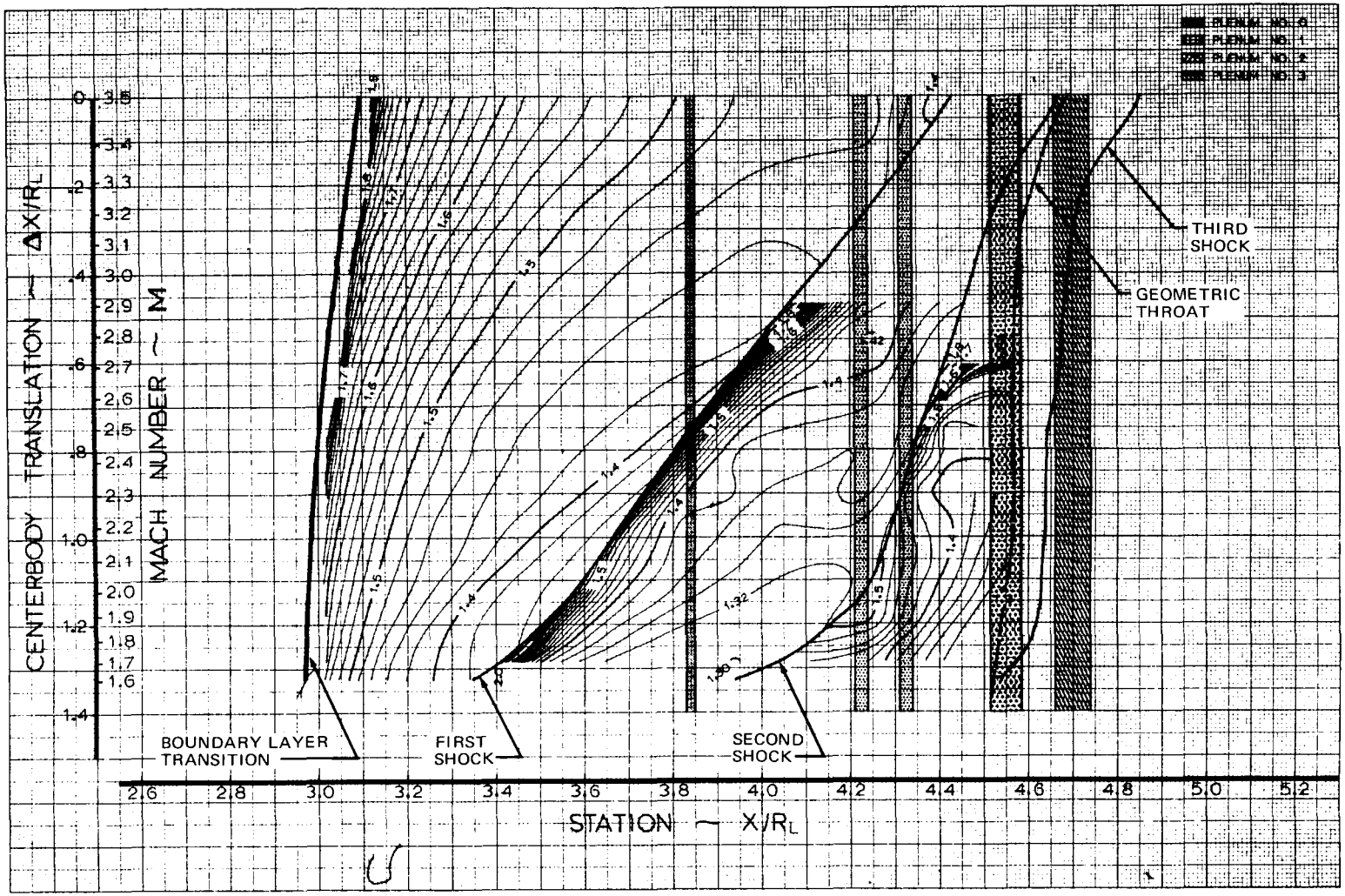

FIGURE 25.–BLEED BANDS SUPERIMPOSED ON COWL H_i MAP WITHOUT BLEED

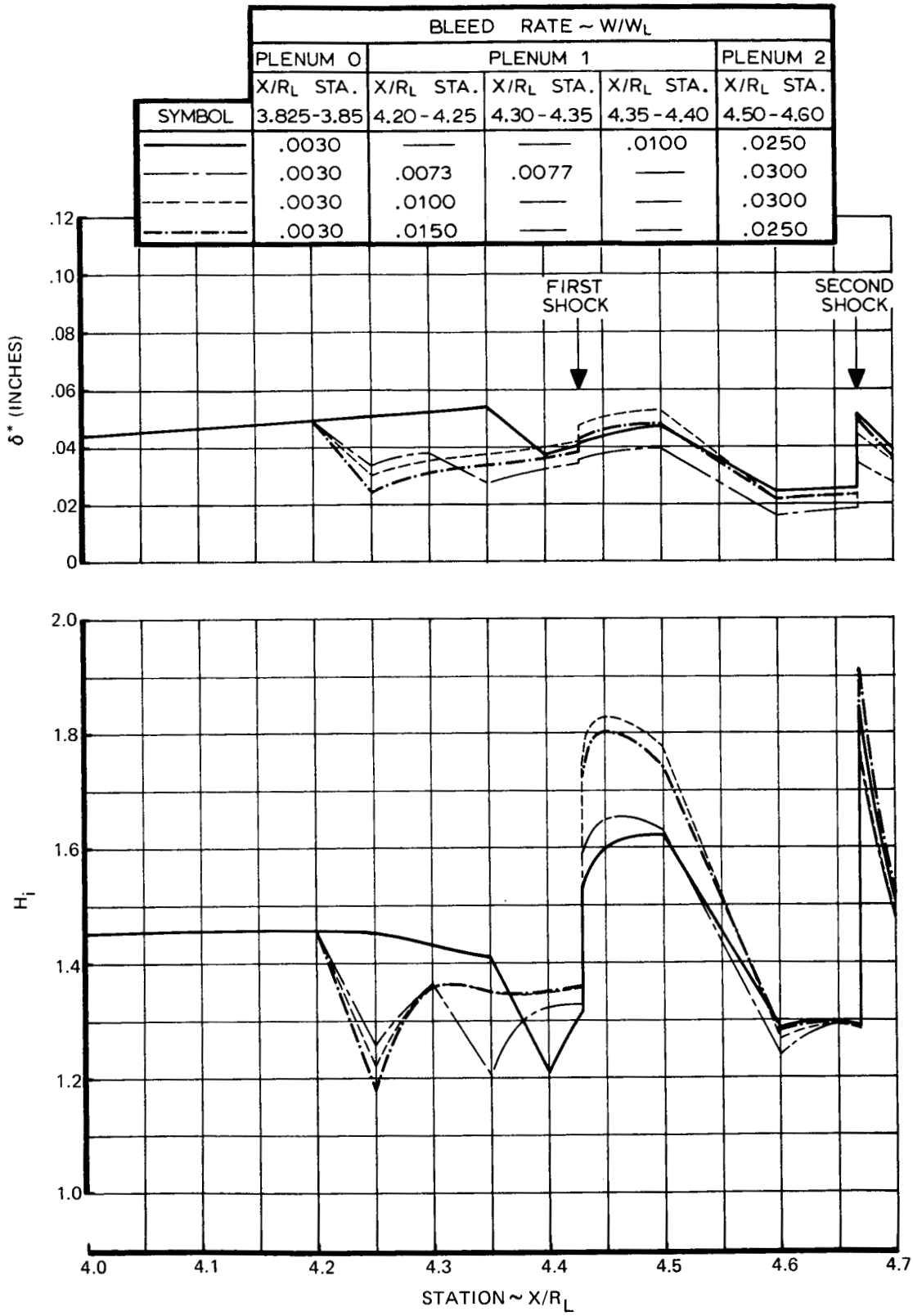

FIGURE 26.–FORWARD COWL BLEED REQUIREMENTS AT MACH 3.5

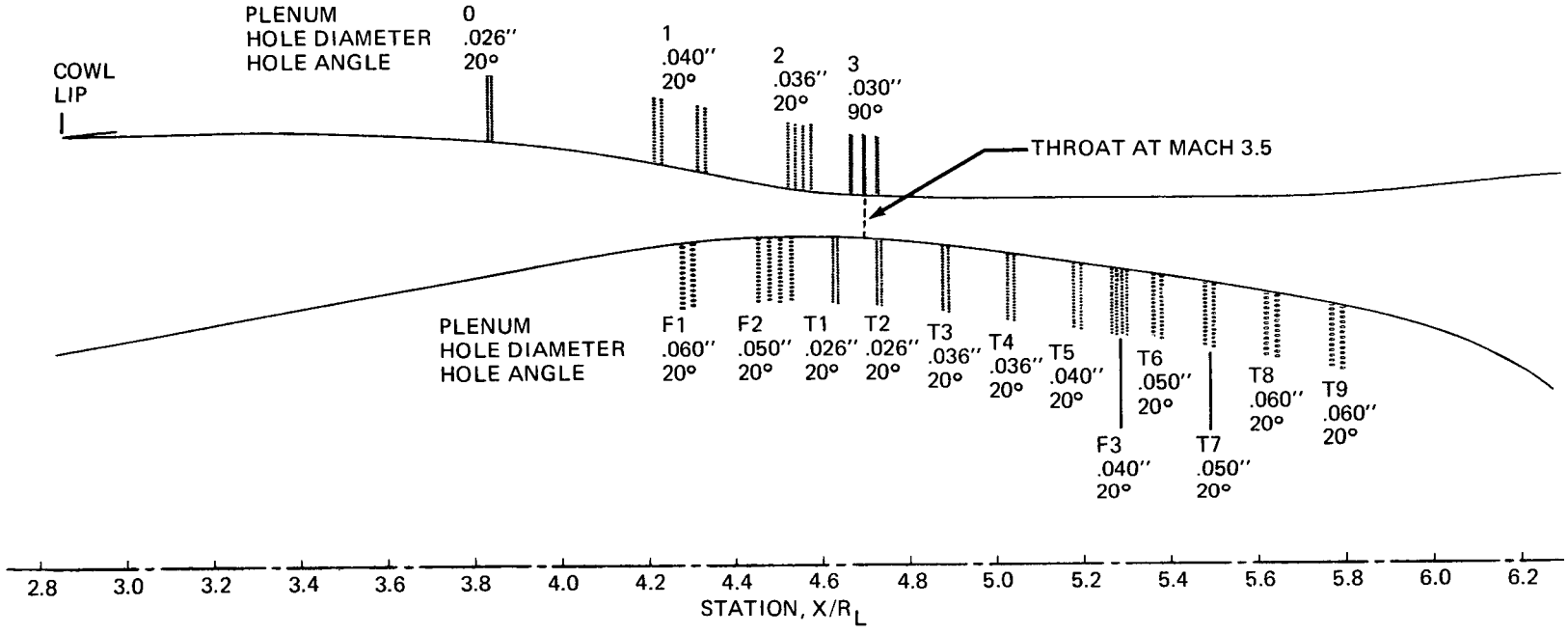

FIGURE 27.–INLET SCHEMATIC WITH PROPOSED BLEED HOLE PATTERN

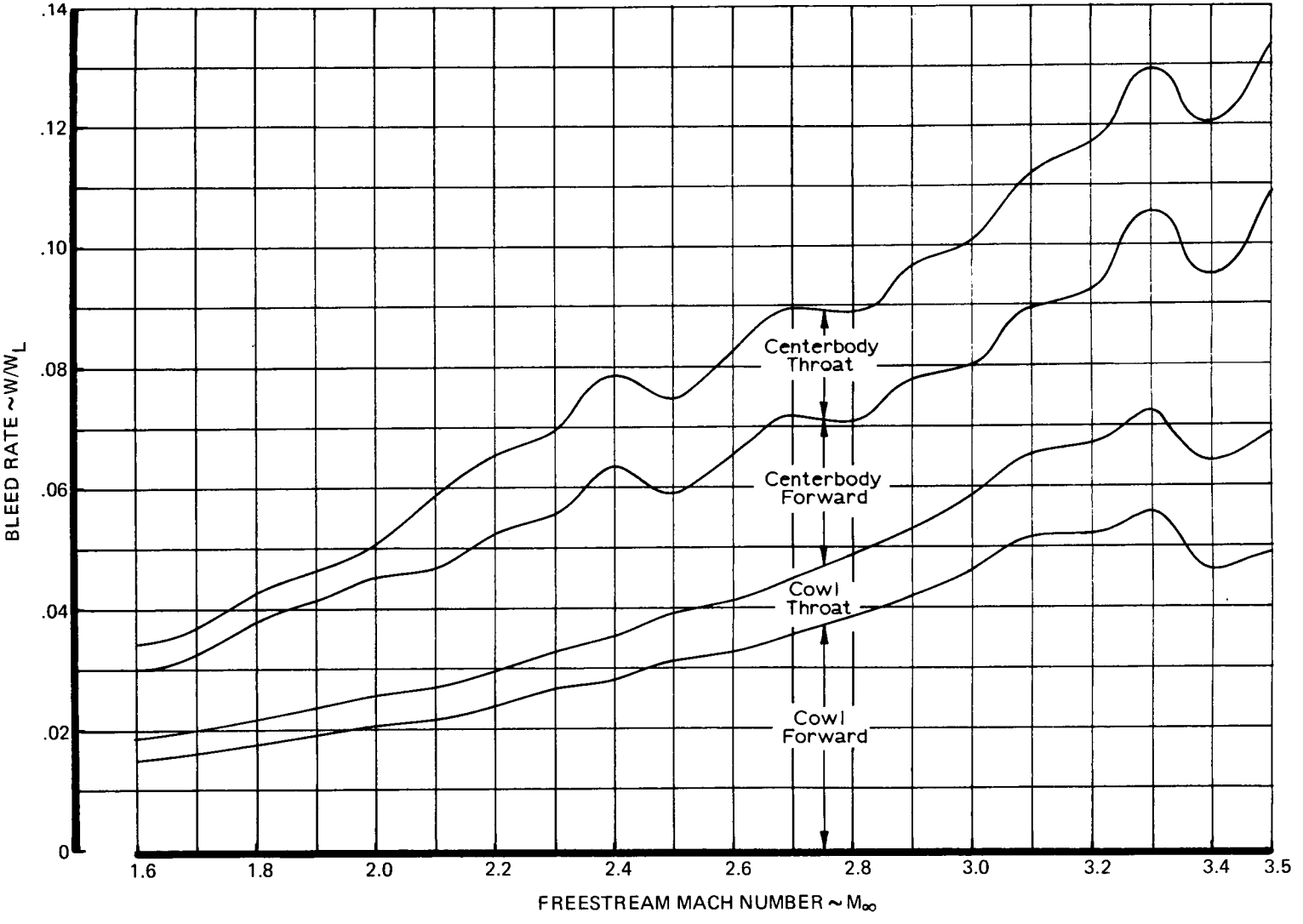

FIGURE 28.–INLET BLEED FLOW RATES IN THE STARTED MACH NUMBER RANGE

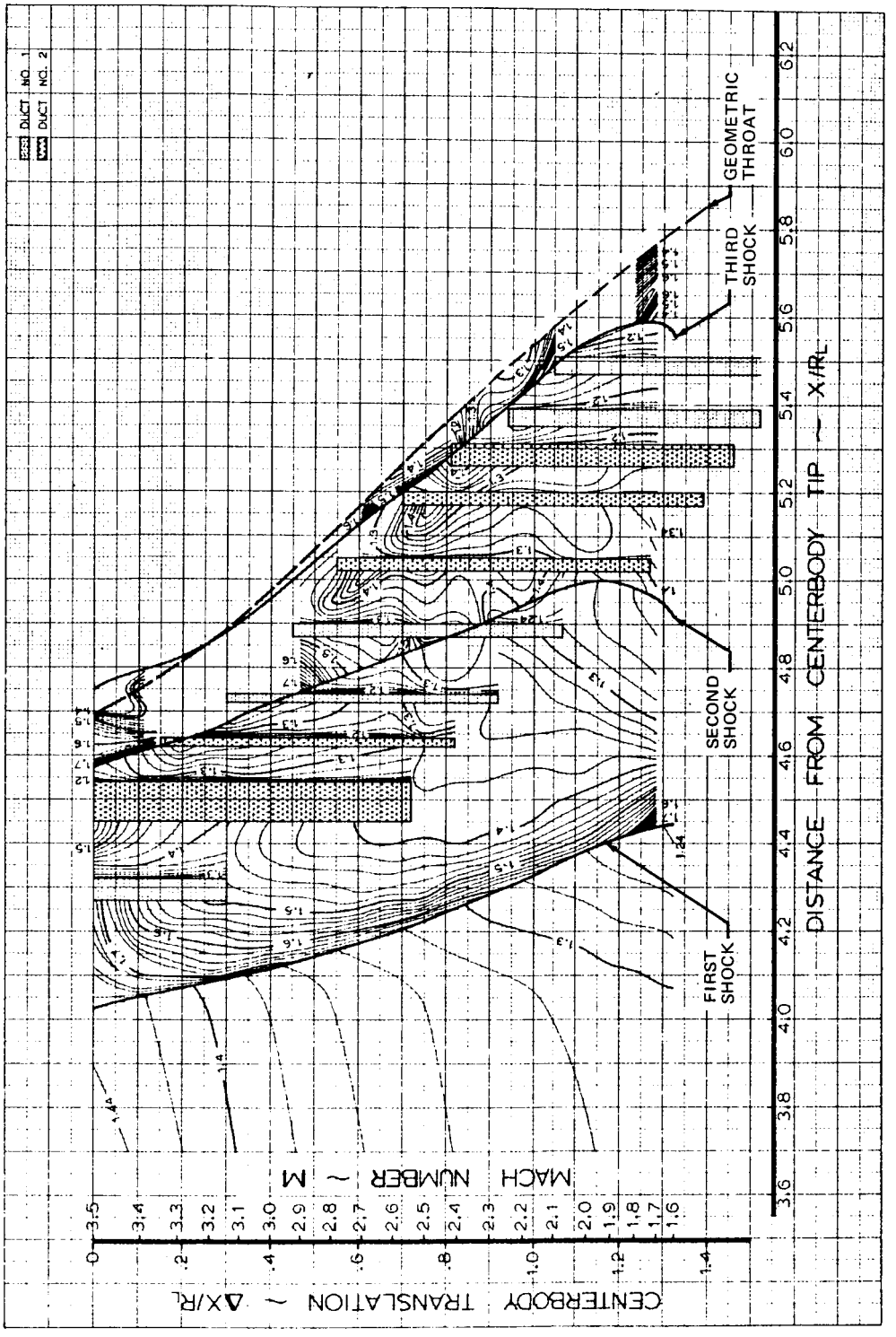

FIGURE 29.—CENTERBODY H_i MAP WITH PROPOSED BLEED SYSTEM

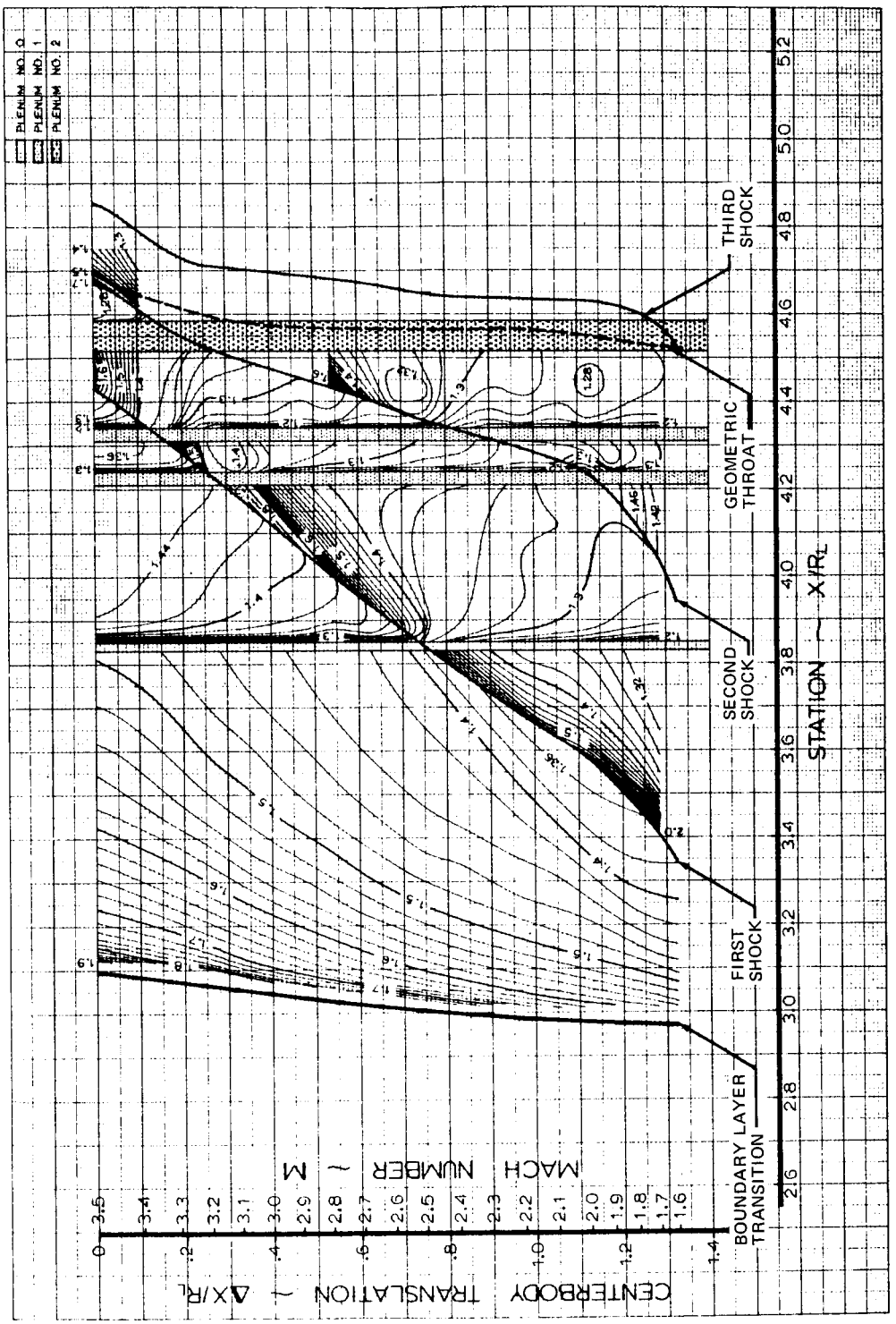

FIGURE 30.–COWL H_1 MAP WITH PROPOSED BLEED SYSTEM

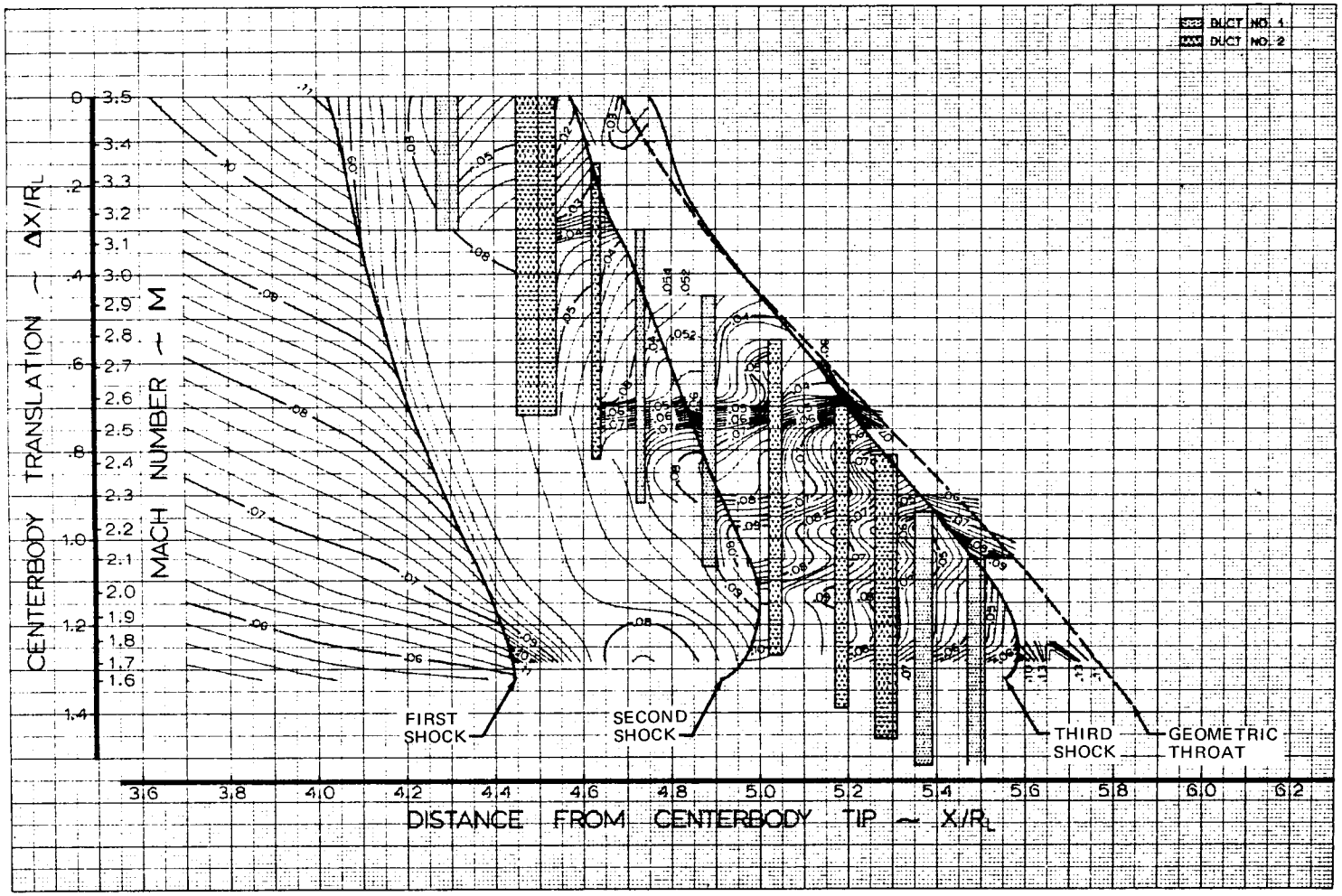

FIGURE 31.–MAP OF CENTERBODY BOUNDARY LAYER DISPLACEMENT THICKNESS, δ, WITH PROPOSED BLEED SYSTEM*

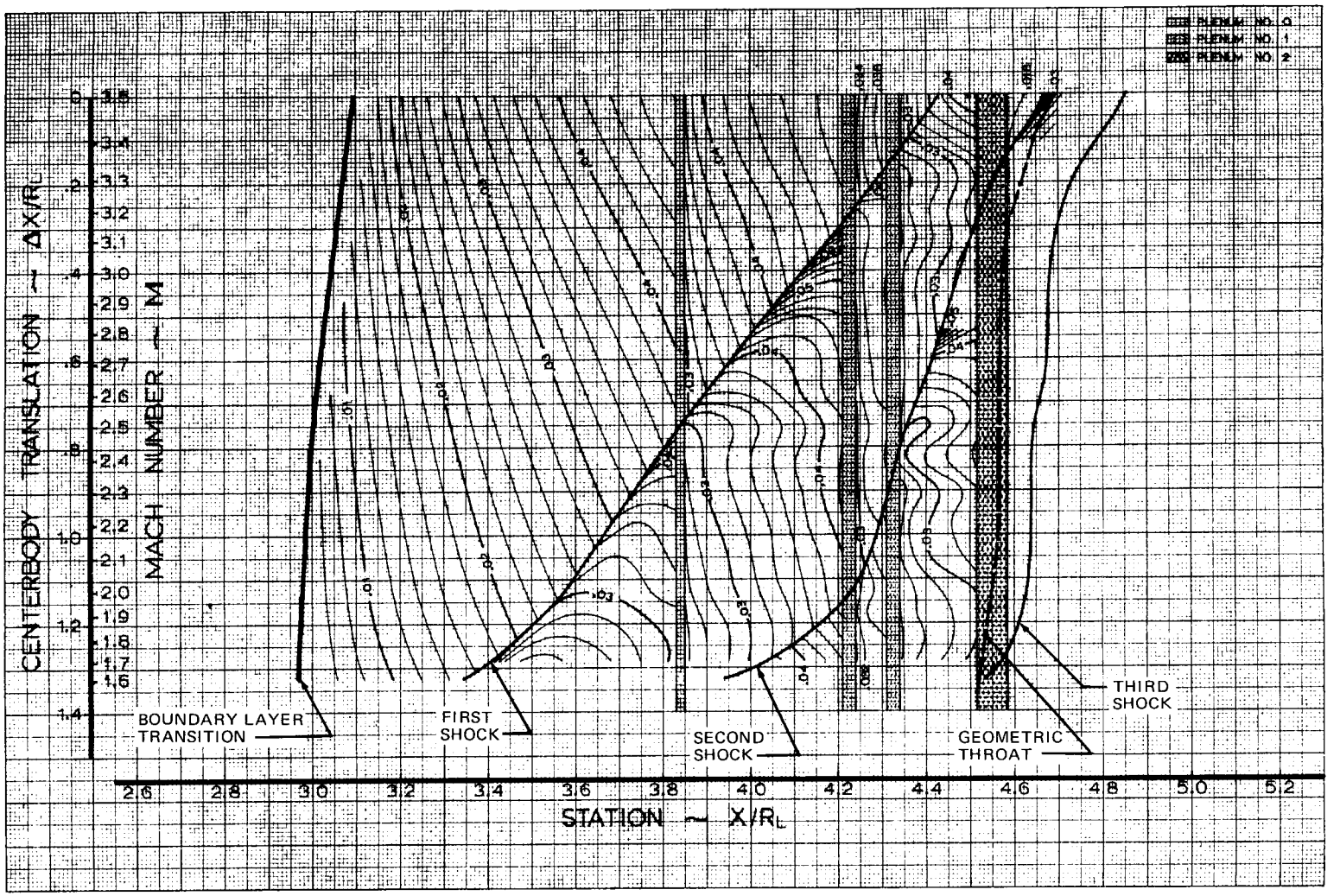

FIGURE 32.–MAP OF COWL BOUNDARY LAYER DISPLACEMENT THICKNESS, δ, WITH PROPOSED BLEED SYSTEM*

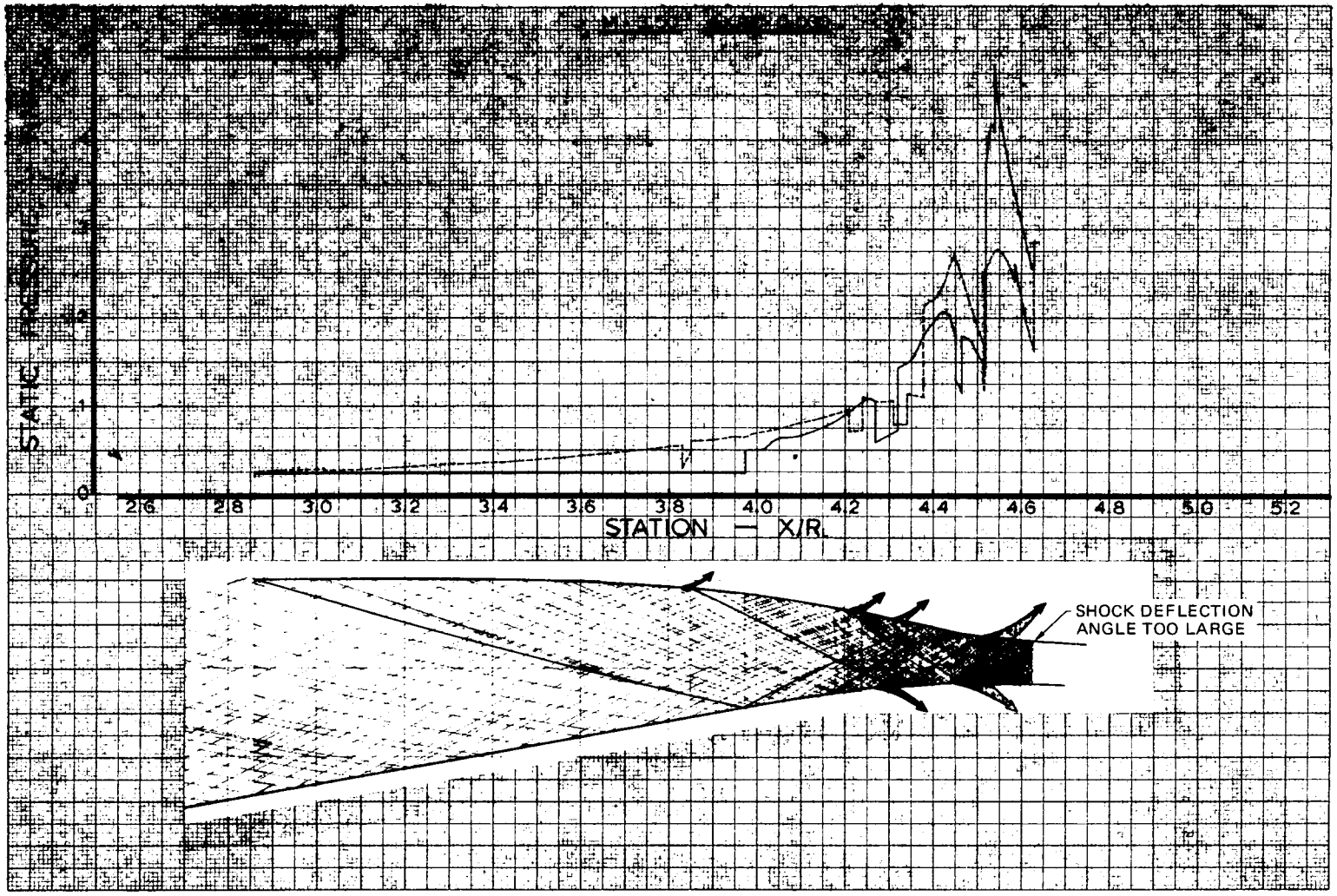

FIGURE 33.—COMBINED FLOWFIELD ANALYSIS, MACH 3.5

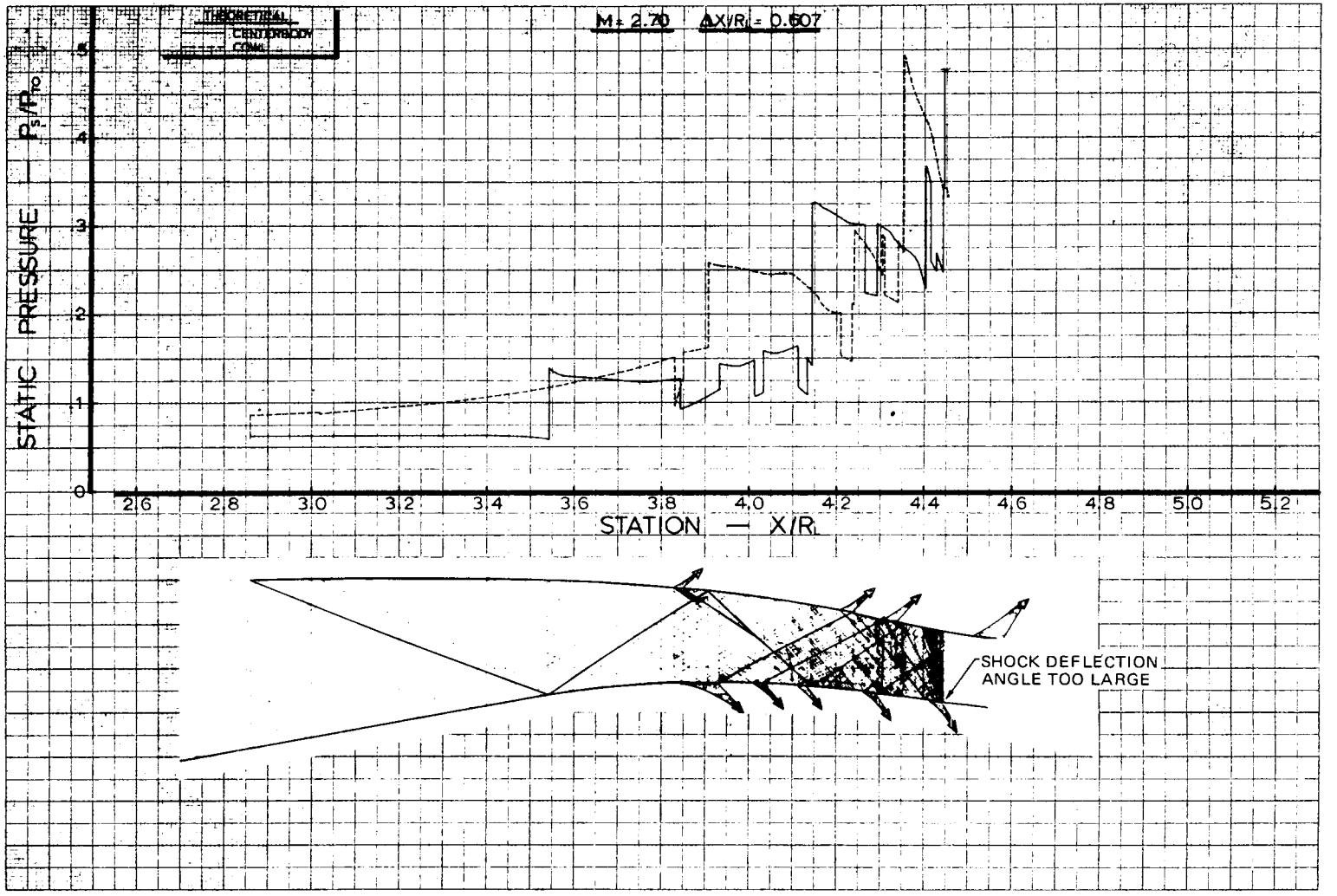

FIGURE 34.–COMBINED FLOWFIELD ANALYSIS, MACH 2.7

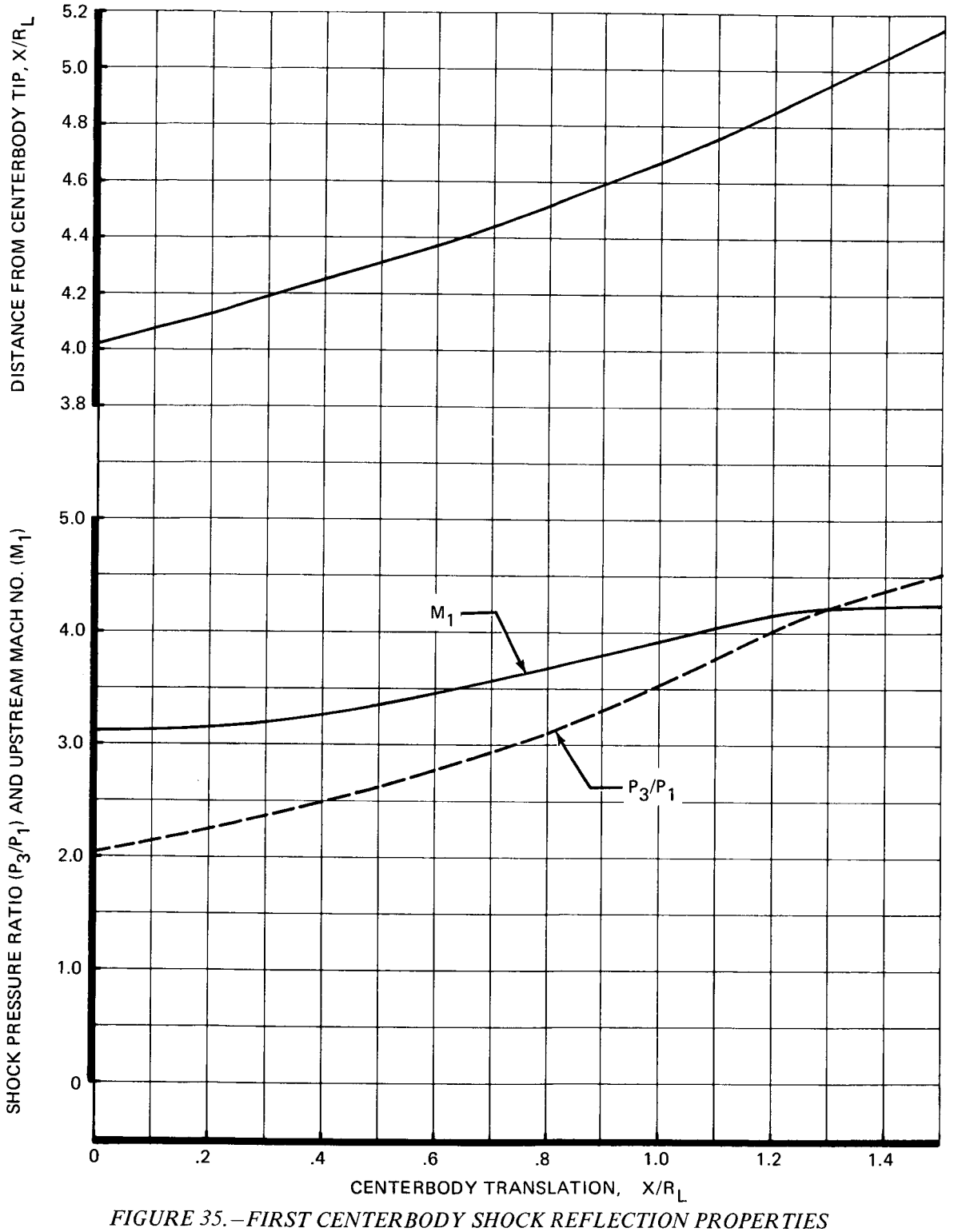

FIGURE 35.–FIRST CENTERBODY SHOCK REFLECTION PROPERTIES DURING RESTART AT MACH 3.5

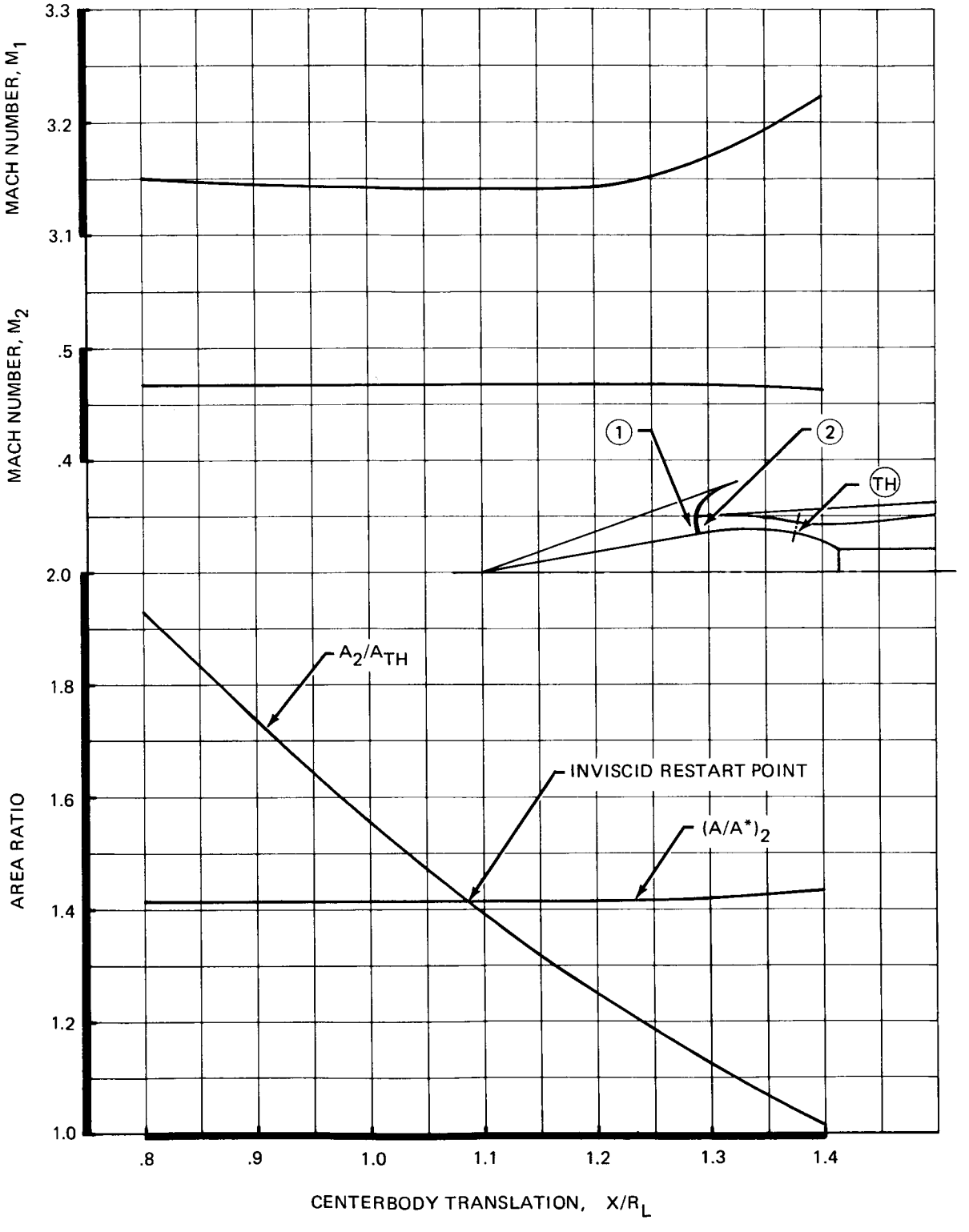

FIGURE 36.–MACH 3.5 RESTART POSITION

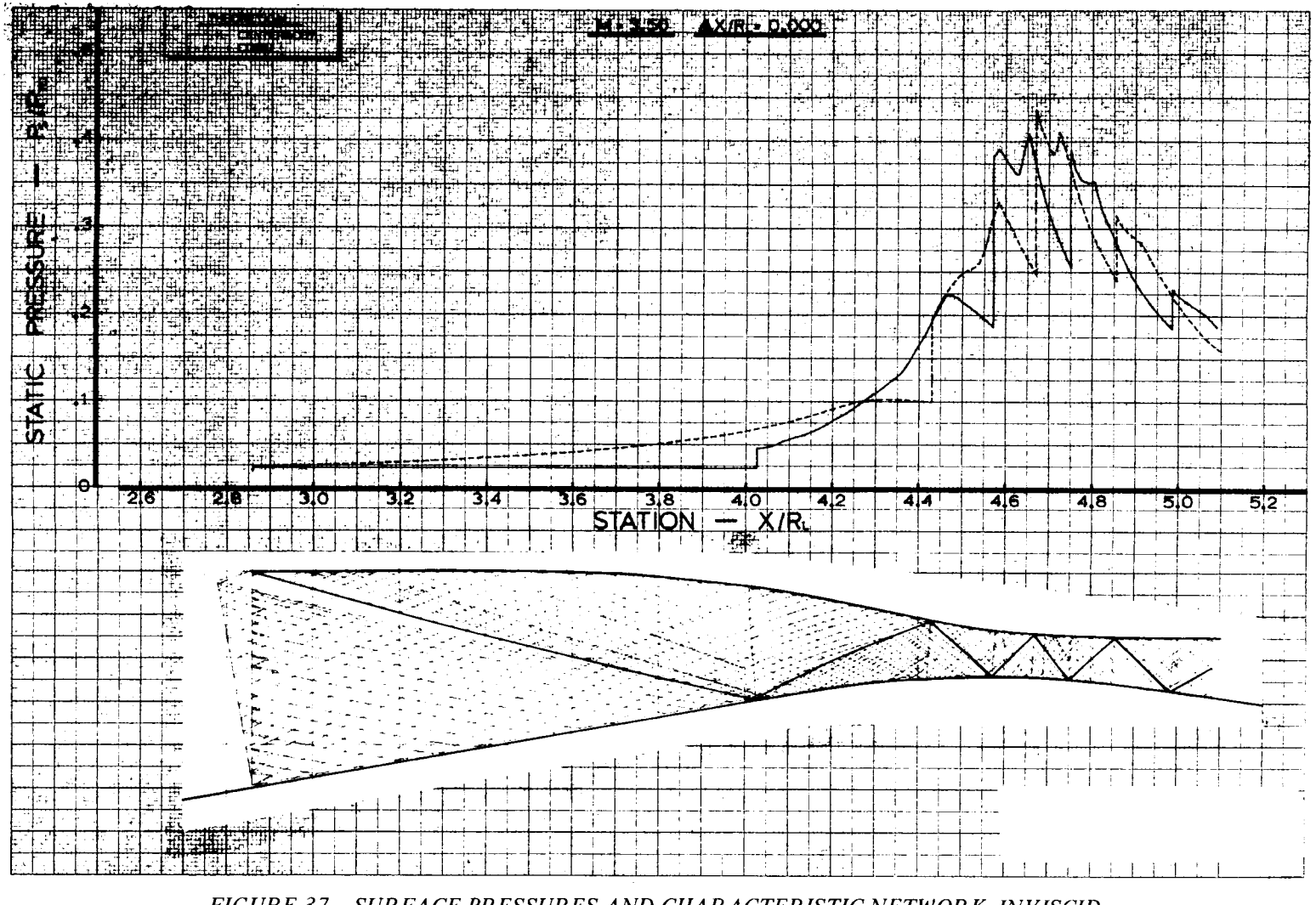

FIGURE 37.—SURFACE PRESSURES AND CHARACTERISTIC NETWORK. INVISCID ANALYSIS, MACH 3.5

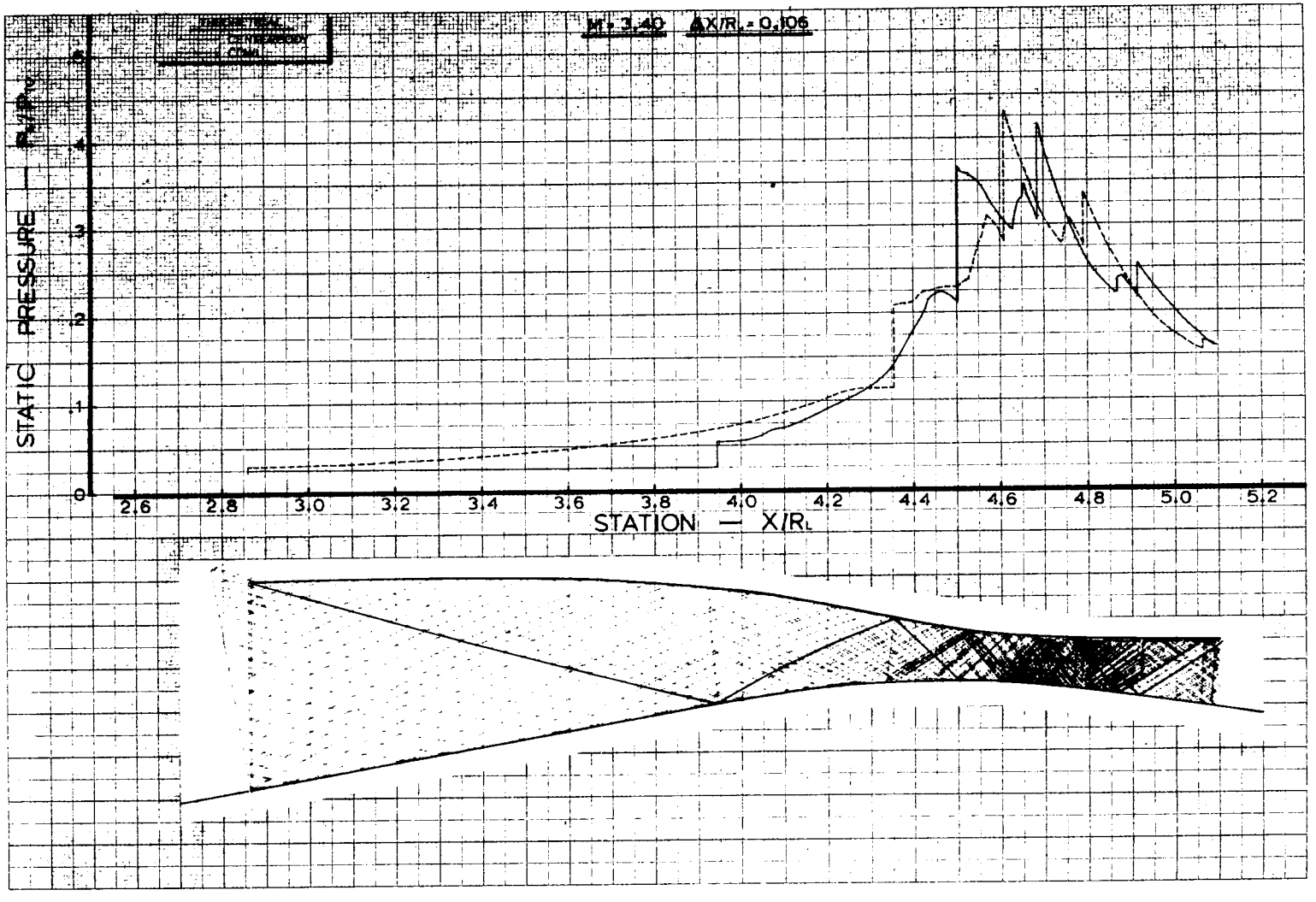

FIGURE 38.–SURFACE PRESSURES AND CHARACTERISTIC NETWORK. INVISCID ANALYSIS, MACH 3.4

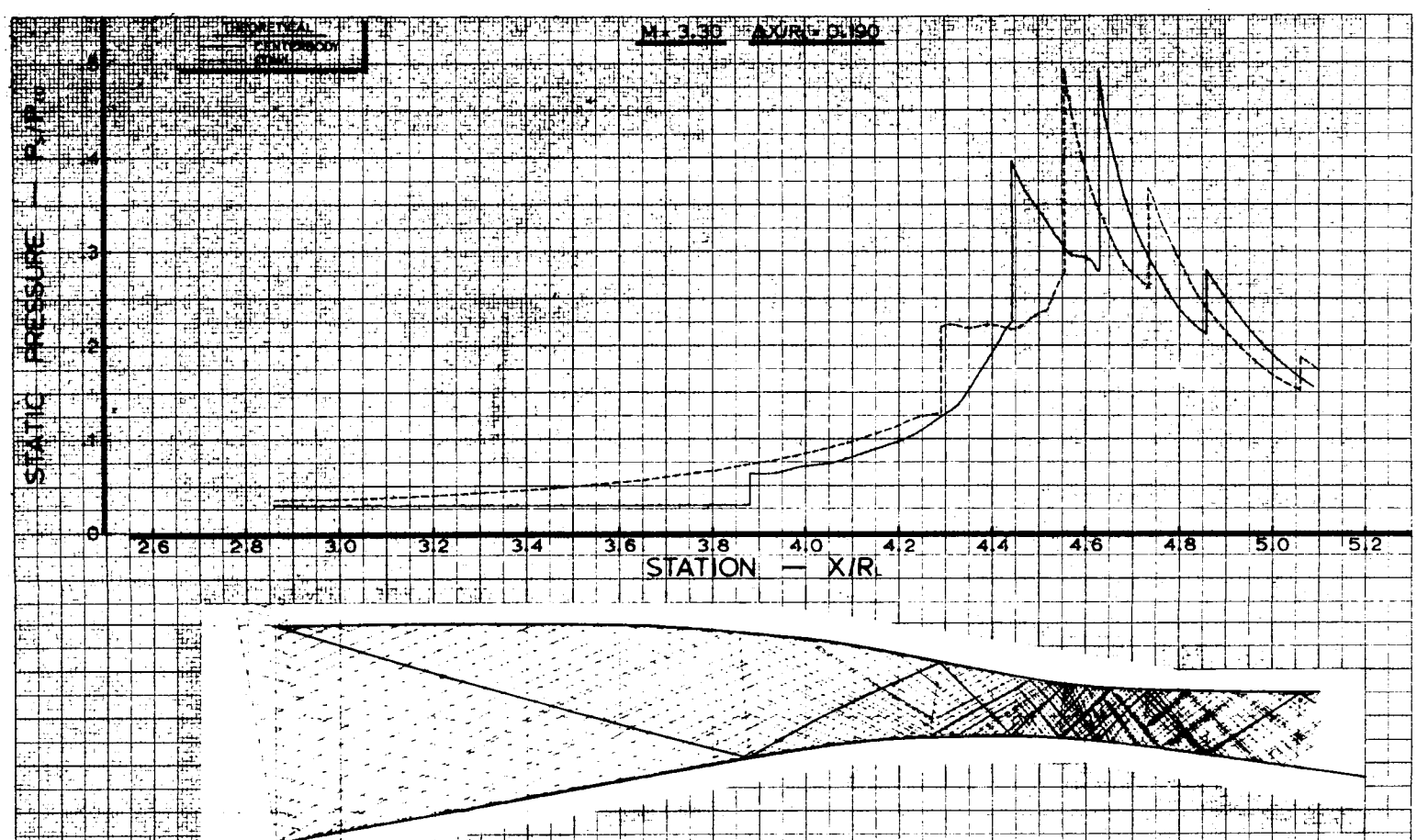

FIGURE 39.–SURFACE PRESSURES AND CHARACTERISTIC NETWORK. INVISCID ANALYSIS, MACH 3.3

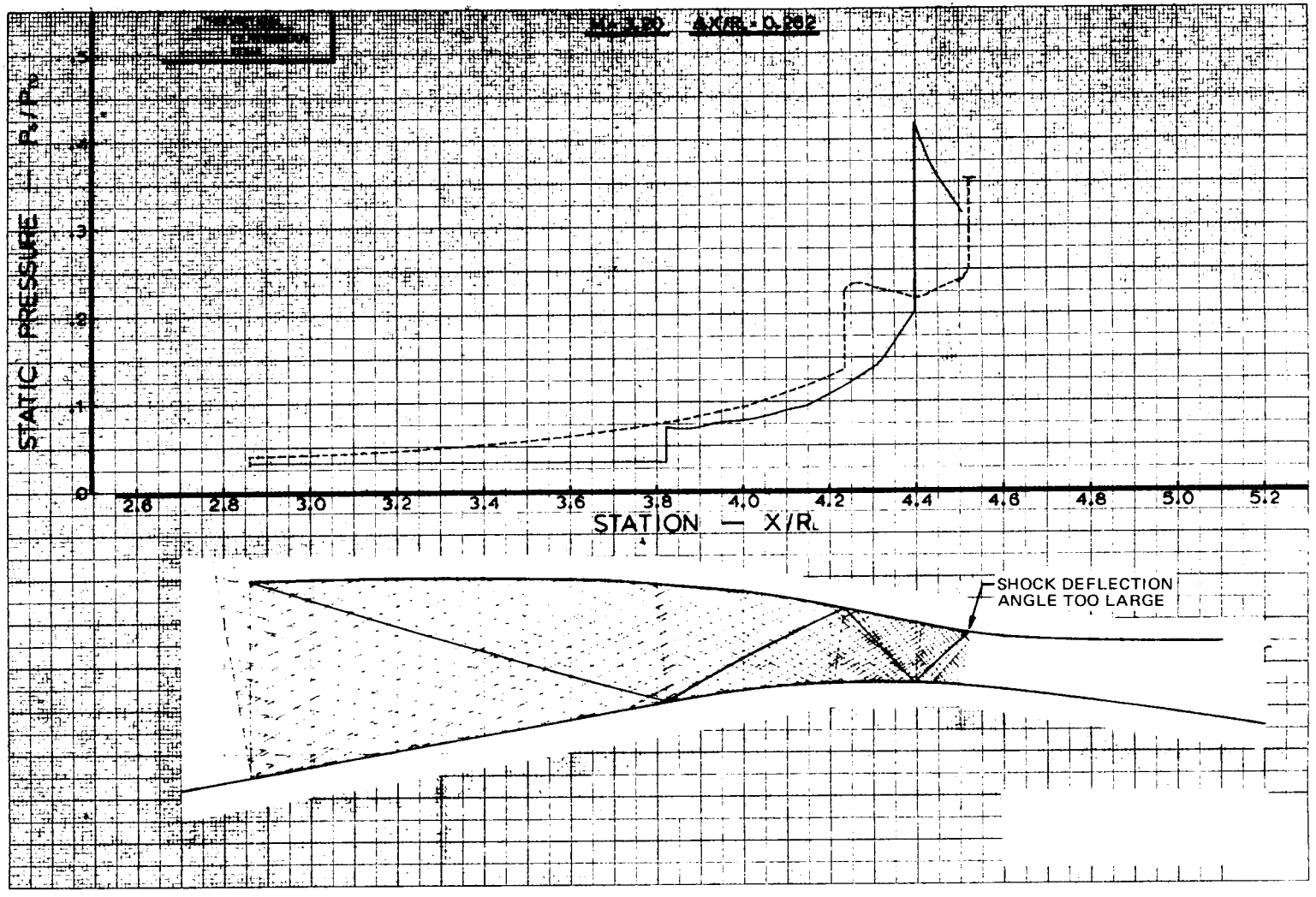

FIGURE 40.—SURFACE PRESSURES AND CHARACTERISTIC NETWORK. INVISCID ANALYSIS, MACH 3.2

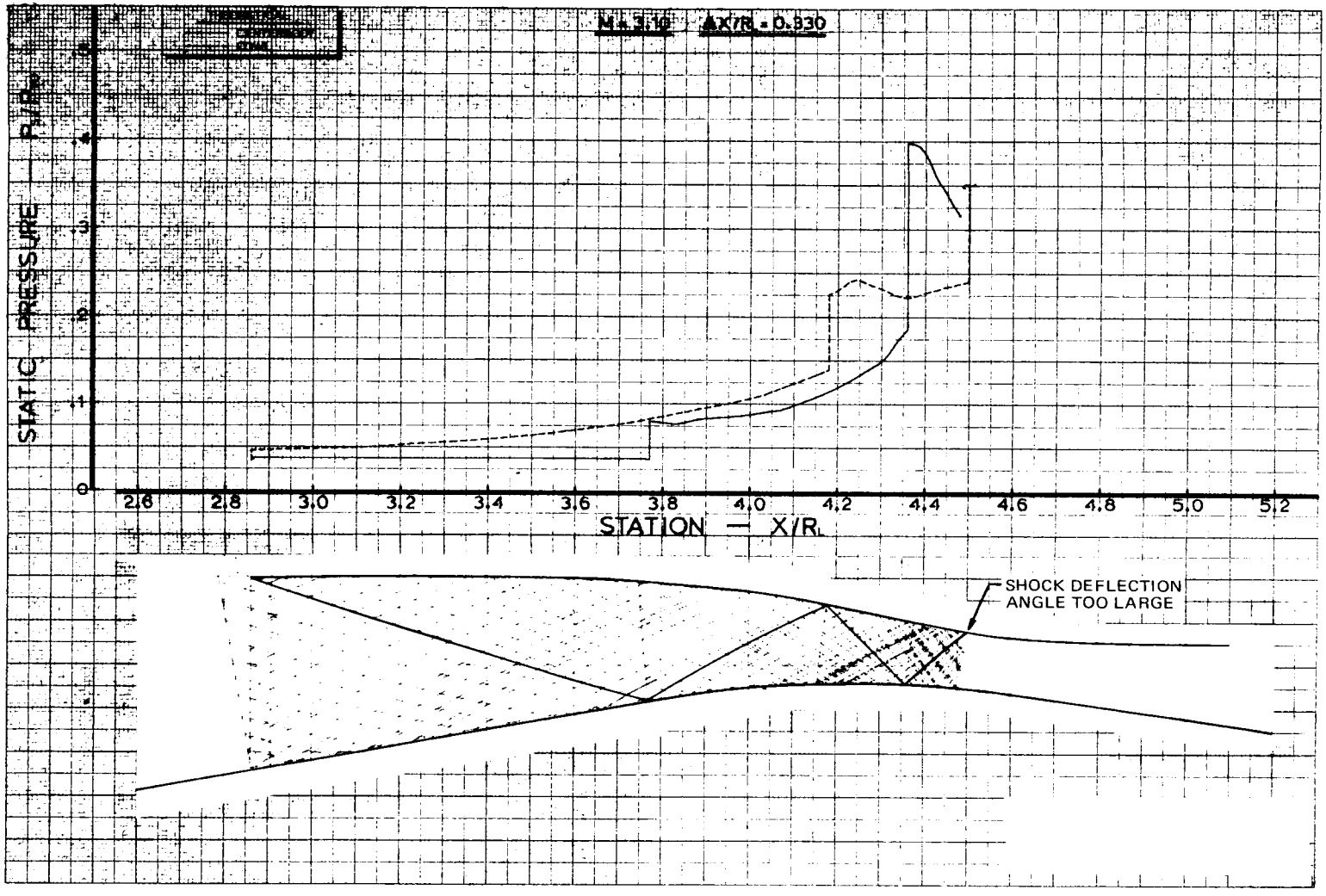

FIGURE 41.– SURFACE PRESSURES AND CHARACTERISTIC NETWORK. INVISCID ANALYSIS, MACH 3.1

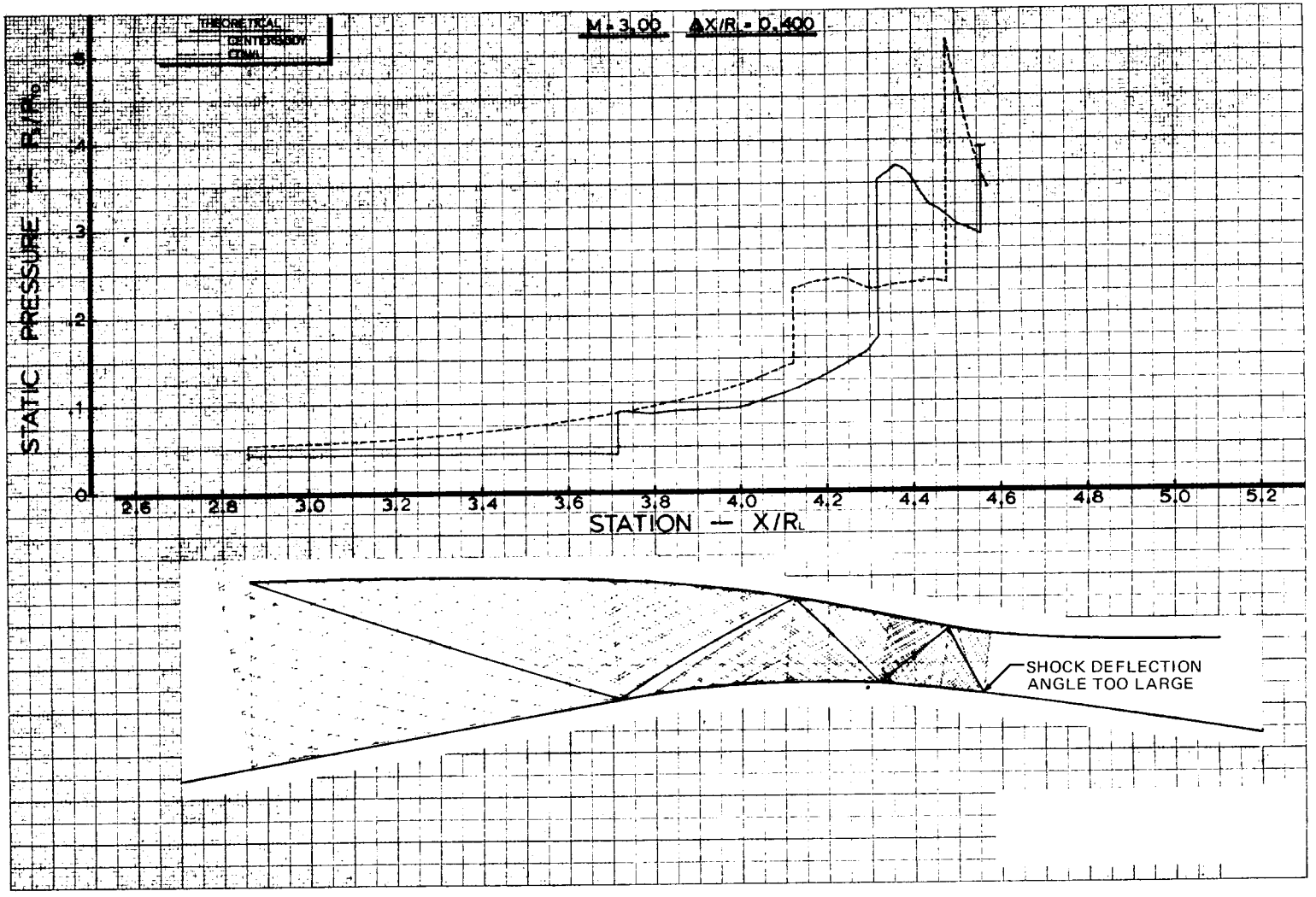

FIGURE 42.– SURFACE PRESSURES AND CHARACTERISTIC NETWORK. INVISCID ANALYSIS, MACH 3.0

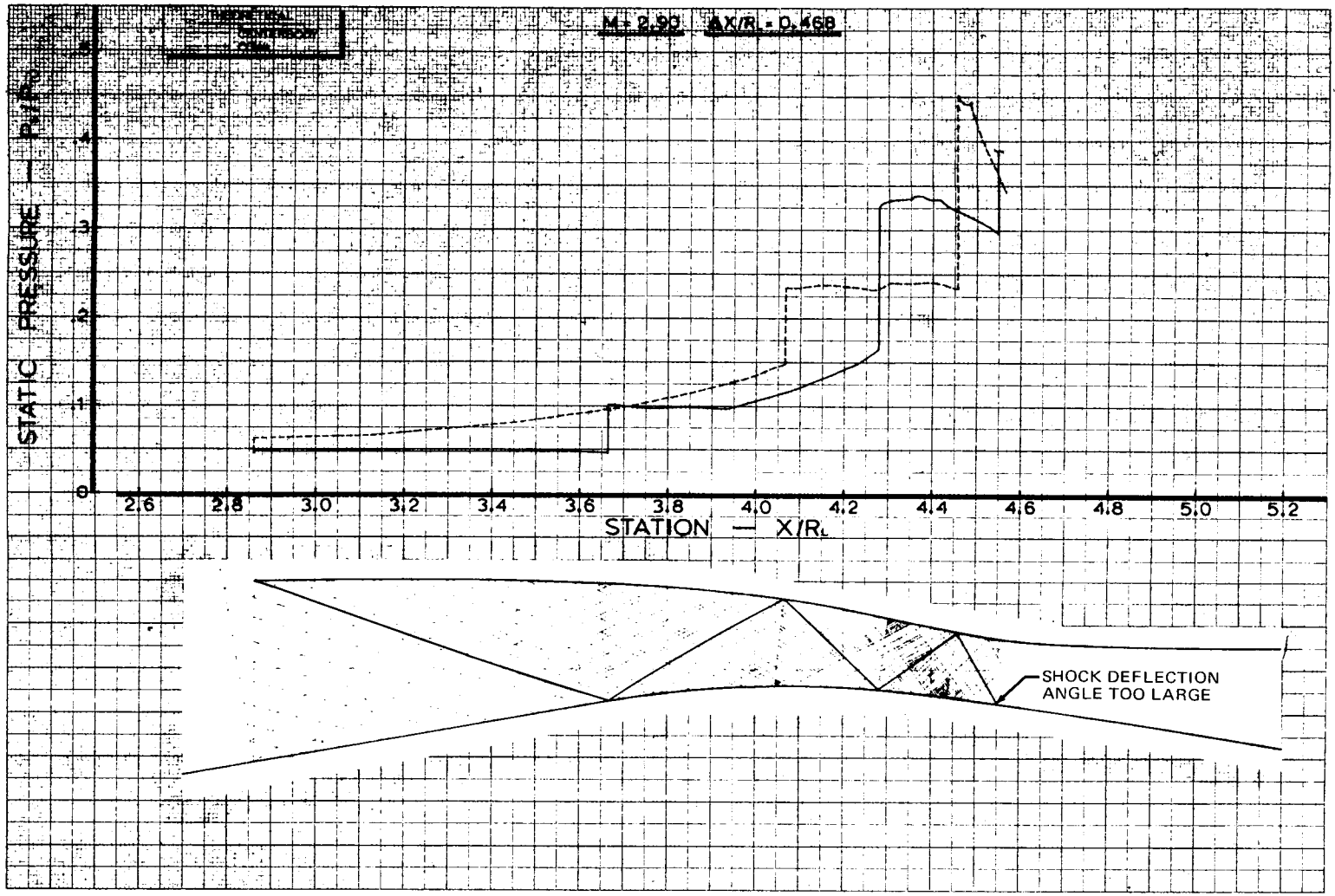

FIGURE 43.—SURFACE PRESSURES AND CHARACTERISTIC NETWORK. INVISCID ANALYSIS, MACH 2.9

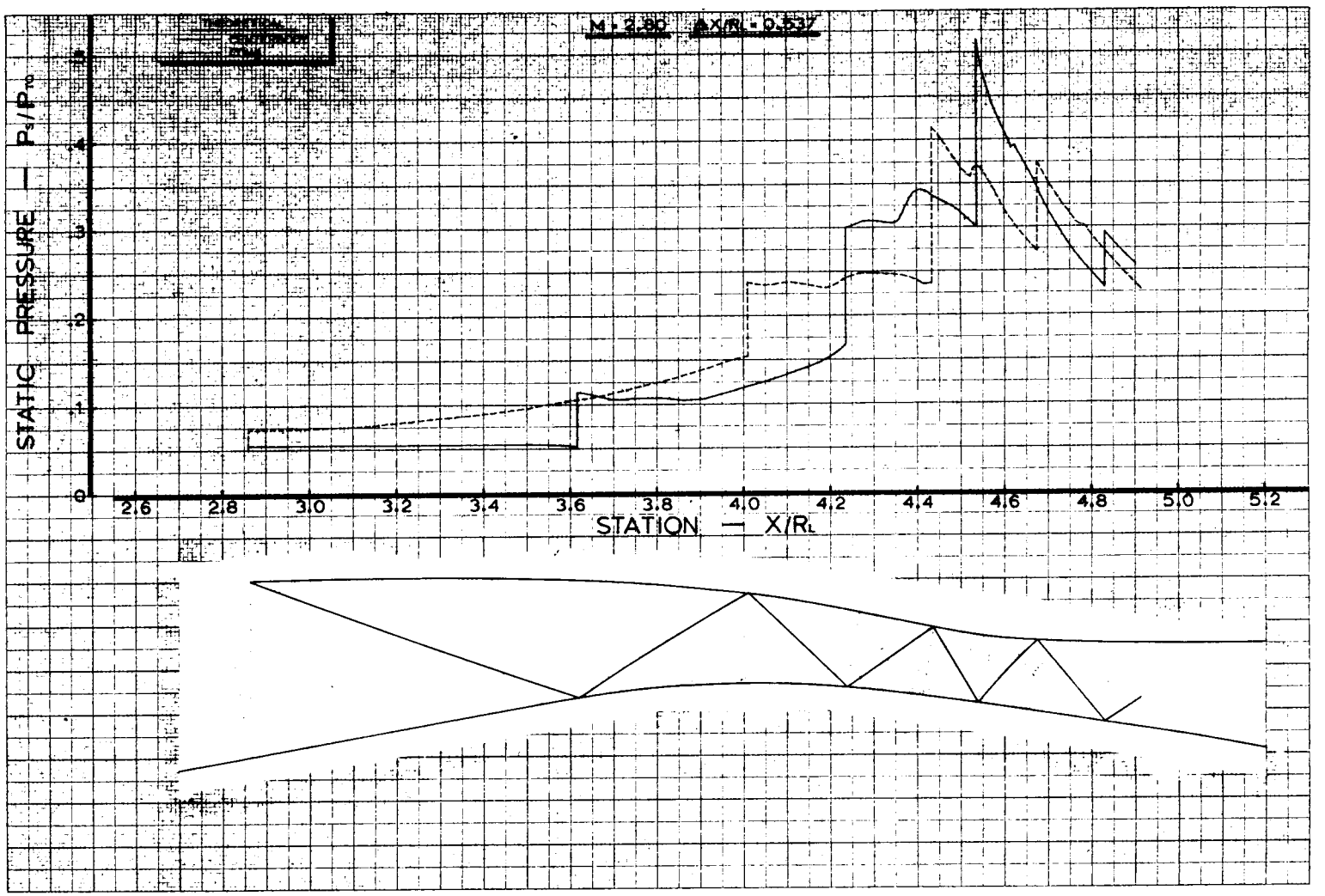

FIGURE 44.—SURFACE PRESSURES AND CHARACTERISTIC NETWORK. INVISCID ANALYSIS, MACH 2.8

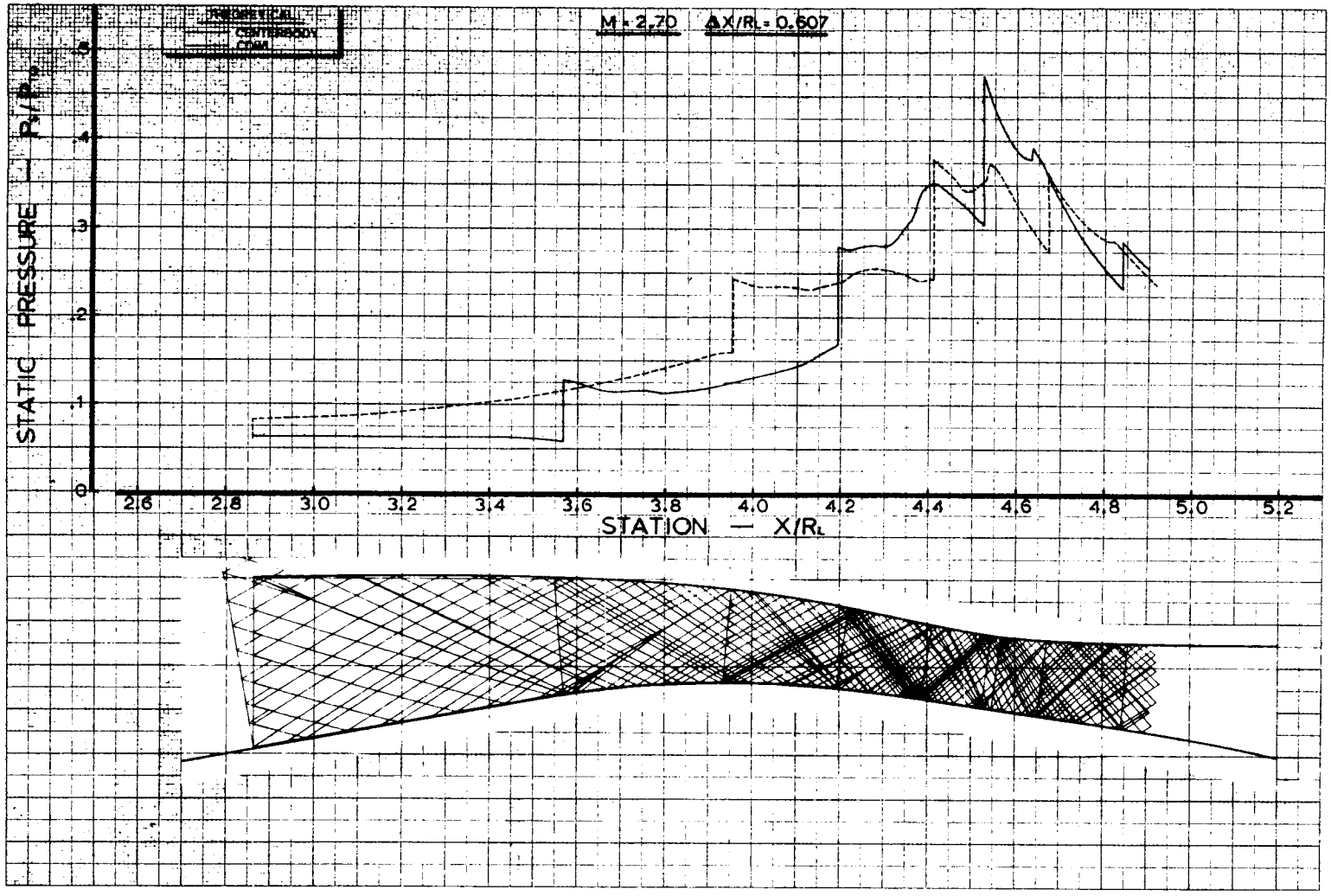

FIGURE 45.—SURFACE PRESSURES AND CHARACTERISTIC NETWORK. INVISCID ANALYSIS, MACH 2.7

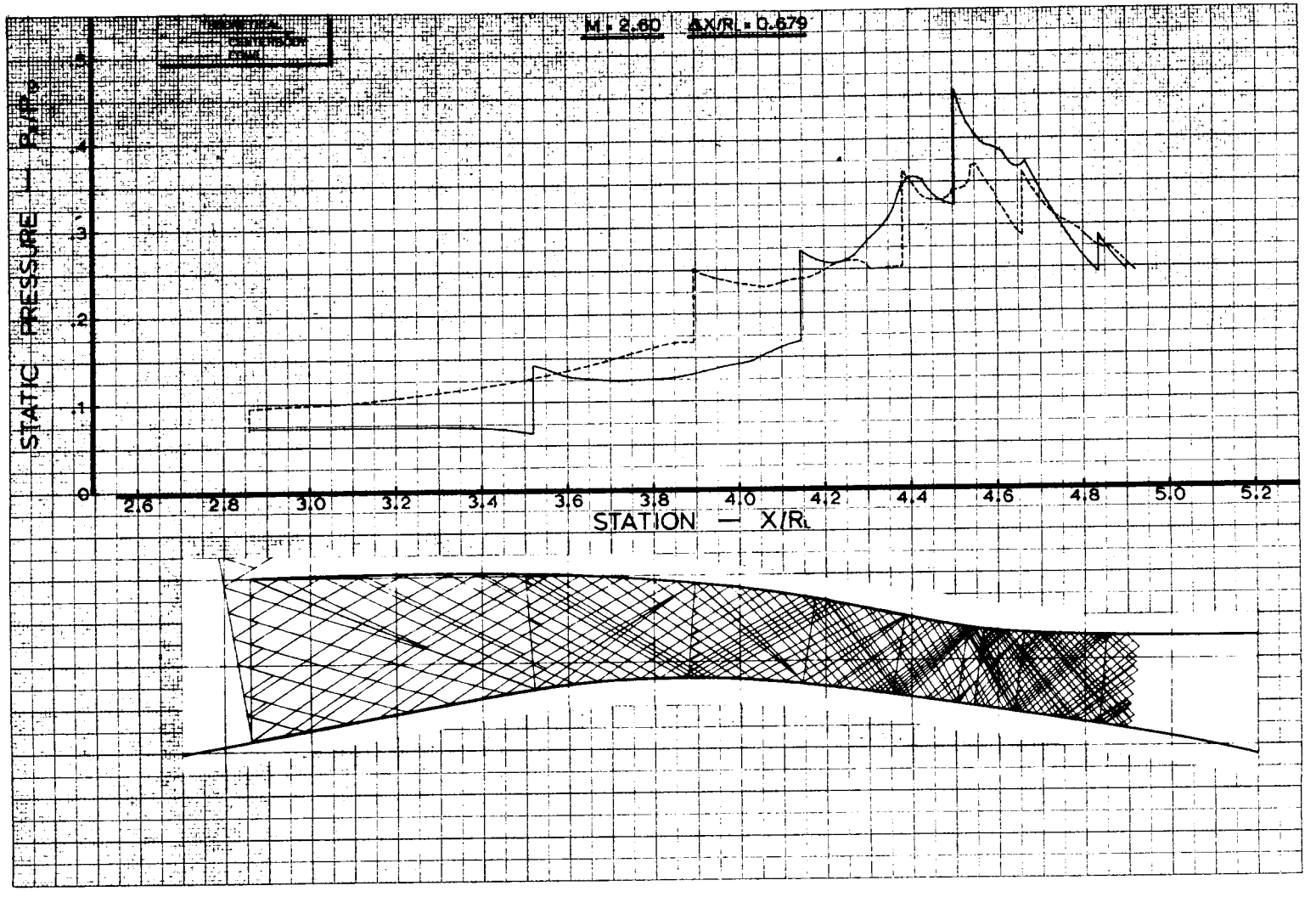

FIGURE 46.– SURFACE PRESSURES AND CHARACTERISTIC NETWORK. INVISCID ANALYSIS, MACH 2.6

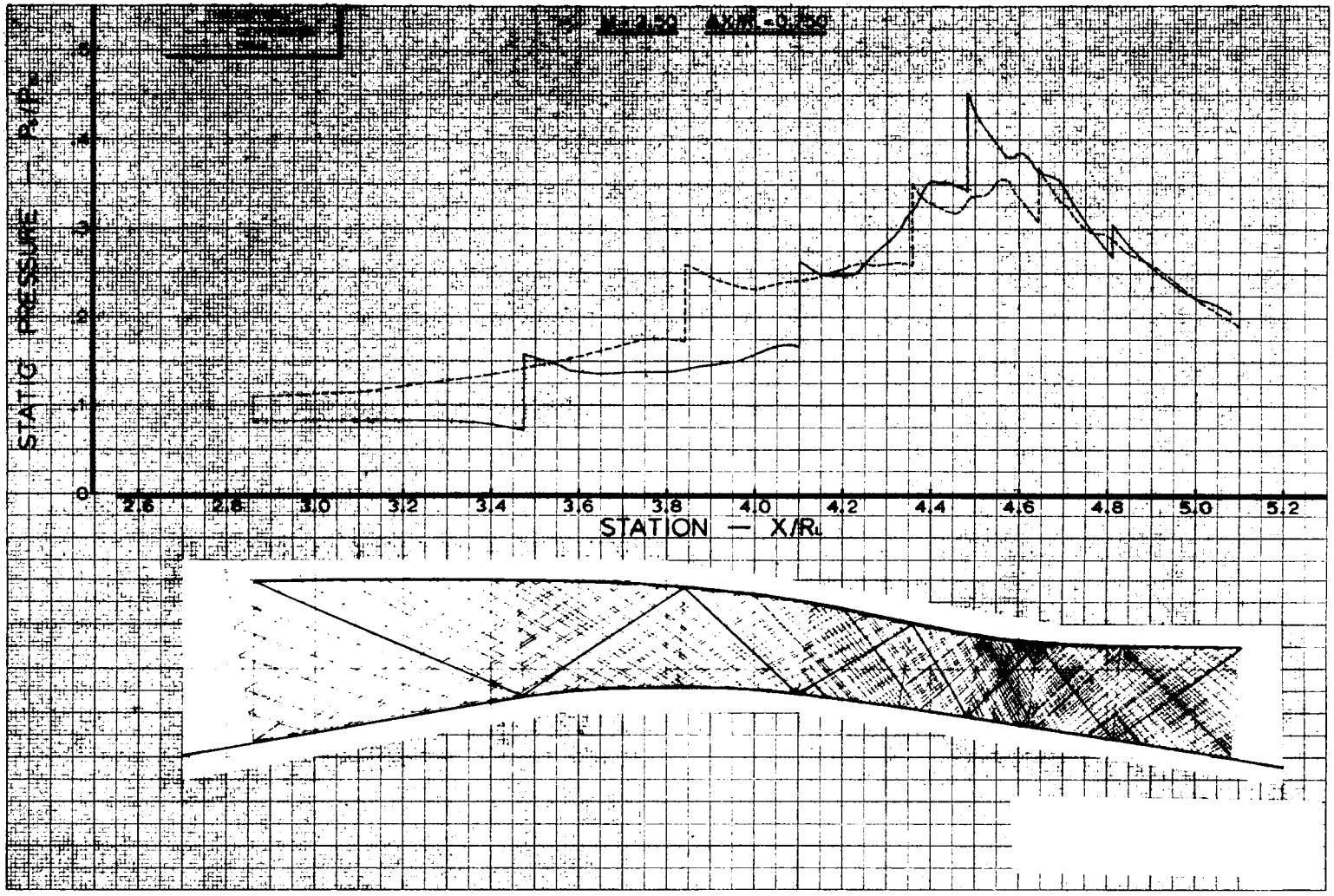

FIGURE 47.–SURFACE PRESSURES AND CHARACTERISTIC NETWORK. INVISCID ANALYSIS, MACH 2.5

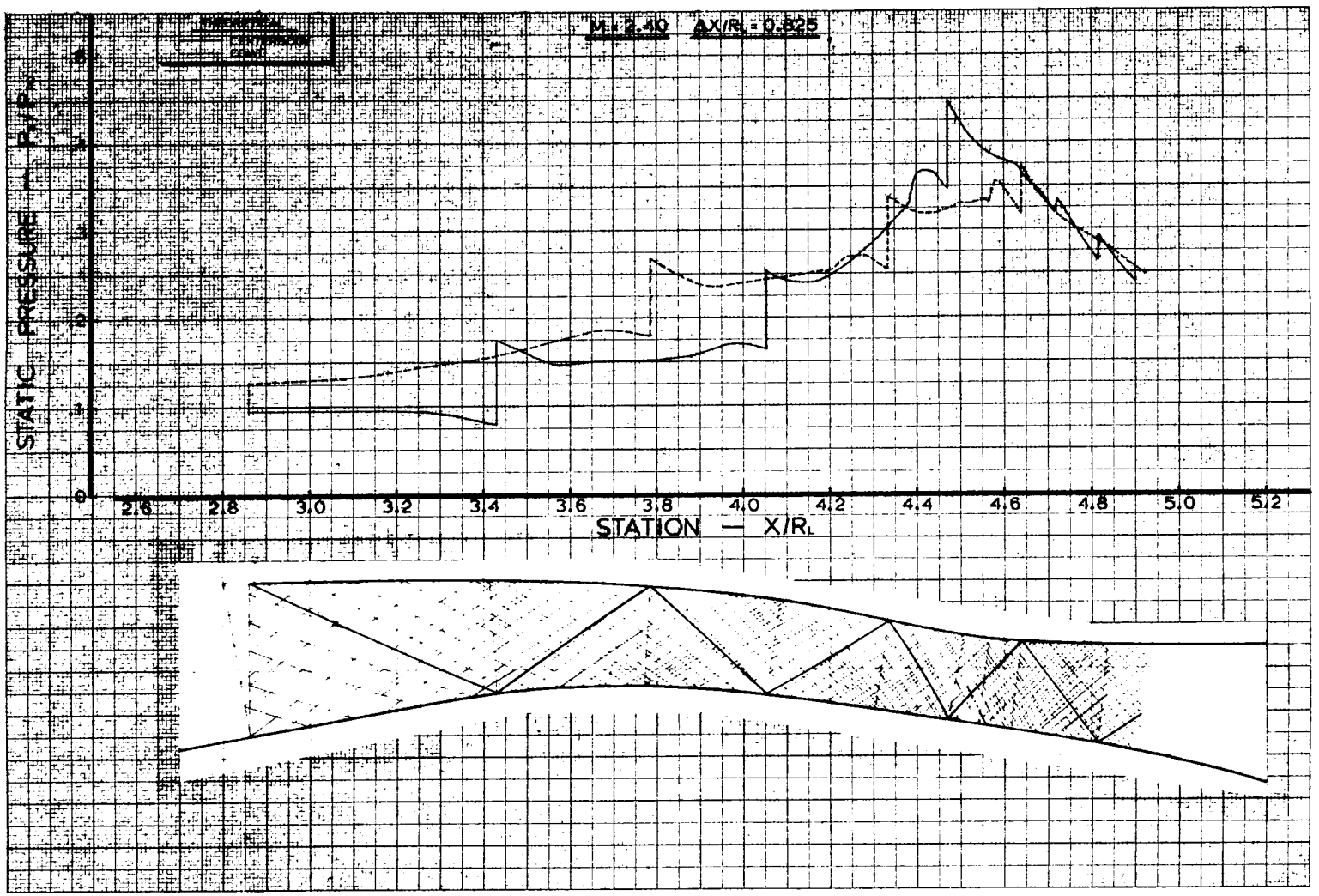

FIGURE 48. – SURFACE PRESSURES AND CHARACTERISTIC NETWORK. INVISCID ANALYSIS, MACH 2.4

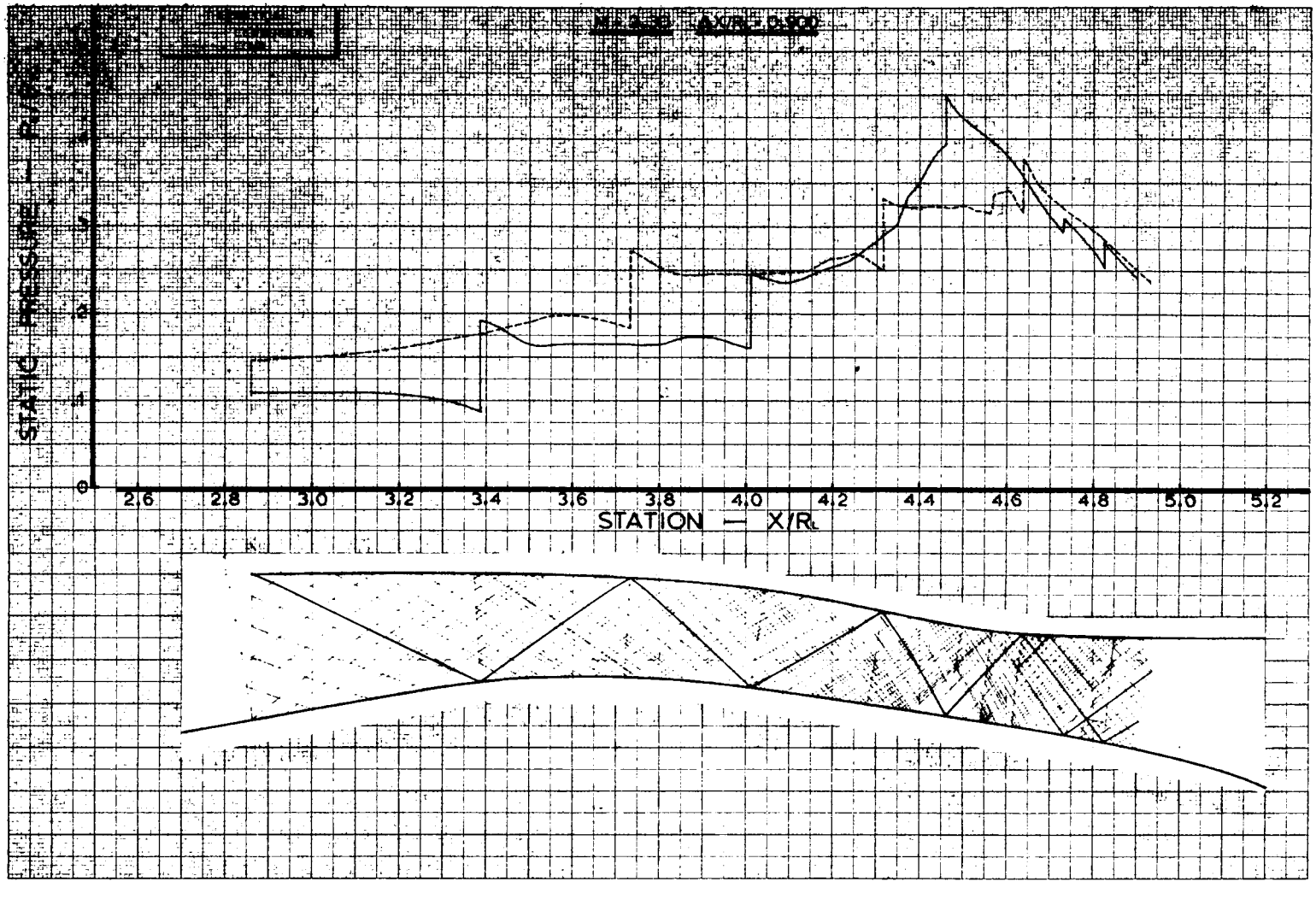

FIGURE 49.–SURFACE PRESSURES AND CHARACTERISTIC NETWORK. INVISCID ANALYSIS, MACH 2.3

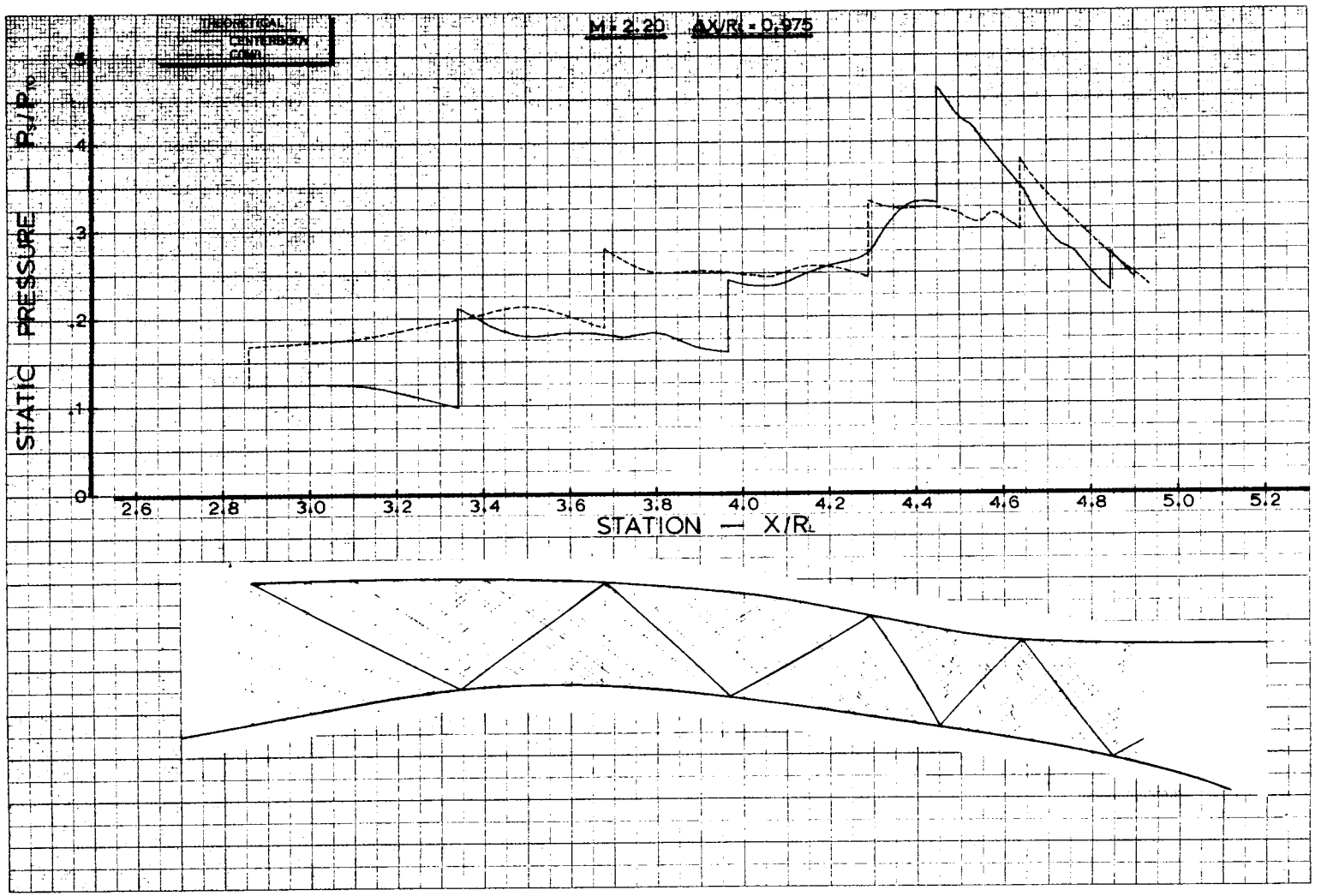

FIGURE 50.–SURFACE PRESSURES AND CHARACTERISTIC NETWORK. INVISCID ANALYSIS, MACH 2.2

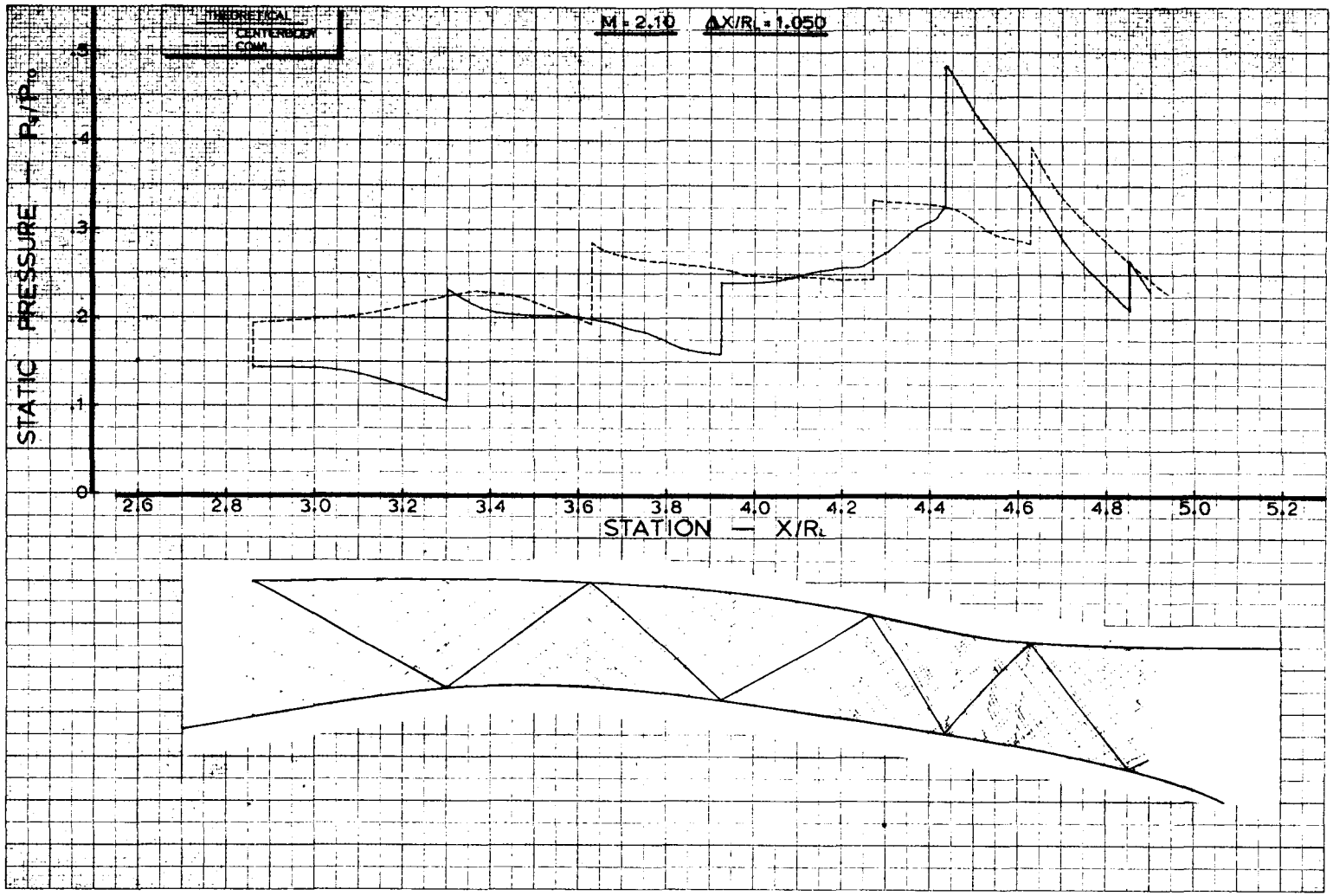

FIGURE 51.– SURFACE PRESSURES AND CHARACTERISTIC NETWORK. INVISCID ANALYSIS, MACH 2.1

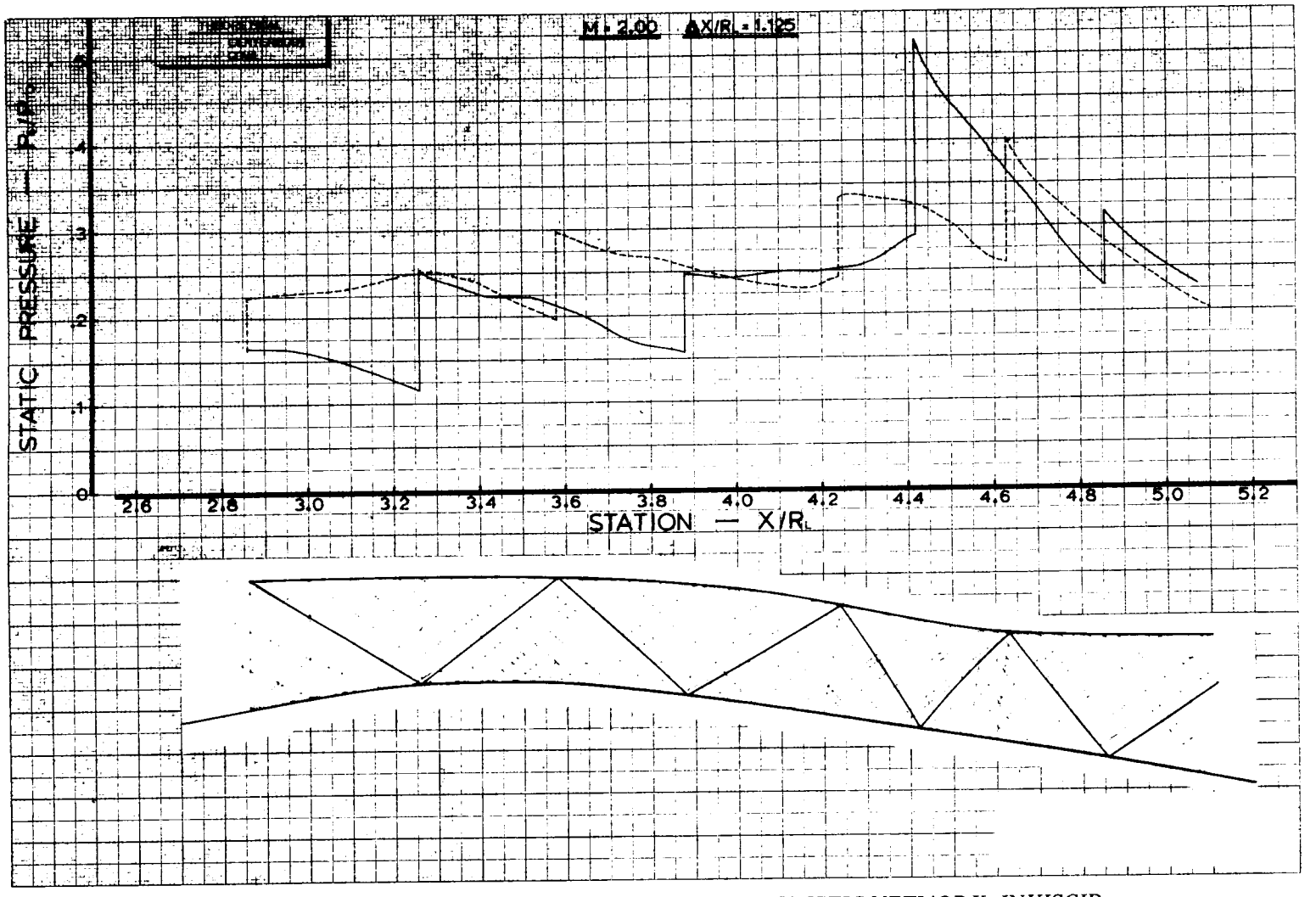

FIGURE 52.–SURFACE PRESSURES AND CHARACTERISTIC NETWORK. INVISCID ANALYSIS, MACH 2.0

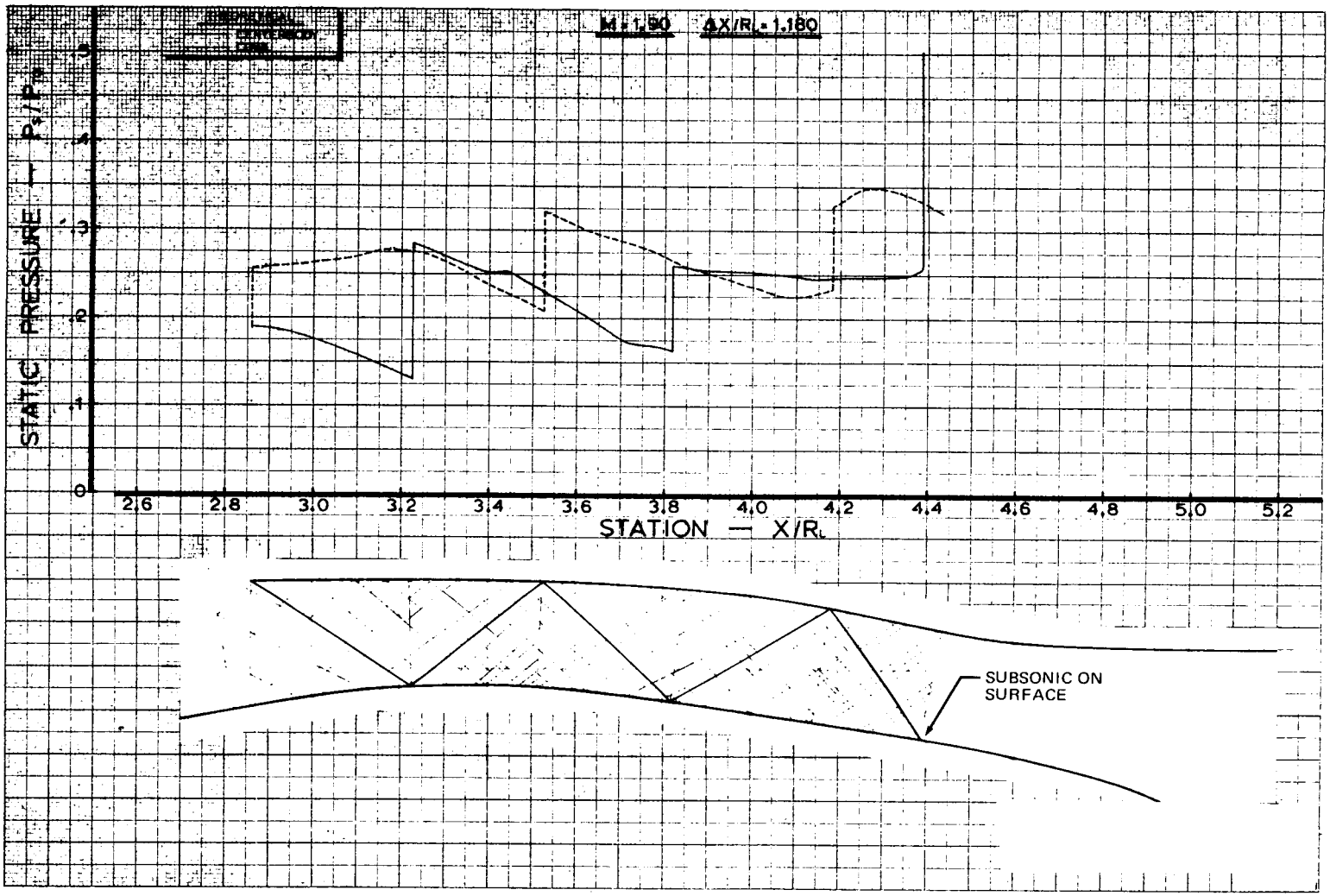

FIGURE 53.—SURFACE PRESSURES AND CHARACTERISTIC NETWORK. INVISCID ANALYSIS, MACH 1.9

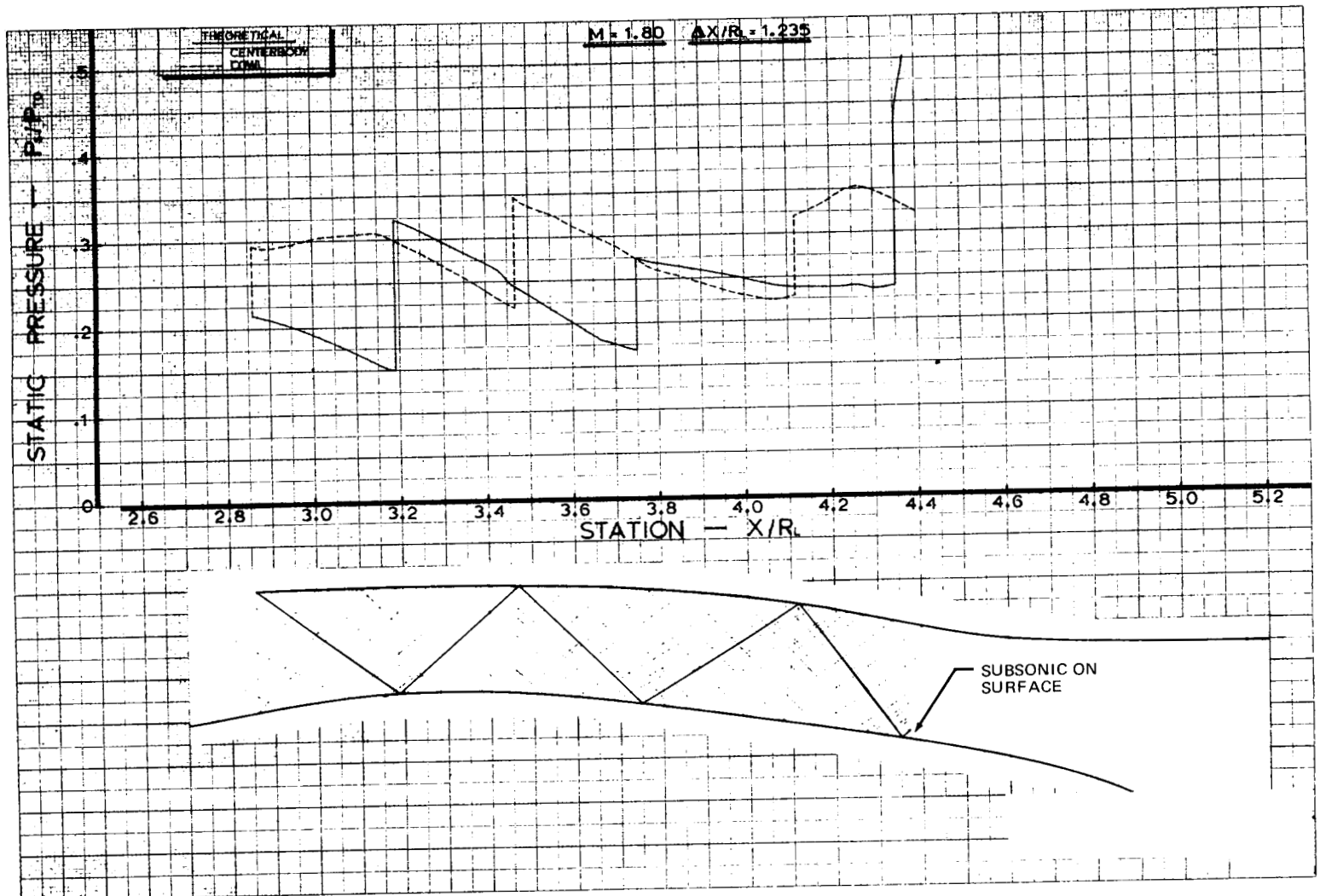

FIGURE 54.–SURFACE PRESSURES AND CHARACTERISTIC NETWORK. INVISCID ANALYSIS, MACH 1.8

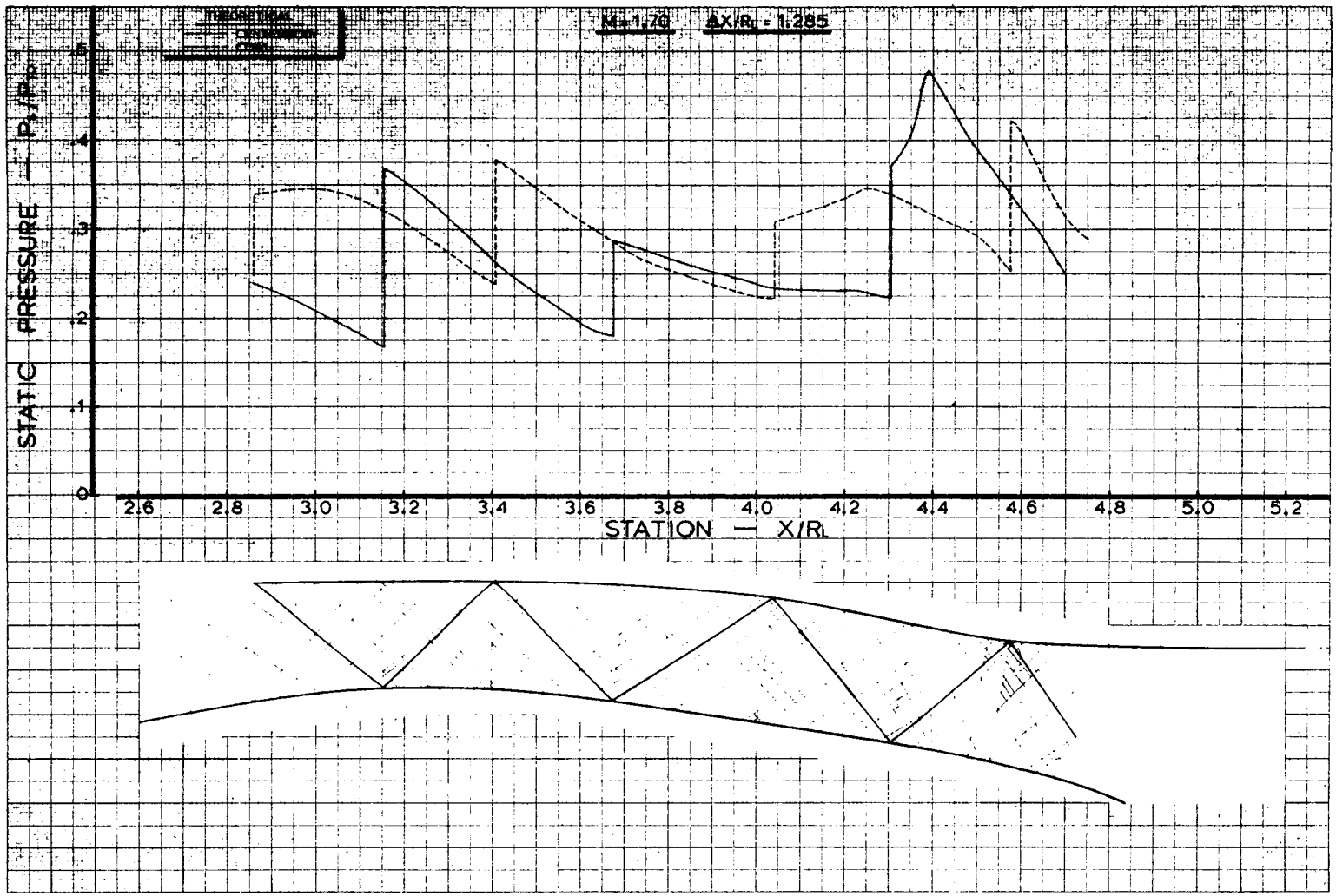

FIGURE 55.–SURFACE PRESSURES AND CHARACTERISTIC NETWORK. INVISCID ANALYSIS, MACH 1.7

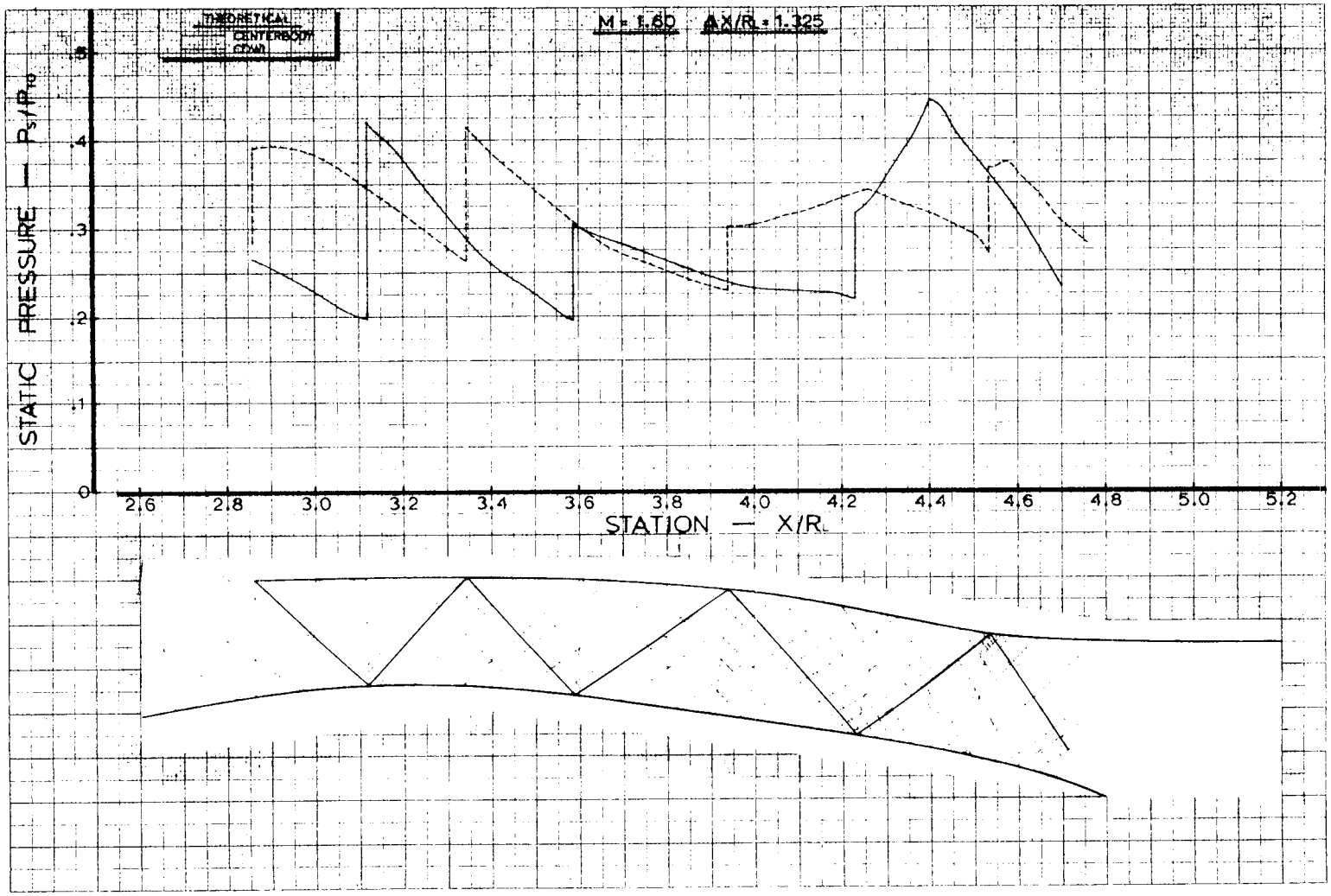

FIGURE 56. SURFACE PRESSURES AND CHARACTERISTIC NETWORK. INVISCID ANALYSIS, MACH 1.6